From THE DEPARTMENT OF NEUROSCIENCE
Karolinska Institutet, Stockholm, Sweden

INTER- AND INTRACELLULAR RESISTANCE AND VULNERABILITY IN MOTOR NEURON DISEASES

Jik Nijssen

Karolinska Institutet

Stockholm 2020

The cover image shows the band of synapses (neuromuscular junctions) between spinal motor neurons and the lumbrical muscle in the hind limb of a mouse

Published by Karolinska Institutet.
Printed by US-AB

ISBN 978-91-7831-841-4

Inter- and intracellular resistance and vulnerability in motor neuron diseases

THESIS FOR DOCTORAL DEGREE (Ph.D.)

By

Jik Nijssen

Public thesis defense at Eva & Georg Klein lecture hall, Solnavägen 9, Karolinska Institutet
Wednesday, 27 May 2020, 9:30.

Principal Supervisor:
Associate Prof. Eva Hedlund
Karolinska Institutet
Department of Neuroscience

Co-supervisor(s):
Prof. Ole Kiehn
University of Copenhagen / Karolinska Institutet
Department of Neuroscience

Associate Prof. Qiaolin Deng
Karolinska Institutet
Department of Physiology and Pharmacology

Prof. Rickard Sandberg
Karolinska Institutet
Department of Cell and Molecular Biology

Dr. Nigel Kee
Karolinska Institutet
Department of Neuroscience

Dr. Julio Aguila Benitez
Karolinska Institutet
Department of Neuroscience

Opponent:
Prof. Andreas Hermann
University of Rostock
Translational Neurodegeneration

Examination Board:
Associate Prof. Johan Holmberg
Karolinska Institutet
Department of Cell and Molecular Biology

Prof. Mats Nilsson
Science for Life Laboratory, Stockholm University
Department of Biochemistry and Biophysics

Prof. Fatima Pedrosa-Domellöf
Umeå University
Department of Integrative Medical Biology

ABSTRACT

Amyotrophic lateral sclerosis (ALS) and spinal muscular atrophy (SMA) are fatal diseases presenting with degeneration and loss of lower motor neurons in the brainstem and spinal cord. However, oculomotor and trochlear motor neurons that control eye movement, are resistant until late stages of disease. Moreover, individual motor neurons degenerate in a distinct pattern. Firstly, the distal synapse between motor neuron and muscle, the neuromuscular junction (NMJ), becomes denervated. Subsequently, the neuron degenerates in a retrograde manner, until the cell body in the spinal cord is lost later in disease. This highlights the distal axon and NMJ as the most vulnerable subcellular compartment of motor neurons.

We set out to investigate the mechanisms that underlie the resistance of oculomotor neurons, as well as the differential vulnerability within motor neurons themselves. We first validated the resistance of oculomotor neurons in two mouse models of ALS and SMA in *Paper I*. Next, we performed a large transcriptomic screen of differentially vulnerable motor pools in SMA mice throughout disease progression in *Paper II*. We used laser capture microdissection (LCM) to dissect motor neurons from different pools in the brainstem and spinal cord. Here we revealed pathways and transcripts that were enriched only in the resistant oculomotor neurons that serve to prevent them from going into apoptosis, as well as promote their regeneration. We showed that applying one of the oculomotor-enriched transcripts, *Gdf15*, to vulnerable spinal motor neurons derived from stem cells improved their survival. Next, in *Paper III* we utilised *in vitro* approaches and generated a model of oculomotor resistance in ALS by deriving both spinal and oculomotor neurons from mouse embryonic stem cells. Here we found that *in vitro* oculomotor neurons are more resistant to excitotoxic stress and have increased levels of pro-survival Akt-signaling, which also held up in LCM-dissected post-mortem human spinal and oculomotor neurons.

To investigate the vulnerability of the distal axon, we generated a technique called Axon-Seq in *Paper IV*, that allows transcriptomic profiling of isolated motor axons by culturing motor neurons in microfluidic chambers. We subsequently used this technique in *Paper V* to show that human stem cell-derived motor neurons carrying ALS-causative mutations in FUS and TDP-43 showed unique transcriptome dysregulation in somas and axons. This implies that different pathways of degeneration are at play between subcellular compartments, and provides novel targets for therapeutic intervention directed at different compartments of the motor neuron.

LIST OF SCIENTIFIC PAPERS

I. Comley LH, **Nijssen J,** Frost-Nylen J and Hedlund E. Cross-Disease Comparison of Amyotrophic Lateral Sclerosis and Spinal Muscular Atrophy Reveals Conservation of Selective Vulnerability but Differential Neuromuscular Junction Pathology. *J Comp Neurol* 524(7):1424-1442

II. Nichterwitz S, **Nijssen J***, Storvall H*, Schweingruber C, Comley LH, Allodi I, van der Lee M, Deng Q, Sandberg R and Hedlund E. LCM-seq reveals unique transcriptional adaption mechanisms of resistant neurons and identifies protective pathways in spinal muscular atrophy. *In revision*

III. Allodi I, **Nijssen J**, Aguila Benitez J, Schweingruber C, Fuchs A, Bonvicini G, Cao M, Kiehn O and Hedlund E. Modeling Motor Neuron Resilience in ALS Using Stem Cells. *Stem Cell Rep* 12(6):1329-1341

IV. **Nijssen J***, Aguila J*, Hoogstraaten R, Kee N and Hedlund E. Axon-Seq Decodes the Motor Axon Transcriptome and Its Modulation in Response to ALS. *Stem Cell Rep* 11(6):1565-1578

V. **Nijssen J**, Aguila J, Schweingruber C, Reber S, Ruepp MD and Hedlund E. Mutations in the ALS-causative genes FUS and TDP-43 cause distinct dysregulation of somatic and axonal transcriptomes. *Manuscript*

** These authors contributed equally to this work*

SCIENTIFIC PAPERS NOT INCLUDED IN THE THESIS

I. **Nijssen J**, Comley LH and Hedlund E. Motor neuron vulnerability and resistance in amyotrophic lateral sclerosis. *Acta Neuropathol* 133(6):863-885

II. Lund H, Pieber M, Parsa R, Grommisch D, Ewing E, Kular L, Han J, Zhu K, **Nijssen J**, Hedlund E, Needhamsen M, Ruhrmann S, Guerreiro-Cacais AO, Berglund R, Forteza MJ, Ketelhuth DFJ, Butovsky O, Jagodic M, Zhang XM and Harris RA. Fatal Demyelinating Disease Is Induced by Monocyte-Derived Macrophages in the Absence of TGF-β Signaling. *Nat Immunol* 19(5):1-7

III. Nizzardo M, Taiana M, Rizzo F, Benitez JA, **Nijssen J**, Allodi I, Melzi V, Bresolin N, Comi GP, Hedlund E and Corti S. Synaptotagmin 13 Is Neuroprotective Across Motor Neuron Diseases. *Acta Neuropathol* 139(5):837-853

CONTENTS

LIST OF ABBREVIATIONS

ALS	Amyotrophic lateral sclerosis
CN3/4	Cranial nerves 3 (Oculomotor) and 4 (Trochlear)
CN5	Cranial nerve 5 - Trigeminal
CN7	Cranial nerve 7 – Facial
CN10	Cranial nerve 10 – Vagus nerve
CN12	Cranial nerve 12 - Hypoglossal
DEG	Differentially expressed gene
ESC	Embryonic stem cell
GO	Gene ontology
iPSC	Induced pluripotent stem cell
NMJ	Neuromuscular junction
SMA	Spinal muscular atrophy
WGCNA	Weighted gene co-expression network analysis

1 INTRODUCTION

Motor neurons are highly polarised cells that send axons across large distances in the body. They can be subdivided in two groups: the upper motor neurons, which project down from the cerebral motor cortex into the brainstem and spinal cord, and lower motor neurons, projecting outward from the brainstem and spinal cord towards skeletal muscles. At the skeletal muscle, a specialised synapse termed the neuromuscular junction (NMJ) is responsible for signal transmission from the motor neuron to the contractile myofibre, thereby controlling voluntary muscle movement.

In the fatal diseases amyotrophic lateral sclerosis (ALS) and spinal muscular atrophy (SMA) the motor system is selectively affected, with degeneration of lower motor neurons in both diseases as well as degeneration of upper motor neurons in ALS. This results in the loss of voluntary motor control and ultimately severe muscle wasting and paralysis. Depending on the degree of upper motor neuron degeneration in ALS, additional symptoms can include spasticity and hyperreflexia. The cause of death is respiratory failure due to paralysis of the intercostal and diaphragm muscles, both responsible for breathing.

1.1 AMYOTROPHIC LATERAL SCLEROSIS

ALS is an adult-onset disease, typically starting between 30 and 60 years of age, with a fast progression. Initial symptoms are heterogeneous, largely depending on the level of upper motor neuron degeneration, but classically involve muscle fasciculations and muscle weakness starting at the distal extremities. Around 20% of patients first present with bulbar (speech and swallowing) difficulties (Swinnen and Robberecht, 2014). Approximately 25% of patients survive until 5 years after diagnosis, and this decreases to around 10% at 10 years post-diagnosis (Pupillo et al., 2014).

Currently no cure exists for ALS, and treatment is limited to Riluzole (Rilutek) and, only in the US and Japan, Edaravone (Radicava). Both drugs extend lifespan by a few months at most (Luo et al., 2018; Miller et al., 2012), and are not effective for all patients. More general symptomatic treatments include medication against pseudobulbar affect (uncontrolled emotional outbursts), excessive saliva production (to aid with swallowing) and muscle

relaxants (to counter fasciculations and spasms). In addition, physiotherapy is often prescribed in an attempt to maximise muscle strength and control.

1.1.1 Genetics and disease mechanisms of ALS

The majority of ALS cases appear sporadic (90%, sALS), while the remaining 10% are familial (fALS), meaning there is a clear family history of the disease. Mutations in several genes are known to cause ALS, the most common being *C9orf72*, as well as *SOD1*, *TARDBP* (TDP-43) and *FUS* (reviewed in Renton et al., 2014 and Taylor et al., 2016). Mutations are present in both sALS and fALS cases, and knowledge from fALS inheritance shows that the disease is almost always transmitted as a dominant trait with high penetrance (Taylor et al., 2016). Disease presentation and progression is not sufficient to pinpoint the underlying mutation, or even to distinguish fALS from sALS (Swinnen and Robberecht, 2014). Nonetheless, some genetic variants predispose to certain characteristics, for example an early (sometimes juvenile) onset with certain *FUS* mutations (Naumann et al., 2019) and strong initial lower-limb involvement and paralysis with certain *SOD1* mutations (Cudkowicz et al., 1998).

A common neuropathological hallmark of the disease is the presence of intracellular inclusions of ubiquitinated TDP-43, the protein product of the *TARDBP* gene, in the vast majority (> 95%) of all ALS cases, regardless of their genetic aetiology (Neumann et al., 2006). Approximately 4% of cases are comprised of SOD1- and FUS-ALS, presenting with mutations in, and protein aggregates of these two genes (Mackenzie et al., 2007; Vance et al., 2009). FUS-positive inclusions have also been observed in non-FUS ALS, but what proportion of non-FUS ALS cases present with these inclusions is unclear (Deng et al., 2010; Ikenaka et al., 2020; Tyzack et al., 2019).

Mutations in Cu-Zn superoxide dismutase (*SOD1*) were the first ALS-linked variants to be discovered in 1993 (Rosen et al., 1993). SOD1 is an important and highly conserved antioxidant enzyme, present in all cells. The most widely studied mouse model of ALS is based on overexpression of the human $SOD1^{G93A}$ mutation. This model recapitulates the disease well, with an adult-onset neurodegeneration and a fast progression of paralysis (Gurney et al., 1994). Misfolded SOD1 protein can aggregate and form cytoplasmic inclusions. While such $SOD1^{+}$ inclusions are universally observed in post-mortem tissue of mutant SOD1-related ALS patients, the role and presence of $SOD1^{+}$ inclusions in non-SOD1 fALS and sALS is not entirely clear yet. While some studies find virtually no presence of SOD1 misfolding and aggregation in sALS (Ayers et al., 2014; Cruz et al., 2017), others do show the presence of

misfolded SOD1 in post-mortem tissue from sALS patients (Forsberg et al., 2010; Paré et al., 2018; Ruegsegger et al., 2015). This discrepancy has been attributed to differences in tissue staining protocols (Paré et al., 2018), epitopes that are missed by certain antibodies (Ayers et al., 2014) and misidentification of normal staining patterns as aggregation (Cruz et al., 2017). Nonetheless, it seems that at least in a small proportion of sALS cases misfolded and possibly aggregated SOD1 pathology is present. How commonly it presents and to what extent it contributes to disease progression is yet unclear. It is possible that it represents a downstream process that only shows in severe cases.

Mutant SOD1 also impacts motor neurons in a non-cell-autonomous manner. Chimeric mice containing wild-type (non SOD1-overexpressing) motor neurons that were surrounded by SOD1-mutant cells still showed pathology and degeneration (Clement et al., 2003). Later it was shown that targeted removal of mutant $SOD1^{G37R}$ from motor neurons only delayed onset and early progression of disease, but did not prevent it (Boillée et al., 2006). Conversely, targeted removal of the mutant transgene only from microglia or astrocytes did not prevent disease, but slowed progression drastically (Boillée et al., 2006; Yamanaka et al., 2008). This suggests that mutant protein in motor neurons is the driver of disease onset and early progression, while glial cells contribute to later disease progression. Furthermore, expression of mutant transgenes solely in motor neurons is sufficient to trigger motor neuron loss and an ALS-like phenotype in animals, even though the surrounding cells were not genetically compromised (Huang et al., 2012; Jaarsma et al., 2008). Taken together, this paints the picture that, at least for SOD1 mutations, carrying the mutant protein in motor neurons is sufficient, but not required for disease initiation. Meanwhile glial cells, not required for disease initiation, play an important role in progression.

The pathogenic ALS phenotype in SOD1 mice does not strongly rely on changes in the regular enzymatic activity of the protein. Rather, a toxic gain-of-function of the misfolded protein is thought to cause ALS. Most SOD1 mutants have intrinsically normal antioxidant activity (Bruijn et al., 1998; Hayward et al., 2002; Wong et al., 1995), and mutations in patients are for the vast majority autosomal dominant, instead of recessive as would be expected in a loss-of-function paradigm. Genetic removal of SOD1 systemically in mice also does not lead to a motor system phenotype, although motor neurons become less effective in their response to injury and muscle fibres show aberrant properties (Nagahisa et al., 2016; Reaume et al., 1996). Vice versa, overexpression of wild-type SOD1 also does not result in an ALS-like phenotype, but it does cause mild NMJ denervation, resembling that normally seen in ageing mice (Epstein et al., 1987; Gurney et al., 1994). Interestingly, SOD1 was shown to be exported from cells and

released from dead cells in culture, triggering aggregation in other cells in a prion-like way (Grad et al., 2014).

In the *C9orf72* gene, a large $(GGGGCC)_n$ hexanucleotide repeat expansion was identified that is currently the most common genetic variant in both fALS and sALS (DeJesus-Hernandez et al., 2011; Renton et al., 2011). In healthy people this gene carries around 20 expansions, which rises to several hundreds or even thousands of repeats in ALS patients. Interestingly, this repeat expansion also underlies frontotemporal dementia (FTD). The function of the C9ORF72 protein is not entirely clear. While haploinsufficiency of C9ORF72 in *in vitro* motor neurons results in decreased survival under stressed conditions (Shi et al., 2018), full knock-out approaches of the homologue gene in mice have not been able to recapitulate a motor phenotype. Instead, mice display an immunological phenotype characterised by cytokine storm, splenomegaly, lymphocyte infiltration in many tissues and elevated autoantibodies (Atanasio et al., 2016; Jiang et al., 2016; Sudria-Lopez et al., 2016). Thus, it is likely that a gain-of-function causes the ALS phenotype.

The hexanucleotide repeat sequence was found to give rise to so-called repeat-associated non-ATG dependent translation (RAN-translation) (Zu et al., 2010). RNA is transcribed directly from the repeat sequence and being translated into long dipeptide repeat proteins based on all reading frames in the DNA sequence, sense and anti-sense. These dipeptide repeat proteins aggregate and a subset of them, particularly the arginine-containing peptides, result in cellular stress (Ash et al., 2013; Mori et al., 2013). In addition, RNA transcripts from *C9orf72* aggregate in intranuclear RNA-protein inclusions (RNA-foci), which also confer stress to the neurons and result in axon outgrowth and branching defects in zebrafish (Donnelly et al., 2013; Swinnen et al., 2018). The importance of RNA-induced toxicity is still debated, however. Depending on the model system used, RNA-foci appear to be contributing strongly to disease (Swinnen et al., 2018) or rather the opposite, with the dipeptide repeat proteins being the main culprit (Mizielinska et al., 2014; Moens et al., 2018). Several groups reported that nucleocytoplasmic transport was impaired in drosophila models expressing expanded *C9orf72* repeats that gave rise to toxic dipeptide proteins (Freibaum et al., 2015; Jovičić et al., 2015; Zhang et al., 2015). Still, in what order these events occur and which can actively trigger or contribute to neuronal degeneration is debated. TDP-43 pathology was detected in C9ORF72-ALS patient tissue, though often not in the same aggregates (Mackenzie et al., 2013; Murray et al., 2011). Yet, the link between C9ORF72-induced pathology and TDP-43 pathology is unclear. It is plausible that dipeptide repeat proteins or RNA-foci could initiate aggregation of RNA-binding proteins, such as TDP-43, providing an upstream disease process

that culminates in TDP-43 pathology similar to other forms of ALS. Thus far only one report directly linked dipeptide repeat proteins to accumulation of TDP-43 pathology in a *Drosophila* model of C9ORF72-ALS (Solomon et al., 2018). It therefore remains to be investigated where C9ORF72-ALS converges with other types of ALS.

After the discovery that the vast majority of ALS cases present with TDP-43 positive inclusions (Neumann et al., 2006), it was found that mutations in *TARDBP* also underlie a moderate portion of fALS cases (Sreedharan et al., 2008). Soon after, mutations in *FUS* were also identified to cause fALS (Kwiatkowski et al., 2009; Vance et al., 2009), with both *FUS* and *TARDBP* underlying approximately 4-5% of fALS cases (Lattante et al., 2013). *TARDBP* and *FUS* both encode RNA-binding proteins with diverse functions. Mutations in both genes cluster in the RNA-binding domains, while in *FUS* many mutations also localise to the nuclear localization signal domain. The functional homology between these genes implicates abnormal RNA biology as an upstream mechanism in ALS.

FUS-ALS cases present with cytoplasmic FUS^{+} inclusions (King et al., 2015; Vance et al., 2009). Inclusions of FUS have also been detected in human sALS post-mortem tissue, sometimes co-localising with TDP-43 (Deng et al., 2010; Ikenaka et al., 2020; Tyzack et al., 2019). It is not clear how widespread FUS aggregates are in sALS and non-FUS fALS, as many studies have not actively looked for these inclusions. Interestingly, the otherwise so ubiquitous TDP-43^{+} inclusions are absent in *FUS*-linked ALS, potentially placing TDP-43 further upstream to FUS. Both TDP-43 and FUS positive inclusions have been shown to co-localize with stress granules. These are a pan-cellular stress response comprised of membrane-less aggregates of all components of the translation pre-initiation complex: poly-adenylated mRNAs, RNA-binding proteins and ribosomal subunits (reviewed in Aulas and Vande Velde, 2015). They only appear under cellular stresses, such as osmosis or oxidative stress. Normally when the stressor subsides, stress granules dissolve and disappear again shortly after. Functionally, they are thought to protect the mRNA from harmful circumstances, as well as provide time to decide whether certain mRNAs still need to be translated or should be stored or degraded in the face of stress. In the context of ALS, it has been shown that after TDP-43 co-aggregates with stress granules upon their formation, it can remain aggregated even when the stress granules are dissolving again, possibly leading to more toxic types of aggregates (Becker et al., 2017; Gasset-Rosa et al., 2019).

Since both mutant FUS and TDP-43 appear to aggregate in the cytoplasm, whereas they are normally mainly present and functional in the nucleus, a partial loss of (nuclear) function of

these proteins was thought to cause ALS. A complete loss of function seems unlikely, as complete knockout of either *FUS* or *TARDBP* is embryonically lethal in inbred animals (Hicks et al., 2000; Kraemer et al., 2010). For *FUS*, however, it is clear that disease occurs even when wild-type FUS is present at close to normal levels in the nucleus, indicating that a cytoplasmic gain-of-function mechanism is more likely (Mitchell et al., 2012; Sharma et al., 2016). Moreover, postnatal loss of FUS does not influence motor neuron survival, again implying a gain-of-function to underlie ALS (Sharma et al., 2016).

Somewhat contrarily, for TDP-43 it appears that exclusion from the nucleus by inducible removal of the nuclear localization signal is sufficient to induce neurodegeneration (Walker et al., 2015). This leaves the question open whether neurodegeneration is triggered due to aberrant localization in the cytoplasm or due to loss of TDP-43 in the nucleus. However, an inducible post-natal knock-out of TDP-43 in mice results in death after 9 days (Chiang et al., 2010). This indicates that even if TDP-43 is absent from the nucleus in an ALS context, cytoplasmic TDP-43 presumably retains a physiological and necessary function for survival. Overexpression of TDP-43, however, causes an ALS-like phenotype, indicating that protein levels of TDP-43 need to be tightly regulated to prevent dysfunction (Wils et al., 2010). In summary, it appears that *FUS* mutations cause motor neuron death due to a toxic gain-of-function in the cytoplasm. *TARDBP* mutations, on the other hand, most likely cause motor neuron degeneration due to both a loss-of-function in the nucleus, combined with a toxic gain-of-function in the cytoplasm. It is important to identify where these different mechanisms intersect further downstream to result in motor neuron degeneration.

1.2 SPINAL MUSCULAR ATROPHY

SMA in its most severe forms (type 0 and I) is an infantile onset motor neuron disease, with death before 2 years of age. At the other end of the spectrum are type III and IV SMA, which have an onset later in life and often do not affect life expectancy, although patients are likely to become wheelchair-bound at some point in their life.

Recent years have seen the development and approval of two breakthrough therapies: nusinersen (Spinraza, Finkel et al., 2016) and onasemnogene abeparvovec-xioi (Zolgensma, clinical studies still ongoing). Both treatments were shown to result in dramatic improvement in motor functions and lifespan, although the outcome seems highly dependent on the age of the infant when the drug is administered (the earlier the better).

1.2.1 Genetics and disease mechanisms of SMA

SMA is characterised by the progressive loss of lower motor neurons and resulting paralysis. In contrast to ALS, SMA is a monogenetic disease. It is caused by homozygous loss-of-function mutations in the *SMN1* gene (Lefebvre et al., 1995). In humans, a paralogous gene called *SMN2* is present in varying copy numbers. This gene can partially compensate for the loss of *SMN1*. However, due to a single base pair substitution in *SMN2* compared to *SMN1* in exon 7, this exon is spliced out in approximately 90% of *SMN2* transcripts, rendering it unstable (Lefebvre et al., 1995). Thus, the *SMN2* gene only produces about 10% full-length SMN protein. As a result, patients with a loss-of-function of *SMN1* develop SMA, while the copy number of *SMN2* determines severity of disease, among likely other modifying factors (Harding et al., 2015). It is this process that nusinersen acts on, as it affects the splicing of *SMN2*, resulting in an increased proportion of transcripts from this gene that include exon 7. Zolgensma on the other hand is an AAV9 viral vector-mediated delivery of a fully functional copy of the *SMN1* gene.

SMN is known to perform a variety of functions in cells, being linked to translation, intracellular transport, endocytosis and more. However, the first and most well described role for SMN is in the nuclear biogenesis of snRNPs, by chaperoning the interaction between snRNAs and their accompanying proteins in nuclear structures termed ‘gems’ (Chaytow et al., 2018; Liu et al., 1997). Subsequently, additional proteins and pre-mRNAs are added to this complex to form the spliceosome. Gems are not equally present in every tissue and their highest numbers are in fact present in neurons, particularly motor neurons, highlighting their importance for motor neuron diseases (Young et al., 2000). As the number of gems are reduced in SMA and this correlates with disease severity, splicing defects are thought to play an important role in SMA disease initiation (Gabanella et al., 2007). One particularly striking alteration in SMA is the preferred downregulation of components of the minor spliceosome (Gabanella et al., 2007). These complexes are required for splicing of minor introns, a subgroup that makes up only ~0.5% of all introns in humans. Genes containing minor introns are highly conserved and are involved in a subset of key cellular pathways, such as DNA damage repair, RNA processing and vesicle/axonal transport (Burge et al., 1998).

SMN protein was also detected in axons and growth cones, where it is typically devoid of other protein components of the snRNPs or spliceosome, highlighting that it likely does not perform its canonical function here (Zhang et al., 2006). SMN was found to be responsible for mRNA

transport and regulation of local translation in axons, as well as cytoskeletal dynamics, mainly by modulating actin (Nölle et al., 2011).

Several studies have linked FUS and TDP-43 to SMN, highlighting possible cross-disease pathways. FUS interacts directly with SMN, as it is also involved in the snRNP complex, specifically with U1 snRNP. FUS was shown to be required for gem formation, and in cells from both FUS and TDP-43 fALS patients, the number of nuclear gems was decreased, similar to SMA (Yamazaki et al., 2012). Furthermore, splicing alterations induced by loss of *SMN* had a significant overlap with those introduced by overexpression of human FUS in mice, which causes neurodegeneration (Mirra et al., 2017). FUS was shown to bind to U11 snRNP, thereby being directly involved in splicing of minor introns, similar to SMN. Splicing of these introns was defective upon expression of ALS-causative mutations in FUS (Reber et al., 2016). Together, this implicates minor spliceosome defects in the pathology of both SMA and ALS (Jutzi et al., 2018).

Less is known about the interaction of TDP-43 with SMN or the spliceosomal complex. However, in TDP-43^{A315T} mice an upregulation of SMN was observed, demonstrating a regulatory interaction between the two. SMN upregulation was likely a beneficial compensatory response, as overexpression of SMN in the TDP-43^{A315T} context extended lifespan of the mice (Perera et al., 2016).

1.3 DIFFERENTIAL VULNERABILITY OF SUBCELLULAR COMPARTMENTS

The affected lower motor neurons in both ALS and SMA follow a distinct pattern of degeneration. Data from mouse models, as well as patient tissue, shows that the distal connection between motor neuron and muscle is lost first. This ‘dying-back’ pathology causes the muscle to be denervated, after which the motor neurons degenerate proximally, back to the soma (Cifuentes-Diaz et al., 2002; Fischer et al., 2004; Frey et al., 2000; Liu et al., 2015). This highlights the NMJ as a highly vulnerable element of the motor neuron. Processes culminating in axonal degeneration are likely driven by the soma, as is the case for trophic factor deprivation (Simon et al., 2016). However, preserving the NMJ as the initial site of degeneration can provide a therapeutic target to slow down progression of the disease. Moreover, rescuing motor neuron somas by preventing cell death does not protect against axonal degeneration and consequently muscle denervation (Gould et al., 2006).

1.3.1 The motor axon contains a distinct mRNA composition

While it is intuitive to think of the nucleus and cell body as the centre of the cell, this does not entirely hold true for motor neurons. With axons that can span up to a meter in length, an average spinal motor neuron holds more than 95% of its volume in the axon. The remainder is mostly taken up by dendrites, while only around 0.1% is contained in the soma.

The large distance between the soma of a motor neuron and the NMJ implies that the distal axon must contain a distinct micro-environment to be able to rapidly respond to local cues. The fast-anterograde axonal transport system relies on kinesins and it carries vesicles and organelles at rates up to 40 cm per day. However, many soluble proteins and cytoskeletal elements travel considerably slower, at rates up to 1 cm per day (Lasek et al., 1984). This would not be sufficient to completely sustain the highly dynamic environment at the NMJ. Local storage of mRNA coupled with local translation could overcome this issue, allowing the distal axon to react to (environmental) cues by targeted translation and protein production.

To investigate this, several techniques have been used to isolate distal axons and analyse their composition. Laser capture microdissection revealed the mRNA repertoire of growth cones of *ex vivo* cultured retinal ganglion cells (Zivraj et al., 2010). However, this technique required over 1,000 growth cones to be dissected to obtain sufficient RNA, although with current day methodologies this number could be reduced. An alternative method was to culture neurons in either Campenot or microfluidic chambers (Taylor et al., 2005). These allow for recruitment of axons by using trophic factor gradients and keep them isolated from the somas (see section 3.2). Due to the size of these devices, material from several hundreds to thousands of axons can be harvested for analysis. Microarray-based detection of axonal RNAs was performed on various types of neurons, such as primary cortical (Taylor et al., 2009), sensory (Gumy et al., 2011) and motor (Saal et al., 2014). These studies revealed the presence of up to 4,000 unique mRNAs in the axonal compartment. Subsequent studies utilized next-generation RNA sequencing, investigating rodent primary motor neurons and sensory neurons (Briese et al., 2015; Minis et al., 2014) and found overlapping results. However, it was not clear what fraction of the detected axonal mRNAs is actually translated into proteins.

To investigate this in developing retinal ganglion axons, Shigeoka et al. (2016) utilised a variant of TRAP (Translating Ribosome Affinity Purification). Here, one ribosome subunit is protein-tagged in a specific neuronal cell type. Pulldown of the tag and thus the ribosomes from the area to which these neurons project and subsequent RNA-sequencing of the mRNAs in these ribosomes revealed the axonal *translatome* at several time points. This

revealed that in adult mice, axonal translation occurs for just over 1,000 unique mRNAs, although it remains possible for mRNA transcripts to sit on ribosomes in a stalled state. At several time points during embryonic and early postnatal development up to 2,000 transcripts were being translated (Shigeoka et al., 2016). This shows that at most half of the unique mRNAs present in axons is actively translated at any given moment. The growing axon goes through successive phases of polarisation, outgrowth, pathfinding and synaptogenesis. It likely carries a repertoire of mRNAs along for all of these functions, to overcome delays that would otherwise arise from transport.

1.4 MODELS OF MOTOR NEURON DISEASES

1.4.1 Rodent models of ALS and SMA

The discovery of *SOD1* as the first causative gene in ALS in 1993 spurred the rapid development of a transgenic mouse model, based on the human $SOD1^{G93A}$ mutation (Gurney et al., 1994). This mouse model grew to become the most popular and widely used rodent model of ALS. It replicates the human disease progression well, as it displays an adult-onset hind limb paralysis that progressively worsens and is ultimately fatal.

While different mouse strain backgrounds, as well as copy number of the $SOD1^{G93A}$ transgene can alter the time course of symptoms, the overall progression of disease is retained. Typically, the first behavioural symptoms are observed between postnatal day (P)60-80, with a decreased motor performance in the rotarod or hanging wire tests. Motor neuron somas in the spinal cord start to decrease in number as of P85-100, and end point survival is around 140-150 days (Fischer et al., 2004; Liu et al., 2015; Mancuso et al., 2012).

This mouse model is in essence a model for SOD1-fALS, which lacks the otherwise so abundant TDP-43 inclusions seen in the vast majority of sporadic ALS cases. However, because the outward symptomatology and pathology is so similar between sALS and fALS, and indeed also SOD1-ALS and other types, it is thought that this model still holds value for ALS as a whole. This is reinforced by consensus findings that at the cellular level, similar stress pathways and events are seen in the $SOD1^{G93A}$ model as in post-mortem human ALS tissue,

such as ER stress, autophagy dysregulation and mitochondrial dysfunction. We utilised this mouse model in *Paper I*, and embryonic stem cells derived from this model in *Paper IV*.
Recent years have now seen the development of mouse models based on known disease-causing mutations in other genes, such as *FUS* (Sharma 2016), *TARDBP* (Walker et al., 2015) and *C9orf72* (Liu et al., 2016). Hopefully this extended number of models will aid in the translation of more therapeutic avenues towards the clinic, as this aspect has been lacking from the $SOD1^{G93A}$ model. To illustrate, mice carrying a TDP-43 mutation were used to validate the therapeutic benefit of reducing levels of ataxin-2 (Becker et al., 2017), a genetic modifier of TDP-43 induced toxicity, identified in yeast (Elden et al., 2010). Similarly, antibody-mediated depletion of toxic dipeptide repeat proteins translated from the *C9orf72* repeat region showed behavioural improvements and lifespan extension in *C9orf72* mutant mice (Nguyen et al., 2020).

The discovery that autosomal recessive loss of the *SMN1* gene caused SMA quickly led to efforts in generating a mouse model of this disease. However, while humans have two distinct copies of *SMN*, called *SMN1* and *SMN2*, mice have only one single *Smn* gene. A complete loss-of-function in mice, due to a homozygous deletion of *Smn*, is embryonically lethal (Schrank et al., 1997). Heterozygous depletion leads to mild motor neuron degeneration, and can serve as a model for SMA type III (Jablonka et al., 2000). However, to model the most severe type I SMA another strategy had to be employed.

It was shown that introducing the human *SMN2* gene (that produces only 10% full length protein compared to human *SMN1*) into the mouse $Smn^{-/-}$ background could rescue the embryonic lethality, and mice survive for approximately 6 days (Monani et al., 2000). When subsequently a copy of human *SMNΔ7* is introduced, a pre-truncated form of SMN lacking exon 7, mice have an extended survival up to approximately two weeks (Le et al., 2005). This effect requires small amounts of full-length SMN from the human *SMN2* transgene to be present. Therefore, it is thought that *SMNΔ7* stabilises full length SMN, thereby exerting its beneficial effect. We used this mouse model, called the SMNΔ7 model, in papers I and II.

1.4.2 *In vitro* modelling of ALS

Cell culture models of ALS assist in understanding and dissecting the mechanisms responsible for generating and maintaining a functional NMJ, as well as the processes that occur in motor neurons that ultimately lead to their demise in ALS and SMA. Here, murine and human pluripotent stem cells have provided a boost to the ALS field. In 2007, embryonic stem cells

(ESCs) were derived from the SOD1^{G93A} mouse, the only available ALS model at the time. These cells could be differentiated into motor neurons using previously established protocols (Wichterle et al., 2002), and contained SOD1 positive inclusions in the cytoplasm, as is seen in *SOD1*-ALS port-mortem tissue from patients (Giorgio et al., 2007). Although the SOD1^{G93A} motor neurons did show a mild increase in cell death compared to controls after a prolonged period in culture, they did not show gross morphological abnormalities or problems with differentiating into motor neurons. Their degeneration was accelerated upon co-culture with SOD1^{G93A}-expressing astrocytes. These also affected the survival of control motor neurons, but to a lesser degree. Later, control human ES-derived motor neurons were also shown to be vulnerable in co-culture with glial cells carrying two different SOD1 mutations (Giorgio et al., 2008; Marchetto et al., 2008).

When human ES-derived motor neurons, but not other cell types in the culture, were expressing constructs carrying various SOD1 mutations, they exhibited a reduced survival and shorter neurite processes (Karumbayaram et al., 2009). This indicates that, even though non-cell-autonomous events can influence progression of degeneration, the initial trigger originates in the motor neurons themselves, justifying the use of motor neuron cell culture systems to study degenerative phenotypes.

With the expansion of the human induced pluripotent stem cell (iPSC) field came the possibility to investigate and compare motor neurons derived from patient cells that carry mutations in other ALS-linked genes, as well as motor neurons derived from sporadic ALS patients. One goal was to be able to identify pathology in cells that did not rely on overexpression of a mutant gene, as is the case for the SOD1^{G93A} mouse and stem cell models.

Patient iPSC-derived motor neurons carrying TDP-43 mutations displayed increased cell death under regular culture conditions (Bilican et al., 2012; Fujimori et al., 2018; Kreiter et al., 2018) and arsenite-induced stress (Egawa et al., 2012). While others did not observe this degeneration, they did observe defects in neuronal firing properties and abnormal ion currents (Devlin et al., 2015). The differences in spontaneous cell death are likely partially dependent on the cell line and different culture conditions with varying levels of stress on the cells. Therefore, the use of CRISPR/Cas9 to edit out a mutation in a patient-derived line, or introduce it in a control genetic background could help reveal whether the specific mutation is responsible for any phenotypes observed, eliminating cell type and culture condition variables. This technique we utilised in *Paper V*. Cytoplasmic TDP-43 mislocalisation and aggregation was also observed in mutant iPSC-lines under stressor conditions (Fujimori et al., 2018; Zhang et

al., 2013), however this cell-autonomous degeneration *in vitro* has not been a consistent observation (Egawa et al., 2012, Kreiter et al., 2018).
Two back to back papers showed that global downregulation of TDP-43, as well as expression of ALS-causative TDP-43 mutations led to a concomitant strong downregulation of stathmin-2 (*STMN2)*, due to splicing defects. Restoration of the levels of this microtubule regulator ameliorated disease phenotypes (Klim et al., 2019; Melamed et al., 2019). General defects in axonal transport and organelle trafficking were also found in TDP-43 mutant neurons *in vitro* and *in vivo* (Kreiter et al., 2018; Sleigh et al., 2020). Together, this highlights a cytoskeletal and particularly microtubule network disruption as a primary pathological process induced by TDP-43 dysfunction. However, this does not account for possible gain-of-function toxicity, as would occur in ALS patients that do not have a complete loss of TDP-43 function.

Finally, in line with data from post-mortem tissue it was shown that sALS patient iPSC-derived motor neurons contained TDP-43 aggregates, whereas SOD1-fALS motor neurons did not (Burkhardt et al., 2013; Fujimori et al., 2018). Neurite outgrowth and survival defects were observed in a large number of the studied sALS lines (Fujimori et al., 2018).

Regarding a non-cell-autonomous effect of TDP-43, studies were conducted *in vitro* to understand the roles of astrocytes and muscle carrying TDP-43 mutations. Human iPSC-derived astrocytes carrying the TDP-43^{M337V} mutation did not affect survival in co-culture of either wild-type motor neurons or motor neurons carrying the same mutation (Serio et al., 2013). However, when mouse ESC-derived motor neurons were co-cultured with muscle overexpressing human TDP-43 mutations, increased motor neuron death was observed, albeit for one of the mutations only (Wächter et al., 2015). Whether this depends on TDP-43 levels, a genuine difference between astrocytes and muscle with regards to TDP-43 or simply different experimental settings is not clear. Experiments using non-overexpressing constructs will be needed to assess the relative contribution of different cell types to disease, although it is not unthinkable that central and peripheral exposure to non-cell autonomous toxicity can exert differential effects.

IPSC-derived motor neurons that carry mutations in FUS are consistently reported to show mislocalisation of FUS to the cytoplasm, as well as occasional cytoplasmic aggregates. However, no spontaneous cell death has been observed (Ichiyanagi et al., 2016; Japtok et al., 2015; Lenzi et al., 2015; Marrone et al., 2018; Naumann et al., 2018). Nonetheless, neurons carrying FUS mutations display various deleterious phenotypes, such as increased

susceptibility to oxidative stress (Ichiyanagi et al., 2016; Japtok et al., 2015; Marrone et al., 2018), axonal fragmentation and increased susceptibility to DNA damage (Naumann et al., 2018).

Genetic correction of $SOD1^{A4V}$ patient-derived iPSCs revealed specific defects in the mutant cells in mitochondrial transport and morphology, as well as increased ER-stress and an activated unfolded protein response (Kiskinis et al., 2014). However, no detergent-insoluble SOD1 or SOD1 aggregates were detected in these motor neurons. The lack of aggregates was also observed in another study investigating the $SOD1^{A4V}$ and $SOD1^{D90A}$ mutations (Chen et al., 2014). More recently, two studies have shown misfolded and aggregated SOD1 in iPSC-derived motor neurons (Fujimori et al., 2018; Imamura et al., 2017). This discrepancy could be explained by the use of different SOD1 mutations, as the latter two studies used L114FVX, H43R and H46R mutations. Genetic background of the lines can also play a role. However, differences in culture conditions may also form an equally likely explanation. Neurons in culture are easily stressed by oxidation, low density culturing, imperfect extracellular matrix conditions or lack of trophic support. Overall, mouse models of SOD1 mutations show a stronger SOD1 aggregation phenotype, even compared to post-mortem human ALS tissue. This is likely due to the forced overexpression of multiple copies of mutant SOD1 in mice. The process of misfolding and aggregation likely takes longer in the human cells, as SOD1 is only expressed at physiological levels. Hence the cases where SOD1 aggregates are observed may represent the more extreme end of the spectrum with stressed neurons displaying early pathological hallmarks.

Several of the pathological hallmarks associated with C9ORF72-ALS have been recapitulated in *in vitro* models. Both RNA-foci as well as dipeptide repeat sequences arising through RAN-translation were present in iPSC-derived neurons. These hallmarks were not only observed in motor neurons but also in other neurons, such as cortical glutamatergic, GABAergic and TH+ dopaminergic neurons (Almeida et al., 2013; Lopez-Gonzalez et al., 2016). These cells suffer from compromised mitochondrial function and a (presumably linked) increase in oxidative stress. Moreover, these cells become more vulnerable to autophagy inhibition, in line with recent papers describing a role for C9ORF72 in the initiation and regulation of autophagy (reviewed in Nassif et al., 2017).

A transcriptomic comparison was made between dysregulated transcripts in *C9orf72* repeat-carrying cells and controls and $SOD1^{A4V}$ carrying motor neurons (Donnelly et al., 2013; Kiskinis et al., 2014) and controls. This revealed only a 5% overlap in transcripts,

whereas there was a larger overlap between the SOD1 mutation and a different SOD1 mutant. This underlines the different aetiologies of SOD1- and C9ORF72-linked ALS. Overlapping pathways represent downstream events leading to neurodegeneration. However, early disease-triggering mechanisms are likely to be very different between SOD1 and C9orf72-linked ALS.

Taken together, the *in vitro* data show that pathological phenotypes such as protein aggregates, RNA foci and stress granules that are observed in post-mortem tissue from both mice and patients can be recapitulated in iPSC-derived motor neurons. However, these cell culture models typically only show minor morphological phenotypes or intrinsic degeneration under regular culture conditions. This makes sense, since these motor neurons are embryonic and fetal neurons that are used to model an adult-onset disease. The use of overexpression systems or the introduction of homozygous mutations (in contrast to the heterozygous mutations in patient cell lines) can provide the tools to study the initial pathological processes in motor neurons that might accumulate to trigger neurodegeneration later in life.

1.5 DIFFERENTIAL VULNERABILITY OF MOTOR NEURON POOLS

Curiously, most of the genes that are implicated in ALS and SMA are ubiquitously expressed throughout the body. Why mutations in these genes cause degeneration of specifically motor neurons is largely unclear. Moreover, certain subpopulations of motor neurons are more resistant to degeneration than others, while carrying the same genetic predisposition. Among the somatic motor neurons, oculomotor neurons that control eye movement typically remain resistant to degeneration until end stage of disease. This allows patients to utilize eye movements as a last means of communication (Caligari et al., 2013; Kubota et al., 2000; Lenglet et al., 2019). In addition, motor neurons of Onuf's nucleus, involved in bladder and sphincter control, are affected to a lesser degree than surrounding sacral motor neurons (Bergmann et al., 1995).

In mouse models of motor neuron disease, the selective resistance of the oculomotor system has been reproduced. At late stages of disease, oculomotor neurons are not lost, unlike other brainstem and spinal cord motor neurons (Ferrucci et al., 2010; Haenggeli and Kato, 2002).

Oculomotor neurons differ from spinal motor neurons in some fundamental anatomical aspects (reviewed in Nijssen et al., 2017). One striking difference is that oculomotor neurons synapse onto multiple NMJs per muscle fibre in the extraocular muscles. This contrasts to all other

skeletal muscle in the body, where each myofibre is innervated by one single NMJ. Consequently, the extraocular muscles contain one band of neuromuscular endplates with the typical *en plaque* morphology, as seen in other skeletal muscles, but also a spatially separate band of so-called *en grappe* endplates. This innervation pattern is thought to allow graded contractions and a finer level of motor control compared to other skeletal muscles (Porter 2002).

In addition, the size of the motor units is distinctly smaller in oculomotor neurons, with a single one typically innervating only between 5-20 myofibres (Enoka, 1995; Gueritaud et al., 1985), while spinal motor neurons innervate in the hundreds of myofibres or even up to 2,000 in specific muscles (Burke and Tsairis, 1973; Burke et al., 1971). This is intriguing, as even within the spinal cord there appears to be a correlation with motor neurons having a smaller motor unit size being more resistant. Slow-twitch (S) motor units are comprised of 'slow' motor neurons innervating type I muscle fibres that are fatigue-resistant and have a highly oxidative metabolism. These motor units typically involve one motor neuron innervating 200 or fewer myofibres. In contrast, fast-twitch motor units (FF and FR) consist of motor neurons that innervate type IIa, IIb and IIx myofibres that are fatigable and glycolytic. It is these motor units that can have ratios of up to 2,000 muscle fibres innervated by one neuron (Burke and Tsairis, 1973). In ALS, it is the 'fast' motor neurons that degenerate first, followed only late in disease by 'slow' motor neurons, that temporarily can compensate for loss of their fast neighbours (Hegedus et al., 2007; Pun et al., 2006; Schaefer et al., 2005). However, although the correlation is there, whether there exists a causal relation between the number of NMJs a motor neuron has to maintain and its vulnerability is unknown.

Given the unique anatomy of oculomotor neurons and their resistance in disease, studies have investigated whether molecular differences confer their resilience. Mechanisms of proteostasis were different between oculomotor and spinal motor neurons, as oculomotor neurons appeared to have improved proteasomal function and thus an improved capacity to degrade misfolded proteins (An et al., 2019).

Gene-expression profiling of spinal and oculomotor neurons in wild-type rats revealed an enrichment of potential protective factors in the oculomotor neurons (Hedlund et al., 2010). Several candidate genes from this study were followed up on, and later work showed that differences in mRNA levels of parvalbumin, Gucy1a3, $GABA_A$ receptor $\alpha 1$, insulin-like growth factor 2 (IGF-2) and synaptotagmin 13 were maintained at protein level in mouse and human post-mortem tissue (Allodi et al., 2016; Comley et al., 2015; Nizzardo et al., 2020). The

potential therapeutic effects of two candidate molecules, IGF-2 and SYT13, were explored further. *In vitro,* overexpression of either IGF-2 or SYT13 in iPSC-derived motor neurons from fALS and sALS patients improved their survival under glutamate-induced excitotoxicity or co-culture with $SOD1^{G93A}$ mutant astrocytes. Similarly, it attenuated the spontaneous degeneration observed in iPSC-derived motor neurons from SMA patients. *In vivo* delivery of IGF-2 or SYT13 to motor neurons extended lifespan of a mouse models of ALS and SYT13 also improved survival of SMA mice, by preserving NMJ innervation and motor function for a prolonged period of time (Allodi et al., 2016; Nizzardo et al., 2020).

Conversely, this paradigm was also used to identify factors highly expressed in the spinal motor neuron population, whose presence could explain their increased vulnerability. This strategy led to the identification of the matrix-metalloprotease *Mmp9,* a factor selectively expressed in fast motor neurons in mice. Reduction of Mmp9 levels in spinal motor neurons in $SOD1^{G93A}$ mice resulted in improved motor functions and extended lifespan, in a dose-dependent fashion (Kaplan et al., 2014). Together, these strategies highlight the validity of identifying molecular differences between oculomotor and spinal motor neurons that confer increased resistance or vulnerability to neurodegeneration across diseases.

2 AIMS

The two main aims of this thesis were to investigate firstly why the subgroup of oculomotor neurons, among all somatic motor neurons, is intrinsically more resistant to degeneration in the motor neuron diseases ALS and SMA. Secondly, we explored the vulnerability of the distal axon, the first cellular part of the motor neuron to degenerate in ALS and SMA. The goal with our approach is to identify therapeutic targets and pathways aimed at improving motor neuron survival, as well as neuromuscular connectivity.

Paper I: To validate oculomotor neuron resistance in two widely used mouse models of ALS and SMA, and to investigate the temporal dynamics of neuromuscular denervation.

Paper II: To identify transcriptional mechanisms underlying resistance and susceptibility to degeneration in differentially vulnerable motor neuron pools in SMA.

Paper III: To generate and characterise an *in vitro* model of oculomotor resistance in ALS.

Paper IV: To develop a technique to study the motor axon transcriptome, and identify both how it differs from the somatic transcriptome and how it is dysregulated in an ALS context.

Paper V: To investigate the effect of ALS-causative mutations in FUS and TDP-43 on the transcriptome of somas and axons in human iPSC-derived motor neurons.

3 METHODOLOGICAL CONSIDERATIONS

3.1 STEM CELL DIFFERENTIATIONS FOLLOW EMBRYONIC DEVELOPMENTAL PATTERNS

Pluripotent stem cells come in two types: embryonic and induced. Both can differentiate into every type of cell in the body, the difference being their origins. Embryonic stem cells are extracted from the inner cell mass of a pre-implantation embryo, a technique that was first performed in 1981 in mice (Evans and Kaufman, 1981; Martin, 1981). Over the next two decades, research would focus on how to maintain ESCs in culture and subsequently generating protocols to differentiate ESCs into various cell types. The first human ESCs were isolated in 1998 from embryos that were not used for implantation after successful *in vitro* fertilisation procedures (Thomson et al., 1998). Their limited availability spurred the field to identify novel ways of obtaining stem cells. In the early sixties experiments by John Gurdon already showed, using frogs, that the genetic material contained in a somatic cell has the capacity to replace the nucleus in a zygote and allow its differentiation into an entire organism (Gurdon, 1962). However, the challenge remained how to instruct a somatic cell to transform itself back into a stem cell and reinitiate all required processes for pluripotency. This was thought to require large-scale gene expression and chromatin reorganisation changes, and would go against the paradigm established by Waddington in 1957 describing that developmental gene expression and regulation is unidirectional (Waddington, 1957).

The game-changing breakthrough came in 2006, when Shinya Yamanaka and colleagues identified four molecules that, when introduced into somatic cells of a mouse, could reprogram these cells into stem cells (Takahashi and Yamanaka, 2006). This feat was shortly after repeated for human cells (Takahashi et al., 2007; Yu et al., 2007). These factors, SOX2, KLF4, OCT4 and c-MYC effectively ‘de-differentiate’ somatic cells and allow the generation of stem cells from any individual. Their shared discoveries led to Gurdon and Yamanaka jointly winning the Nobel Prize in Physiology or Medicine in 2012. This new technique opened up the field of disease modelling immensely, providing the opportunity to obtain stem cells from disease patients and healthy controls for direct comparison. This is especially valuable in the neuroscience field, as neural tissue cannot be biopsied from living patients. Thus, stem cell-derived neurons and neural tissues can provide a window to investigate disease processes in early stages that would otherwise be hardly accessible for research.

Spinal motor neurons were one of the early neuronal subtypes to be generated from mouse ESCs (Wichterle et al., 2002). This protocol employed two key factors that in combination were able to drive stem cells from neural induction to a definitive motor neuron fate: sonic hedgehog (Shh) and retinoic acid (RA). In embryonic development, RA is secreted by the somites that are adjacent to the newly formed neural tube. RA secretion is restricted, and its levels decrease anteriorly throughout the hindbrain. Thus, RA levels are highest in the developing spinal cord, decrease throughout the hindbrain and are absent anterior to the hindbrain-midbrain boundary (Maden, 2002).

Sonic hedgehog is released by the notochord, ventral to the developing neural tube. From there, it specifies the neural floor plate, which then in turn secretes Shh (Fig. 1A). This creates a gradient across the neural tube, with decreasing concentration from ventral to dorsal. This gradient enables a layered patterning that results in distinct domains along this gradient developing specific subgroups of interneurons, as well as motor neurons (Jessell, 2000).

The combined caudalising action of RA and the ventralising action of Shh can be utilised to control the type of neural cells generated and were fine-tuned to generate spinal motor neurons (Fig. 1B) (Wichterle et al., 2002). Using this paradigm, mostly cervical spinal motor neurons are generated. Patterning of further caudal spinal motor neurons has been achieved by integrating additional Wnt and Fgf8 signaling (Lippmann et al., 2015).

For oculomotor neurons located in the midbrain, RA signalling was omitted, as caudalisation is not required in this protocol. Instead the cells are exposed to Fgf8, combined with Shh (Fig. 1C). *In vivo* Fgf8 is secreted from the isthmic organizer, the boundary located between the developing midbrain and hindbrain (Heikinheimo et al., 1994). Gradients of Shh and Fgf8 promote differentiation of neural progenitors to midbrain and hindbrain neurons, such as oculomotor neurons (Wang et al., 1995; Ye et al., 1998). Since the proportion of oculomotor neurons in the midbrain and consequently in stem cell-derived midbrain cultures is low, we employed a combined overexpression of the transcription factor *Phox2a*, a known driver of oculomotor lineage fate (Mong et al., 2014; Pattyn et al., 1997).

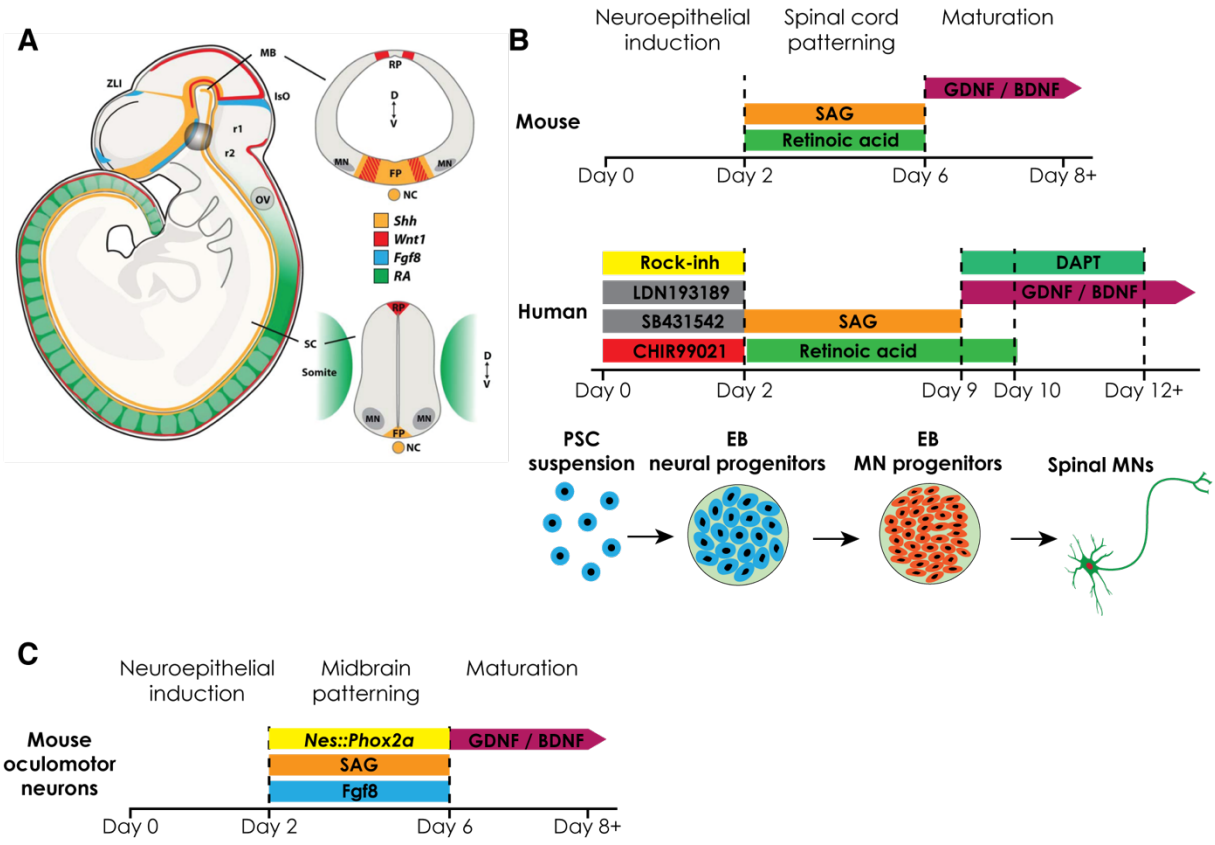

Figure 1. Different factors and gradients specify the developing midbrain and spinal cord. A. Schematic overview showing a sagittal cross-section of an embryo, and transverse sections of the midbrain and spinal cord. Retinoic acid (green) is released parallel to the spinal cord, while sonic hedgehog is released initially by the notochord and subsequently by the floorplate. Fgf8 is released at the isthmic organiser, at the separation between mid- and hindbrain. **B.** Differentiation protocols to specify cervical spinal motor neurons from mouse (top) and human (bottom) stem cells. **C.** Differentiation protocol to specify oculomotor neurons from mouse stem cells carrying the Nestin::Phox2A expression system. *(A) Adapted from Allodi and Hedlund (2014) under the Creative Commons 3.0 licence.*

In 2005 the first motor neurons were generated from human embryonic stem cells (Li et al., 2005) using the combined action of RA and Shh. While several studies used these cells, it was not until the advent of iPSC technology that motor neuron generation from human stem cells for disease modelling became its own research field. Several rounds of protocol optimisations have reduced the time to generate mature motor neurons from approximately one month down to 10-14 days. However, the key component of RA and Shh patterning remained virtually unchanged.

Spontaneous neural induction occurs rapidly in mouse stem cells, but initially took up to two weeks for human cells. The discovery that combined inhibition of SMAD2/3 and SMAD1/5/8 signalling caused rapid induction of neutral progenitors from human stem cells was a

breakthrough in the field (Chambers et al., 2009). This so-called dual-SMAD inhibition has become a highly used method to initiate conversion of human stem cells to any neural cell type. In the differentiation protocol used in *Paper V*, two days of dual-SMAD inhibition preceded one week of RA- and Shh-based patterning (Fig. 1B).

A second advancement was made in the process of neural maturation. Both in our mouse and human protocols, cells are patterned with RA and Shh in a sphere-based culture, where aggregates of cells are floating freely in media. After the patterning period, these spheres contain committed OLIG2-positive motor neuron progenitors, but not yet mature motor neurons. Subsequent dissociation of the spheres and plating of the single-cell suspension on culture dishes then results in terminal differentiation into post-mitotic neurons. Inhibition of Notch-signaling was found to drive this transition and speed up the conversion of neural progenitors into mature motor neurons. An inhibitor of Notch signalling (DAPT), was consequently shown to cause a drastic reduction in the time of motor neuron generation, as well as increasing their proportion over other cell types, as it also avoids the progenitors from going into gliogenesis in a time-dependent manner (Maury et al., 2015).

3.2 USING MICROFLUIDICS TO STUDY THE AXONAL TRANSCRIPTOME

Three main methods have been developed to isolate neural cell bodies from axons. The first method to be developed was the Campenot chamber (Campenot, 1977). In this set-up, a solid divider (typically made from Teflon) is placed in a cell-culture dish and sealed to the bottom surface using a silicone grease layer, or in more recent versions, a hydrogel. When neurons are placed on one side of the divider, their processes can be recruited through the sealant using a gradient of trophic factors. While this method can be highly effective at isolating axons fluidically, it is time consuming and error-prone, as the divider can easily loosen and transect the axons growing underneath.

A second method is based on using well-insets in a traditional cell culture plate. Neurons are seeded on a porous membrane (typically made from PET or similar material) containing pores with diameters in the range of one to a few microns. This membrane is held in suspension in culture media, allowing neurons to grow processes that invade these pores and grow underneath the membrane. While in theory effective at maintaining a separation between soma and axon, this system allows cells that end up in suspension (for example during seeding or media changes) to adhere to the bottom of the membrane and ‘contaminate’ the neurites. In addition, growth of neural processes is not actively directed, making it hard to separate axons

from dendrites without distinct growth cues. Combined with the thin diameter of the membrane, contamination with dendrites or even cellular filopodia can occur.

Lastly, microfluidic chambers made from silicone (typically PDMS) have been developed that can be sealed to a glass or plastic surface and form grooves for axons to grow through (Taylor et al., 2005). They typically contain 2 or more compartments for culturing the cells, with reservoir wells for media on the side (Fig. 2A). We have employed microfluidic devices with groove diameters of 3 micron in our studies. In these devices, a distinct neurotrophic gradient can be created to recruit axons. In addition, the length of the grooves can be as long as desired. We have employed 150 and 450 μm groove lengths. While dendrites *in vitro* can occasionally traverse the 150 μm grooves, they do not grow as long as 450 μm, resulting in highly pure axonal separation at these distances (Taylor et al., 2005, *Paper IV*).

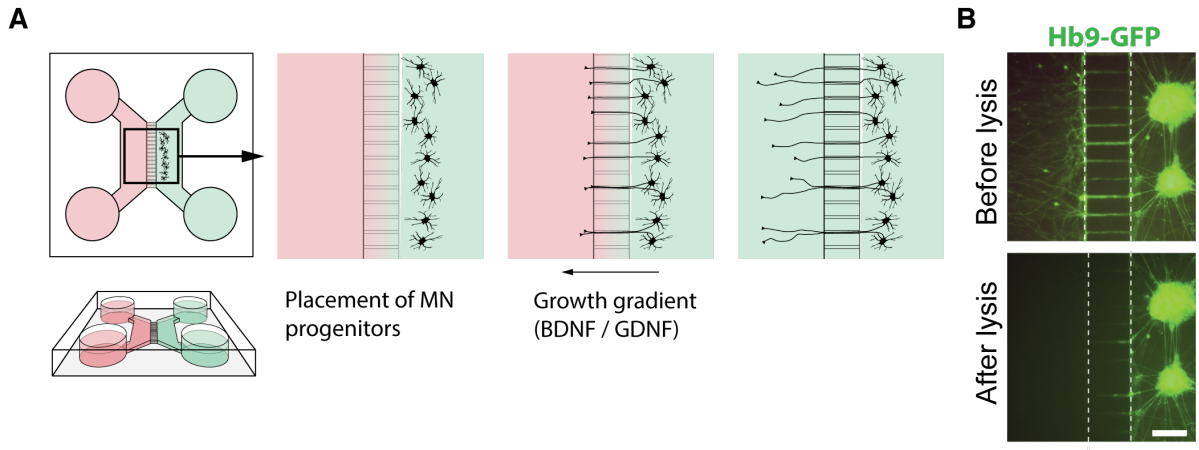

Figure 2. Setup of using microfluidic chambers to culture motor neuron somas and axons in an isolated manner. A. Schematic of the devices. First motor neurons (MNs) are placed inside one of the compartment, after which a gradient of GDNF and BDNF is used to recruit axons to the second compartment. **B.** Hb9-GFP expression showing that the axonal compartment can be lysed without affecting the somas. Scale bar: **B.** 100 μm.

A distinct advantage of the microfluidic system (as well as the Campenot chambers) over cell culture insets is that the two compartments are fluidically isolated. For one this allows the neurotrophic gradient, but it also allows for cells to be grown in entirely different medias (such as motor neurons and muscle cells) or receive different treatments either side. Importantly, they allowed us to lyse the axonal compartment, without affecting the somatic compartment or being contaminated with somas (Fig. 2B). Nonetheless, microfluidic devices have a lower throughput compared to insets, and due to their small size the number of cells that can be grown inside is limited. For certain assays (i.e. transcriptomics or proteomics) this results in too little material from single devices, requiring pooling of devices. To overcome this, we describe a technique

in *Paper IV*, Axon-Seq, that allows the RNA-sequencing of axonal material of one single device, due to the optimisation of a single-cell RNA library preparation protocol for axonal material. This has provided us the benefits of using the fluidically isolated chambers, while still obtaining enough lysis material from single devices to perform analyses.

4 RESULTS AND DISCUSSION

The results in this thesis can be divided in two main parts, covered by papers *I-III* and *IV-V*, respectively. In the first three papers, we focussed on identifying pathways responsible for the selective resistance to degeneration of oculomotor neurons in ALS and SMA.

We first demonstrated this resistance at the level of the NMJ in two mouse models of ALS and SMA, as well as describing a time course of NMJ denervation. Then we performed a transcriptomic study of differentially vulnerable motor neuron pools in the SMA mouse model, where we elucidated pathways of susceptibility or resistance. Thirdly, we generated an *in vitro* system, using mouse ESC-derived motor neurons, to model oculomotor neuron resistance in ALS. We showed that *in vitro* generated oculomotor and spinal motor neurons carry similarity to their *in vivo* counterparts, that the oculomotor neurons are more resilient under excitotoxic stress and that they express a survival-promoting signalling pathway.

In papers *IV* and *V* we uncovered the rodent and human motor axon transcriptome, to study why the distal axon is the most vulnerable part of the motor neuron and why it degenerates first in disease. We showed that the motor axon contains a core set of mRNA transcripts for all essential cellular functions. In addition, dysregulation of the somatic and axonal transcriptomes that occurs in motor neurons expressing ALS-causative mutations may explain their vulnerability.

4.1 PAPER I: CROSS-DISEASE COMPARISON OF AMYOTROPHIC LATERAL SCLEROSIS AND SPINAL MUSCULAR ATROPHY REVEALS CONSERVATION OF SELECTIVE VULNERABILITY BUT DIFFERENTIAL NEUROMUSCULAR JUNCTION PATHOLOGY

In the SOD1^{G93A} mouse model of ALS, oculomotor neurons were shown to persist while other brainstem and spinal cord motor neurons had degenerated (Ferrucci et al., 2010; Haenggeli and Kato, 2002). However, it had not been determined if this resistance held up at the level of the NMJ and if synaptic contacts were preserved. Moreover, in SMA mouse models, oculomotor resistance had not been thoroughly characterised at all yet. We set out to analyse in detail the dying-back phenotype *in vivo* and to perform an extensive analysis of NMJ denervation and post-synaptic morphology changes in two models of motor neuron disease. This also allowed us to pinpoint the order of events regarding pre-synaptic denervation and post-synaptic endplate changes in both ALS and SMA. We chose to investigate three muscle groups. Firstly, the extraocular muscles, innervated by the resistant oculomotor neurons. We chose lumbrical muscles, located in the paw of the mouse, innervated by lumbar spinal motor neurons for the reasons that they are innervated by a motor neuron pool that is known to be vulnerable to degeneration in disease, as well as the accessibility of these muscles for dissection and whole-mount immunohistochemistry. Lastly, we chose the tongue, which is innervated by hypoglossal motor neurons (cranial nerve (CN) 12), as an indicator of bulbar involvement of disease.

4.1.1 Extraocular muscles are resistant to denervation in the SOD1^{G93A} model of ALS

Denervation of NMJs was observed earliest in the lumbrical muscles at P84, before onset of symptoms in the mice, which is a confirmation of the vulnerability of the motor neurons innervating these muscles (Fig. 3A). Tongue muscle showed denervation only at the latest time point measured (Fig. 3E), while extraocular muscles showed no signs of NMJ pathology (Fig. 3I).

When assessing the size of the endplates on the muscle, we found a shrinkage of endplates in lumbrical muscles as of P112, one time point later than denervation was seen (Fig. 3B). This implies that motor nerve retraction is the initial event, leaving the muscle denervated and triggering the endplates to shrink. No endplate shrinkage was observed in tongue and extraocular muscles (Fig. 3F, J).

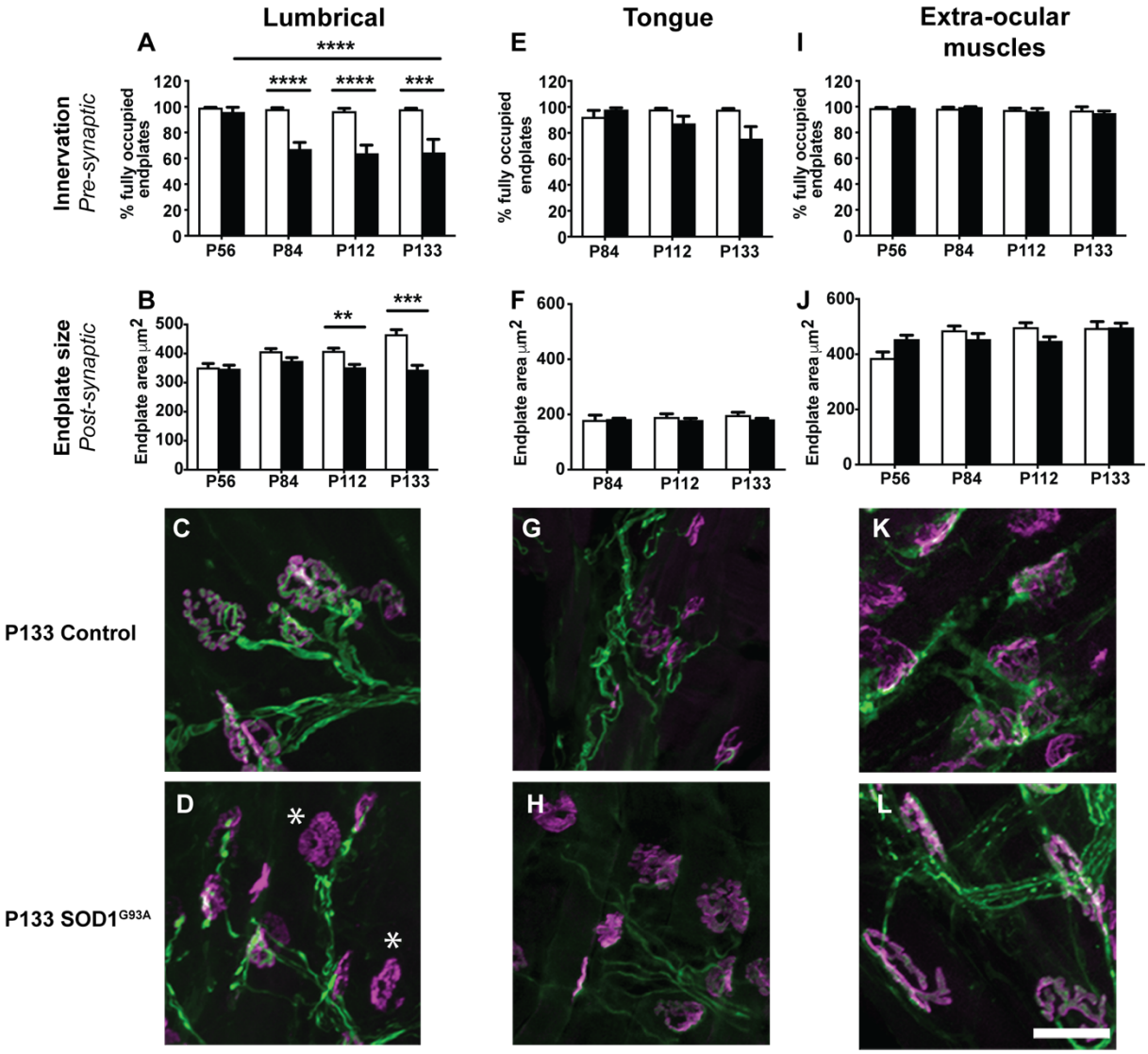

Figure 3. Denervation and endplate shrinkage pathology in three muscle groups of SOD1^{G93A} ALS mice. A. Percentage of fully innervated NMJs in lumbrical (hind limb) muscles. The ALS mice show a loss of innervation as of P84. **B.** Average endplate area in lumbrical muscles. Endplates show shrinkage only as of P112, after NMJ innervation has been lost. **C, D.** Representative micrographs of lumbrical NMJs at P133 in ALS mice and controls. **E.** Percentage of fully innervated NMJs in tongues. No significant denervation is observed up to P133 in ALS mice. **F.** Average endplate area in tongue muscles. No shrinkage is observed at any time point. Also note that tongue NMJs are less than half the size even in control mice compared to lumbrical or extraocular NMJs. **G, H.** Representative micrographs of NMJs in tongue muscles in control and ALS mice. **I.** Percentage of fully innervated NMJs in extraocular muscle. No denervation is seen in extraocular muscles of the SOD1^{G93A} mice. **J.** Endplate area of extraocular muscle NMJs. No shrinkage is present in these muscles. **K, L.** Representative micrographs showing NMJs in extraocular muscle. ** $p < 0.01$, *** $p < 0.001$, **** $p < 0.0001$. Scale bar: **L:** 40 µm, also applies to C, D, G, H and K.

4.1.2 Pre- and postsynaptic pathologies occur in parallel in the SMNΔ7 model of SMA

In the SMA model, NMJ denervation was observed only in lumbrical muscles, and only at the latest P14 time point (Fig. 4A). This is late, given the observable symptoms in the mice as of P5-6. Therefore, we looked at an additional neuromuscular pathology: neurofilament (NF) accumulation at the NMJ (Cifuentes-Diaz et al., 2002), thought to impair synaptic transmission before denervation occurs. We observed a strong increase in NF accumulation as of P10, again exclusively in the lumbricals. We did not observe this in the ALS model. This indicates that presynaptic dysfunction separate from denervation is part of SMA pathology.
Interestingly, a decrease in endplate size was present at P10 (Fig. 4B), before any observable denervation. In addition, endplate maturation, as determined by the number of perforations within the endplate, was delayed in SMA mice already at P10. Additionally, taking the NF accumulation into account, starting at P10, this reveals that pre- and postsynaptic pathology in SMA mice occur at the same time, unlike in ALS.

No denervation and shrinkage were observed in tongue muscles (Fig. 4E, F) and extraocular muscles (Fig. 4I, J). The exception is that from P10 to P14, extraocular NMJs do not grow anymore in the SMA mice, unlike in the controls. This likely due to a general lack of growth in the SMA mice, as they are much smaller than their littermates at this time point. NMJs reach their maximum size between P10 and P14 in the SMA mice. This plateau only appears in the extraocular NMJs, because, compared to the other muscle groups NMJs are biggest in this muscle group.

Taken together, we validated the resistance of oculomotor neurons to degeneration both in the $SOD1^{G93A}$ mouse model of ALS and the SMNΔ7 model of SMA, by demonstrating that these neurons retained NMJ innervation until late stages of disease. Furthermore, we showed a temporal difference in the sequence of events between ALS and SMA. Whereas in the ALS model motor neuron denervation preceded shrinkage of the postsynaptic endplate on the muscle, these events occurred simultaneously in SMA. This implies that motor neuron-intrinsic processes contribute more strongly to the pathophysiology of ALS, while in SMA processes in both motor neurons and muscle appear to simultaneously contribute to pathology. Moreover, endplates did not mature at the same rate in vulnerable lumbrical muscles in the SMA model as they did in controls, implying a developmental delay.

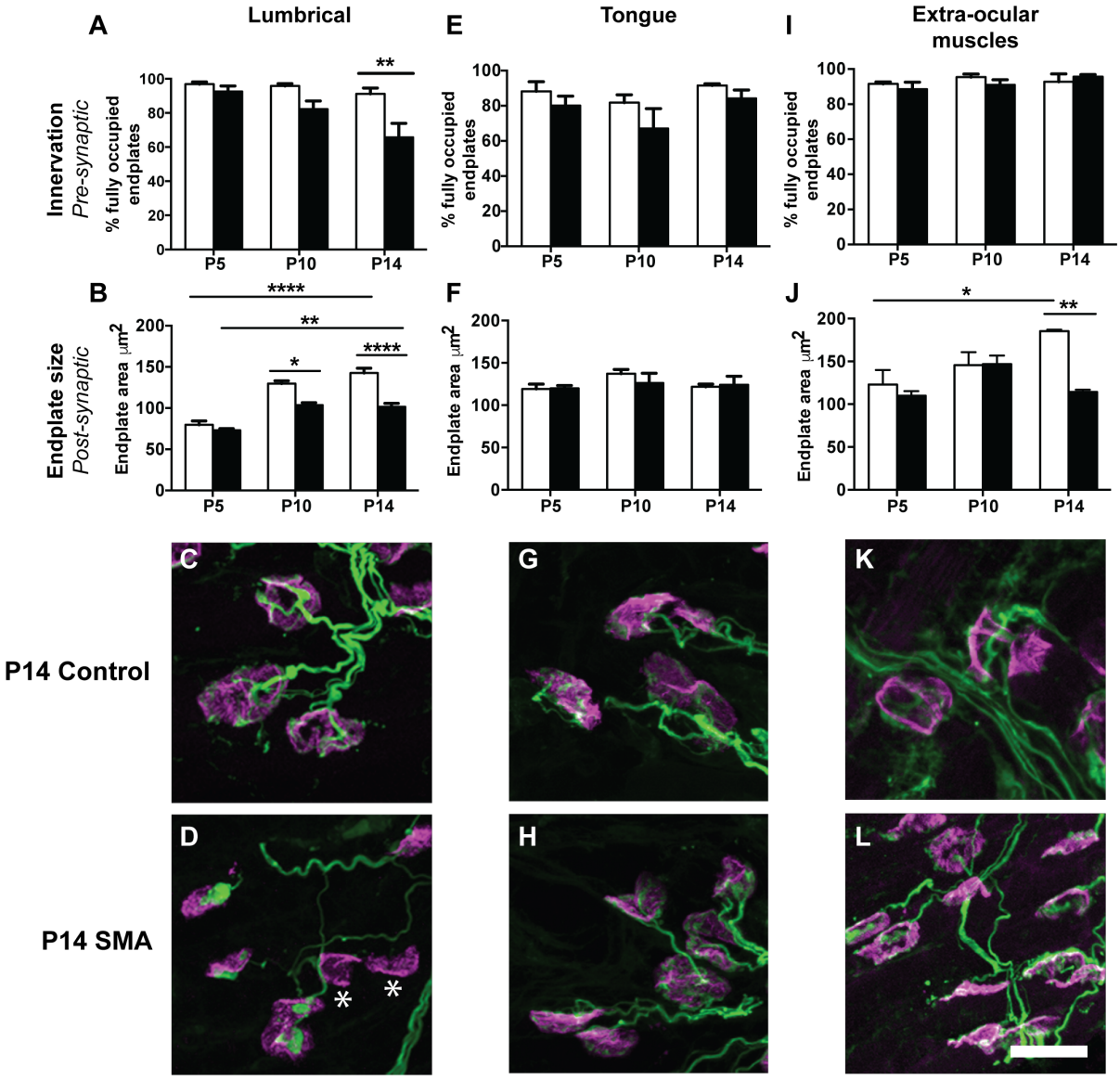

Figure 4. Denervation and endplate shrinkage pathology in three muscle groups of SMNΔ7 SMA mice. A. Percentage of innervated NMJs in lumbrical muscles. The SMA mice show decreased innervation only at P14. **B.** Average endplate area in lumbrical muscles. Endplates show shrinkage already from P10, before NMJ innervation is lost. **C, D.** Representative micrographs of lumbrical NMJs at P14 in SMA mice and controls. **E.** Percentage of fully innervated NMJs in tongues. No significant denervation is observed up to P14. **F.** Average endplate area in tongue muscles. No shrinkage is observed at any time point. **G, H.** Representative micrographs of NMJs in tongue muscles in control. **I.** Percentage of fully innervated NMJs in extraocular muscle. No denervation is seen in extraocular muscles at any time point. **J.** Endplate area of extraocular muscle NMJs. No shrinkage is present in these muscles, except at P14. However, this is likely rather a lack of growth, as SMA mice are generally much smaller than their littermates at this age. **K, L.** Representative micrographs showing NMJs in extraocular muscle. * $p < 0.05$, ** $p < 0.01$, *** $p < 0.001$, **** $p < 0.0001$. Scale bar: **L:** 40 µm, also applies to C, D, G, H and K.

4.2 PAPER II: LCM-SEQ REVEALS UNIQUE TRANSCRIPTIONAL ADAPTATION MECHANISMS OF RESISTANT NEURONS IN SPINAL MUSCULAR ATROPHY

With oculomotor resistance being maintained in the SMNΔ7 mouse model of SMA, we sought to uncover pathways responsible for the relative susceptibility and resistance of these motor neurons in disease. Given the strong role of the SMN protein in the assembly of the spliceosomal machinery, it is highly relevant to investigate transcriptomic dysregulation as it might represent targetable early disease processes. Therefore, we conducted a large-scale transcriptomic study to map gene regulation in resistant and vulnerable motor neuron pools in this model. Several groups of motor neurons were studied: vulnerable spinal and facial motor neurons (CN7), resistant oculomotor (CN3/4) and hypoglossal motor neurons (CN12) and resistant visceral motor neurons (vagus nerve, CN10). In addition, neurons from the red nucleus were included as a non-motor neuron control.

To examine these specific cells in isolation, we employed laser capture microdissection (LCM) coupled with RNA sequencing (LCM-seq, Fig. 5). LCM is a powerful tool that allows tissue dissection at microscopic levels, thereby increasing the power of RNA-sequencing of post-mortem tissue by having highly pure fractions of individual cells of interest. Our lab has demonstrated that LCM-seq can be performed down to the level of single isolated cells, when coupled with the Smart-seq2 protocol for cDNA library preparation (Nichterwitz et al., 2016, 2018; Picelli et al., 2013). While the technique has a drawback in that due to 3'-bias of transcripts it is not optimised to investigate splicing differences, it is still highly accurate for gene-level transcriptomic data.

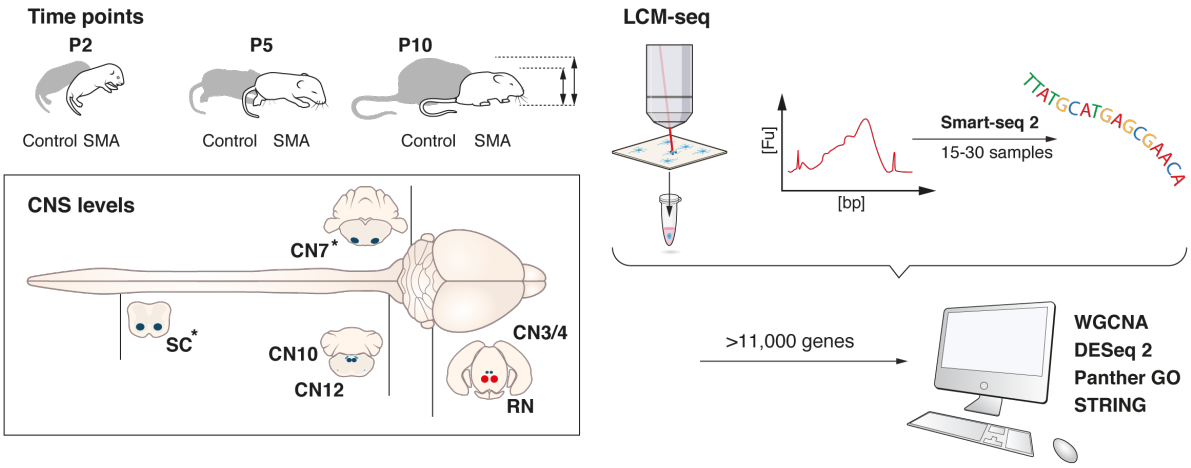

Fig 5. Overview of the LCM-seq procedure. Tissue is collected from the mice and sectioned in a cryostat. Then at the LCM-microscope the cells are isolated and subsequently cDNA libraries are made for RNA-sequencing.

In this manuscript, we collected pools of up to 120 cells per motor nucleus to gain information on the general transcriptome differences between nuclei and pinpoint patterns related to selective resistance or vulnerability across motor neuron pools. Neurons were collected at 3 different ages of the mice. We selected P2 (pre-symptomatic), P5 (early symptomatic) and P10 (late symptomatic) time points to understand the dynamics of the transcriptome in resilient and vulnerable neurons.

4.2.1 Transcriptomic changes in SMA mice are not confounded by a developmental deficit

To assess whether disease-related changes were confounded by age-related changes, weighted gene correlation network analysis (WGCNA) was performed, and gene sets were isolated that correlated with time (i.e. either overall increasing or decreasing in expression from P2 to P10). Gene ontology (GO) analysis revealed an enrichment of the term 'development' among these genes. Principal component analysis based on only these 'GO-developmental' genes did not clearly distinguish SMA from control samples at P2 and P5, and only slightly at P10. However, at P10 the mice are highly symptomatic, and segregation here is likely driven by ongoing disease mechanisms. Together, this shows that gene expression differences that naturally occur over time during development do not differ strongly between SMA and control mice. This implies that at the transcriptional level the SMA mice are not in another (delayed) developmental phase.

Furthermore, we analysed the progressive development of NMJs to exclude a peripheral developmental phenotype. Single NMJs at P0 are poly-innervated by multiple motor axons simultaneously. These are pruned back during the first 2 postnatal weeks, until there is only a single axon remaining. Also post-synaptic endplate densities undergo progressive change. Initially they appear as homogenous plaques, but they gain perforations as they take on a more complex morphology in the first 2 postnatal weeks. We used the number of poly-innervations (Fig. 6A) and endplate perforations (Fig. 6C) as measures for developmental maturity. Based on these traits, SMA mice show no overt phenotype up to P10 in extra-ocular muscles (innervated by CN3/4), tongue (innervated by CN12) and lumbrical muscles (innervated by lumbar spinal motor neurons) for either poly-innervation (Fig. 6B) and endplate perforations (Fig. 6D). Only at P14, the humane terminal endpoint for these mice, the lumbrical muscles in SMA mice show deterioration and a severe lack of complex morphology compared to control mice.

Combined, this gene expression data coupled with the peripheral NMJ analysis demonstrates that the disease process in SMA mice are unlikely to be confounded by a developmental deficit.

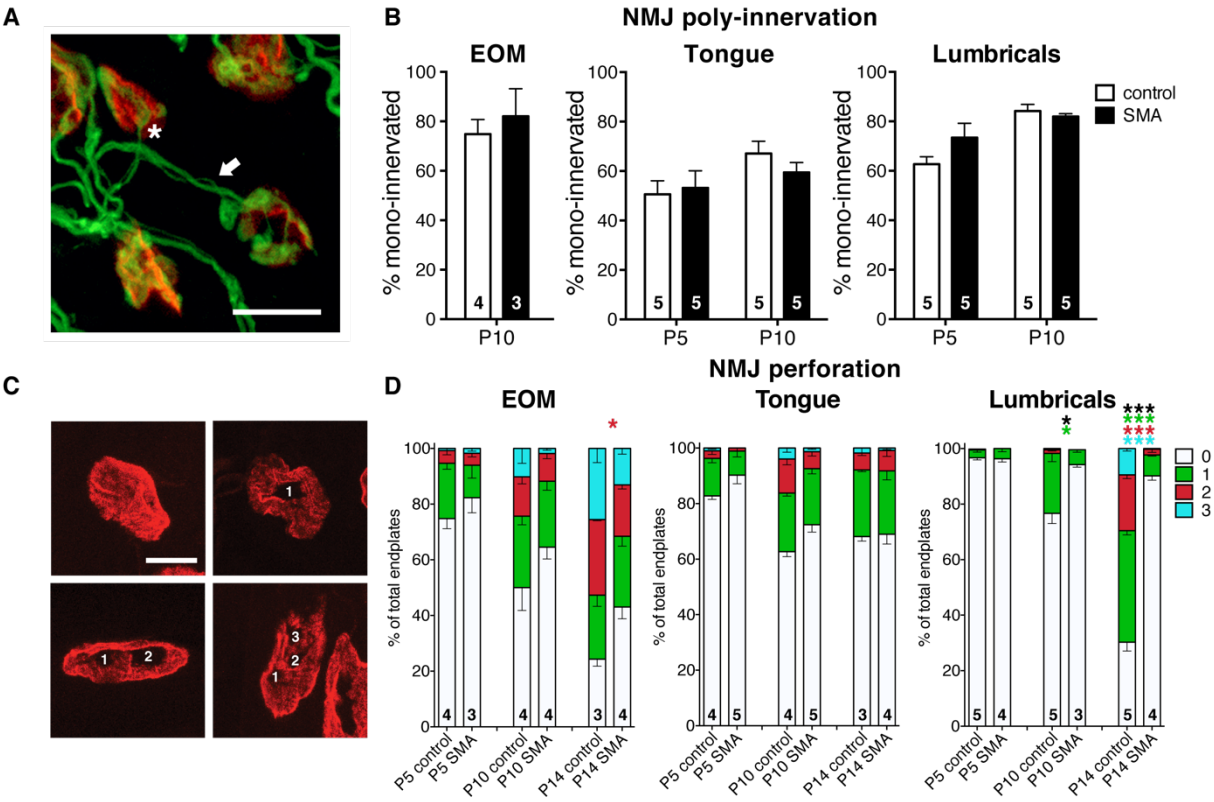

Figure 6. Analysis of development of the motor system in SMA mice. A. Micrograph of an NMJ showing poly-innervation, where multiple axons innervate one single endplate. **B.** Percentages of mono-innervated, and thus most mature, NMJs in three muscle groups in the SMA mice. No differences are observed up to P10 with regards to poly-innervation. **C.** Micrograph of endplates in various degrees of maturation, as signified by their number of perforations. **D.** Average percentage of endplates presenting with 0, 1, 2 or 3 perforations in three muscle groups. Only at P14 do SMA mice show a difference from controls, likely due to disease processes disrupting the NMJs. Scale bars: **A** and **C**: 10 μm.

4.2.2 Somatic motor neurons have both common and unique responses to loss of Smn

Comparisons between SMA and control motor neurons at every time point for every cell type revealed an early change in gene regulation in mainly CN3/4 and CN12 at the early stage (P2), with the highest number of differentially expressed genes (DEGs) at this time point. At P10, however, CN3/4, CN7 and spinal motor neurons had the largest dysregulation of genes, as the number of DEGs per cell type increased from P2. Very few DEGs were detected in the non-disease affected red nucleus neurons, as well as visceral CN10 motor neurons (Fig. 7A).

Surprisingly, also hypoglossal CN12 neurons showed fewer DEGs than the other somatic motor neuron pools, both resistant and vulnerable. When combining DEGs of all 3 time points within each cell type it became evident that, although there is some overlap, most differential gene regulation is unique to each neuron type, implying that neurons cope with Smn-deficiency in various ways (Fig. 7B).

Taking a step back from individual genes, we once again used WGCNA to identify a gene cluster comprised of 251 genes that was correlated to disease in the somatic motor neuron groups, across all time points (Fig. 7C). Principal component analysis based on these genes was unable to segregate SMA from control samples in the non-affected CN10 and red nucleus neurons. This indicates that this module of genes is specific to somatic motor neurons, irrespective of their relative vulnerability.

Among the GO-terms that were enriched in the genes of this module were p53-induced signalling and apoptosis-related signalling (Fig. 7D). Accordingly, GO-term analysis also showed similar enrichment for p53- and apoptosis-related terms when using DEGs as input between control and SMA at P10 in CN3/4, CN7 and spinal cord. Interestingly, even at P5 spinal cord DEGs show an enrichment for these terms.

This indicates that we have uncovered a common disease signature within somatic motor neurons, a gene regulation that is not initiated in red nucleus or CN10 neurons.

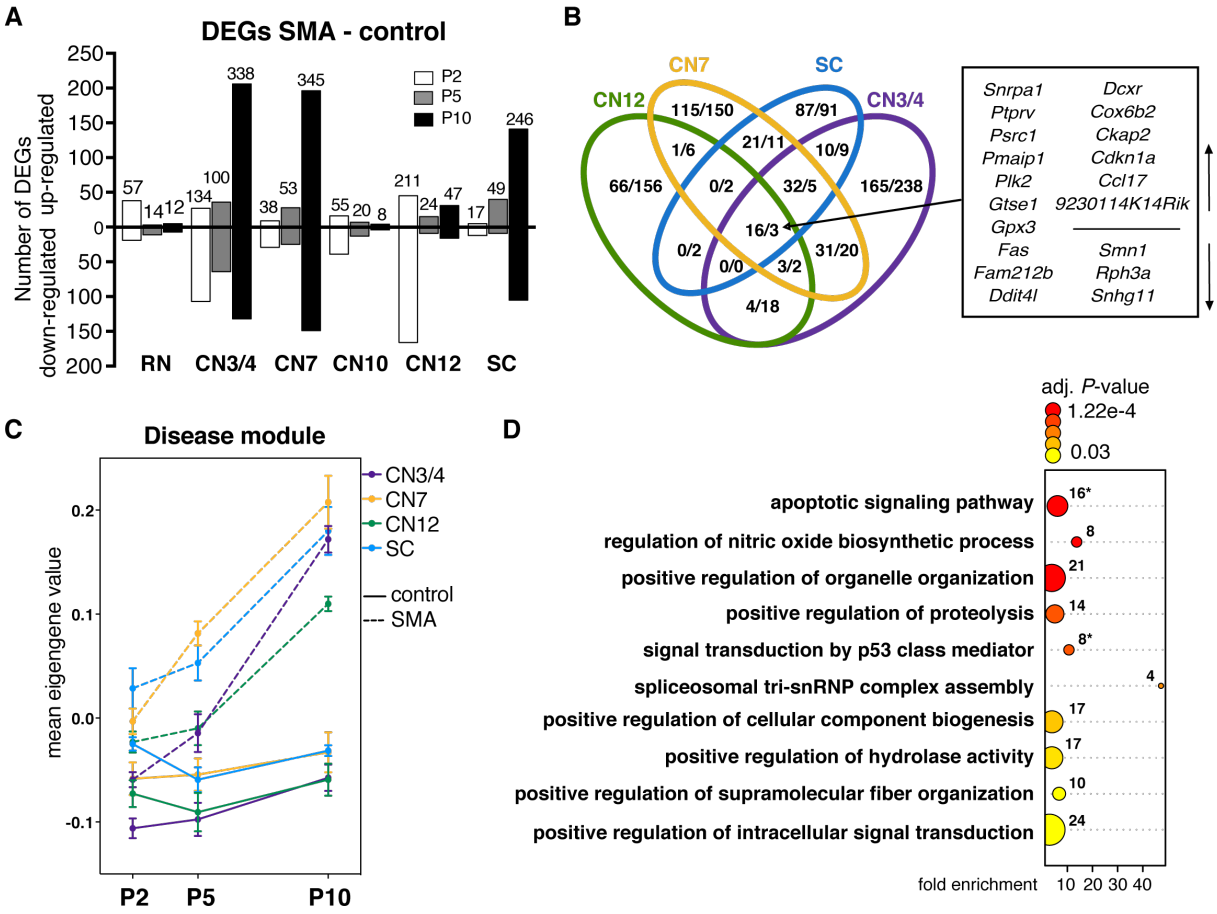

Figure 7. Analysis of gene expression changes in the SMNΔ7 mouse model. A. Number of differentially expressed genes (DEGs) between control and SMA for each nucleus and time point. Bar above and below zero represents up and downregulated genes. The number represents the total number of DEGs. **B.** Venn-diagram of overlapping DEGs between nuclei, with all time points combined. x/y represents x commonly upregulated and y commonly downregulated genes in SMA. **C.** Mean eigengene value of the WGCNA-identified disease module for all nuclei and time points. This shows the expression of genes in the disease module increases only in the somatic motor neurons in the SMA mice. **D.** Selected GO terms for the genes in the disease module (C).

4.2.3 Resistant oculomotor neurons have a distinct transcriptional signature that could confer resistance

Intriguingly, resistant CN3/4 also showed upregulation of apoptotic pathways as well, albeit at later stages than in spinal motor neurons. Subsequently, this group was compared more extensively to the vulnerable spinal motor neurons. STRING analysis for protein-protein interactions showed that of the DEGs at P10 in CN3/4, 46.7% could be embedded in an interconnected interaction network. For spinal motor neurons 35.5% of the genes were interconnected, and spread over two networks. While both spinal cord and CN3/4 showed upregulation of DNA damage sensing and repair proteins (*Trp53* and *Polk*), CN3/4 showed a

specific upregulation of pro-survival factors such as *Pak4, Pak6, Gdf15* and *Chl1*. This was paralleled by a CN3/4-specific downregulation of the pro-apoptotic factors *Itpr1* and *Dffa*.

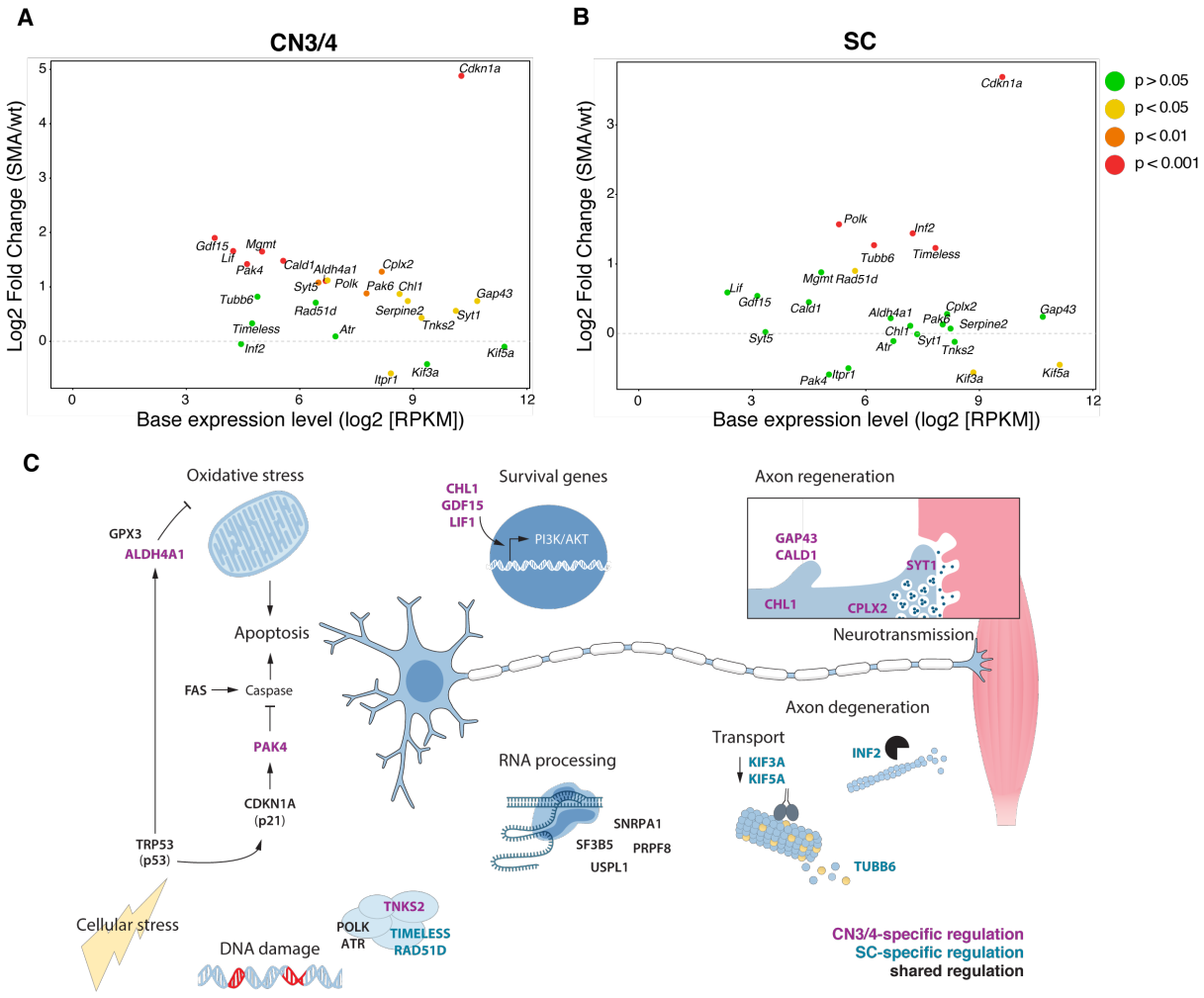

Figure 8. Overview of key genes and their associated functions identified through our LCM-seq analysis. **A.** Key genes dysregulated in oculomotor neurons between SMA and control. **B.** Key genes dysregulated in spinal motor neurons between SMA and control. Colour represents significance value. **C.** Schematic of pathways that some of the key genes in (A) and (B) are involved in that may explain their possible conferred resistance or vulnerability.

Moreover, CN3/4 neurons showed an enrichment of synaptic proteins in disease that are linked to improved neurotransmission (*Syt1, Syt5* and *Cplx2),* as well as factors positively influencing neurite outgrowth and re-innervation *(Gap43, Chl1, Cald1* and *Serpine2*) (Fig. 8A, C). Spinal motor neurons, on the other hand, showed specific enrichment for cytoskeleton destabilising proteins (*Inf2* and *Tubb6*), as well as decreased mRNA levels of key motor proteins (*Kif3a* and *Kif5a*) (Fig. 8B, C).

Finally, we selected *Gdf15* as a candidate to confirm our hypothesis that factors upregulated in resilient neurons can protect more vulnerable neurons. Toward this goal we

generated vulnerable human spinal motor neurons from iPSCs (Fig. 9A) and cultured them in a trophic factor deprivation assay, leading to neuronal death over time (Fig. 9B). Exposing the neurons to different concentrations of GDF15 improved their survival in a dose-dependent manner in all but the last time point measured (Fig. 9C-F).

Taken together, this shows that the resistant and vulnerable somatic motor neuron populations have distinct mechanisms to cope with Smn-deficiency, resulting in either a pro-survival cascade in CN3/4 or a negative cascade leading to neurodegeneration in spinal motor neurons. We also show that a pro-survival factor, *Gdf15*, that was upregulated in resistant CN3/4 motor neurons in SMA has the potential to improve survival of spinal motor neurons *in vitro*.

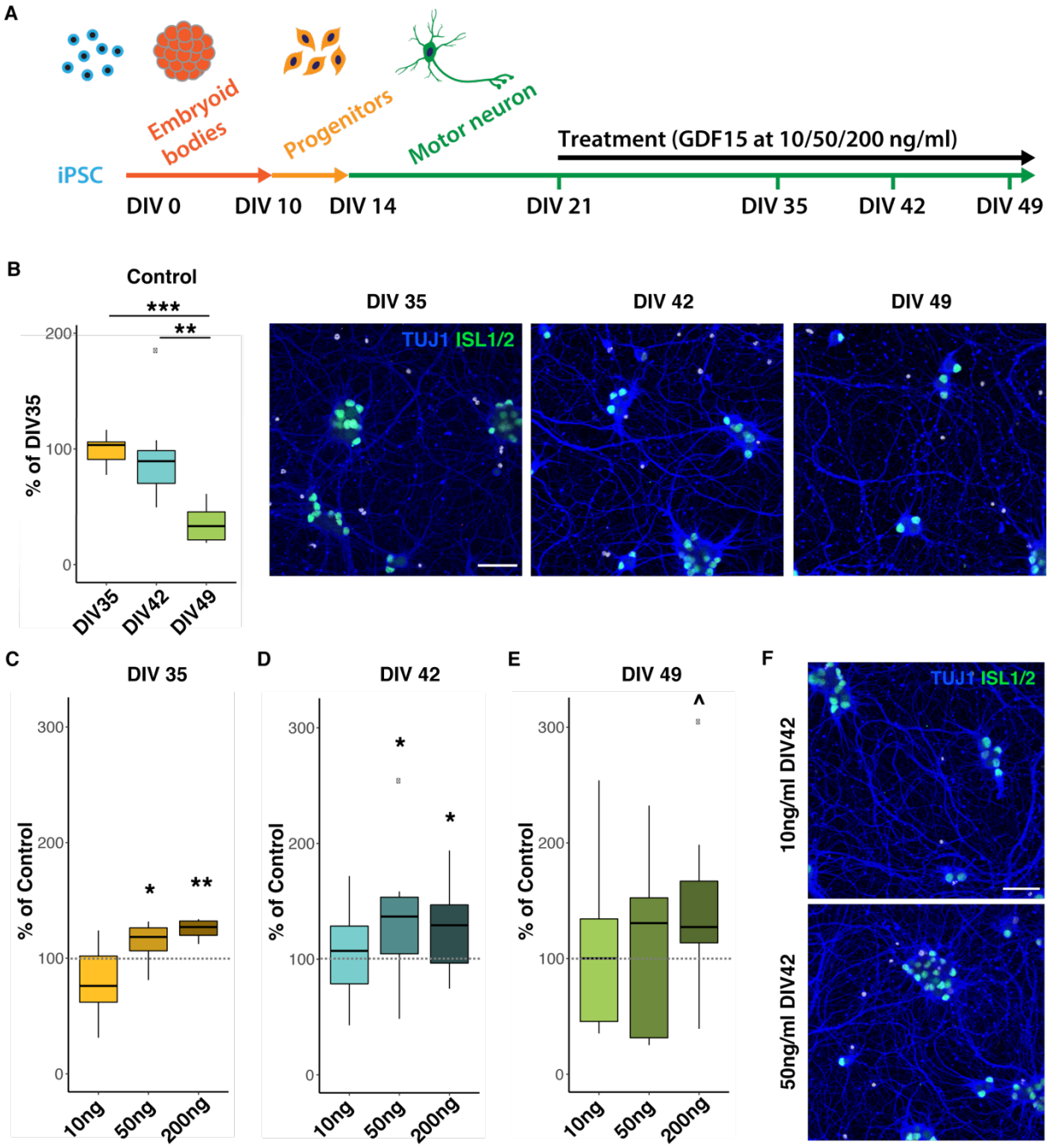

Figure 9. GDF15, a factor enriched in oculomotor neurons in SMA, can protect vulnerable spinal motor neurons. A. Schematic overview of the experimental procedures. GDF15 was added from day in vitro (DIV) 21 forwards and cells were analysed at DIV 35, 42 and 49. **B.** Untreated motor neurons degenerate over time, as also shown in the representative micrograph images. **C-E.** Percent of surviving motor neurons normalised to the untreated condition. GDF15 at both 50 and 200 ng/ml resulted in significantly improved survival at DIV 35 and 42. **F.** Representative images at DIV42 showing the enhanced survival of motor neurons cultured in the presence of GDF15 at 50 ng/ml compared to 10 ng/ml. Scale bars: **B** and **F**: 50 µm. * $p < 0.05$, ** $p < 0.01$, *** $p < 0.001$.

4.3 PAPER III: MODELING MOTOR NEURON RESILIENCE IN ALS USING STEM CELLS

We sought to utilise the potential of oculomotor resistance in ALS as a discovery tool and generate an *in vitro* model of this selective vulnerability. This would allow for an additional angle to uncover and investigate candidate genes and pathways responsible for the protection of oculomotor neurons in ALS.

4.3.1 Mouse embryonic stem cells can be differentiated into oculomotor neurons

Oculomotor neurons are specified in the ventral midbrain by the combined actions of the morphogens sonic hedgehog (Shh), Fgf8 and Wnt. These signals then trigger the expression of transcription factors such as *Phox2a* and *Phox2b*, that further specify and determine oculomotor neuron fate (Deng et al., 2011; Pattyn et al., 1997). To generate oculomotor neurons *in vitro*, we adapted a protocol involving the patterning of mouse ESCs by exposure to Shh and Fgf8, combined with an overexpression of *Phox2a* (Mong et al., 2014). The overexpression was driven by the nestin-promoter, ensuring a pan-neural progenitor activation. In parallel, we utilised an established protocol to generate spinal motor neurons (Wichterle et al., 2002), based on patterning with Shh and retinoic acid.

Utilising overexpression of *Phox2a* (combined with *Ngn2* and *Isl1*) has been used before to generate midbrain motor neurons in the absence of the external patterning factors Shh and Fgf8 (Mazzoni et al., 2013). However, microarray data from the 2013 study showed expression of *Mnx1* (Hb9), a marker that is classically absent in oculomotor neurons (Guidato et al., 2003). The exact brainstem neuronal population was not defined in this protocol, and it might have been a mix of oculomotor neurons along with motor neurons from other brainstem nuclei, such as trigeminal (CN5) or facial (CN7).

In our cultures, we showed, using immunocytochemistry, that half of the neurons in our oculomotor cultures expressed Isl1, an established marker for motor neurons at all anterior-posterior levels (Fig. 10A-C). Of these motor neurons, less than 10% expressed Mnx1. In contrast, in the spinal motor neuron cultures 60% of Isl1+ cells co-expressed Mnx1 (Fig. 10C).

To further validate the identity of our *in vitro* generated spinal and oculomotor neurons, we conducted a transcriptomic analysis on GFP-purified fractions of these cultures. Using an Hb9-

GFP line for spinal motor neurons and an *Isl1*-GFP line for oculomotor neurons (as they lack Hb9), we could isolate motor neurons from both subpopulations using flow sorting and perform bulk RNA sequencing.

This revealed that, as expected, classical neuronal markers were expressed, as well as specific combination of markers for the midbrain oculomotor neurons (*Isl1, Phox2a, Phox2b*) and spinal motor neurons (*Isl1, Mnx1*, *Lhx1, Lhx3, Olig1, Olig2*) (Fig. 10D). Furthermore, the differentially expressed genes between our purified spinal and oculomotor neurons could cleanly separate published RNA-sequencing data from laser-capture microdissected spinal- and oculomotor neurons of early post-natal and adult rodents (Hedlund et al., 2010; Kaplan et al., 2014) (Fig. 10E, F).

We performed an unbiased gene clustering approach using the *Pathway and Gene Set Overdispersion Analysis* (PAGODA) algorithm to elucidate gene sets specific to either our entire midbrain and spinal cord cultures (including GFP-positive motor neurons as well as GFP-negative cells), or to the respective GFP-positive motor neuron groups only (Fig. 10G, H). This way, we were able to separate the differentially expressed genes between spinal motor neurons and oculomotor neurons (green circles in Fig. 10G, oculomotor enriched, and H, spinal motor neuron enriched) in two groups: genes that reflected a difference between the two cultures (midbrain / spinal cord) and those genes that were specific to oculomotor neurons or spinal motor neurons. This analysis revealed that some of the differentially expressed genes only reflected differences between midbrain and spinal cord and the anterior-posterior axis (e.g. *Phox2a* and *Hox*-genes, blue circles in Fig. 10G, H). When pinpointing the motor neuron-specific genes (orange circles in Fig. 10G, H), we confirmed, among others, the specificity of *Mnx1* for spinal motor neurons but not other cells in our 'spinal' cultures, while identifying several genes including *Eya1, Eya2, Sema6d* and *Rgs4* to be specific to oculomotor neurons, rather than the whole midbrain.

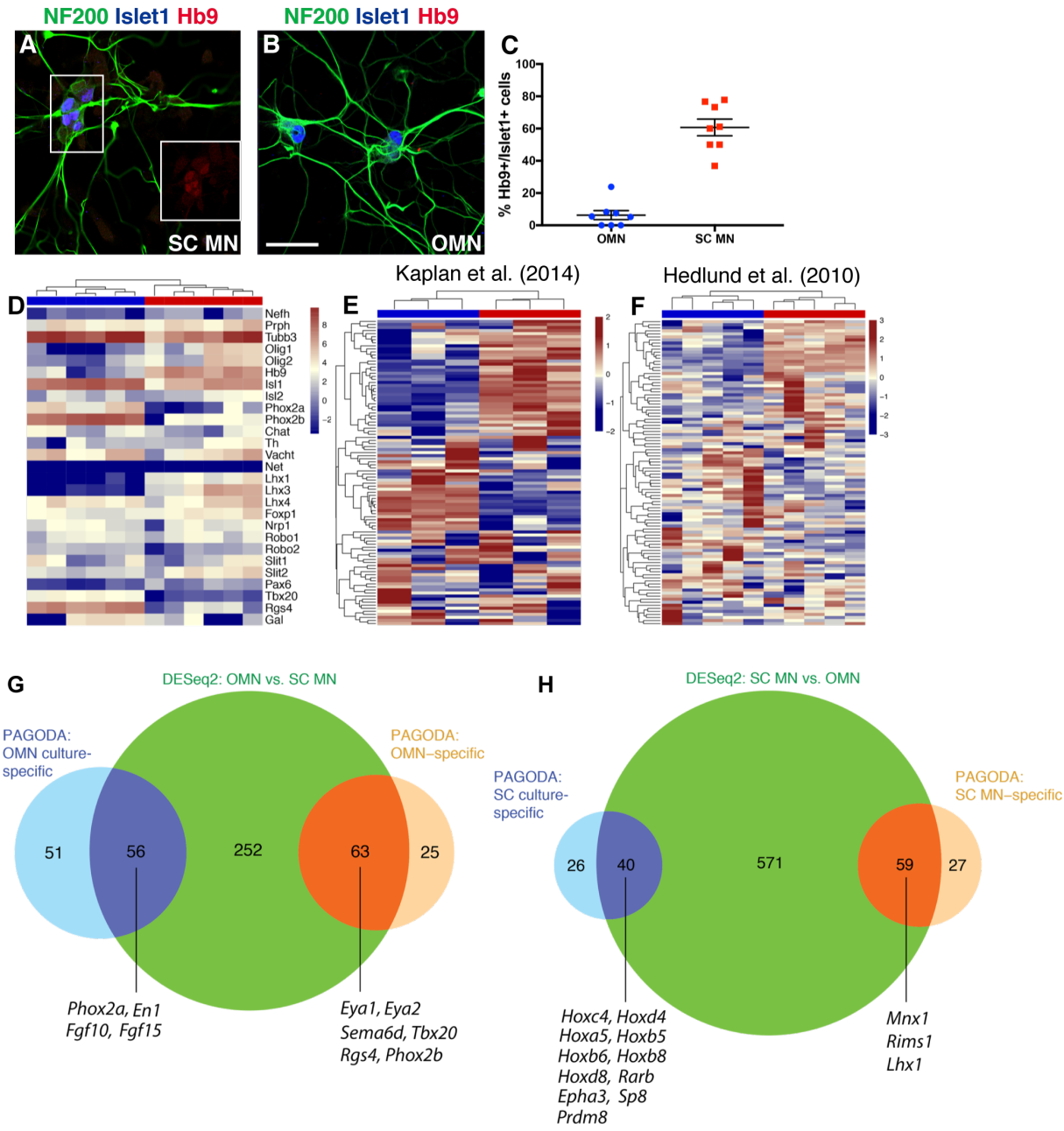

Figure 10: *In vitro* derived oculomotor neurons resemble their *in vivo* counterparts. A,B. Micrographs showing immunocytochemical staining of motor neurons generated with the spinal and oculomotor protocols. Spinal motor neurons express Hb9 and Islet1, while our *in vitro* generated oculomotor neurons lack Hb9 expression. **C.** Quantification showing the lack of Hb9-expression in the oculomotor neurons. **D.** Selection of classical (motor) neuronal marker genes, as well as genes that are more specific to oculomotor or spinal motor neurons. **E, F.** Using the top 100 differentially expressed genes between our oculomotor and spinal motor neurons, we could separate microarray data from early post-natal (E) and adult (F) *in vivo* rodent oculomotor and spinal motor neurons. **G, H.** Visualisation of the pathway and geneset overdispersion analysis (PAGODA) on all our samples, i.e. GFP-sorted motor neurons from both spinal and oculomotor cultures, as well as GFP-negative cells from either culture. Scale bar: **B**: 60 µm, also applies to A.

4.3.2 *In vitro* oculomotor neurons are more resilient during excitotoxicity

One of the downstream events in ALS is thought to be glutamate-driven excitotoxicity. Therefore, we exposed our two types of motor neurons to excitotoxic stress using kainic acid, an agonist of glutamate receptors. In the face of this stress, oculomotor neurons survived better than spinal motor neurons (Fig. 11A-C). In addition, oculomotor neurons did not change the length and branching of their processes, indicating that no axonal or dendritic degeneration was occurring.

To explain this resistance, we turned again to the RNA sequencing data. Here we found that oculomotor neurons have an increased expression of calcium-buffering transcripts such as *Cald1*, *Esyt1* and *Camk2a*. A higher calcium-buffering capacity has previously been mentioned as one factor explaining oculomotor neuron resistance in ALS (Vanselow and Keller, 2000). We also observed increased levels of Akt signalling, as exemplified by higher expression levels of *Akt1* and *Akt3*, and higher protein levels of phosphorylated Akt (Fig. 11D-F) and β-catenin (Fig. 11 G-I). Our group has previously shown the importance of pro-survival AKT-signalling in motor neuron resilience after treatment with insulin-like growth factor 2 (IGF2), a factor that was discovered based on an *in vivo* transcriptomic screen between laser-capture microdissected spinal and oculomotor neurons in rats (Allodi and Hedlund, 2014; Hedlund et al., 2010).

We subsequently showed that AKT signalling is also elevated in human post-mortem laser-capture microdissected oculomotor neurons compared to spinal motor neurons (Fig. 11J). However, this was not the case in motor neurons from Onuf's nucleus, a small group of neurons in the sacral spinal cord that are also resistant to degeneration in ALS (Mannen et al., 1982). This implies that the higher levels of pro-survival Akt signalling are an oculomotor-specific protection mechanism (Fig. 11K).

In conclusion, this paper demonstrated that the resistance of the oculomotor system observed in ALS patients and rodent models of disease can also be recapitulated *in vitro,* and that these stem-cell derived motor neurons can serve as tools to uncover new protective factors in oculomotor neurons that hold up in human post-mortem tissue.

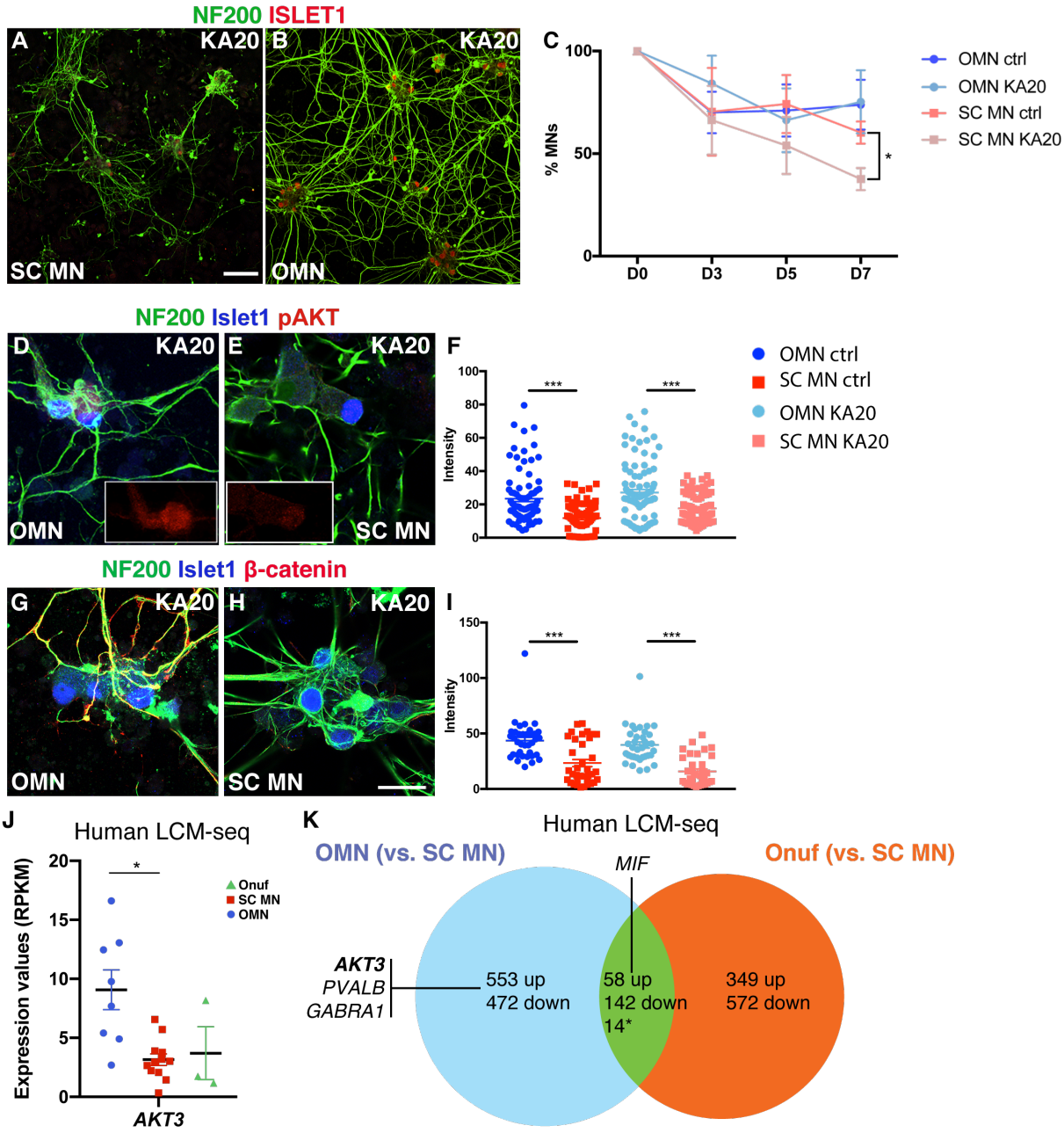

Figure 11: Oculomotor neurons are more resistant to excitotoxicity and have increased pro-survival Akt-signalling. A,B. Micrographs showing spinal and oculomotor neuron cultures after 7 days of exposure to 20 µM kainic acid. **C.** Quantification of surviving motor neurons, by islet-1 staining. Oculomotor neurons survive better in the face of excitotoxicity than spinal motor neurons. **D, E.** Images showing increased staining for phosphorylated Akt in oculomotor neurons compared to spinal motor neurons. **F.** Quantification of phosphorylated Akt staining. Oculomotor neurons maintain phosphorylated Akt in excitotoxic conditions. **G, H.** Images showing increased presence of beta-catenin in oculomotor neurons compared to spinal motor neurons. **I.** Quantification of beta-catenin staining. Again, oculomotor neurons maintain beta-catenin during excitotoxicity. **J.** Expression levels of *AKT3* in human spinal motor neurons, oculomotor neurons and neurons of Onuf's nucleus. **K.** Venn diagram of differentially expressed genes between oculomotor neurons and Onuf's nucleus neurons, both compared to spinal cord motor neurons. Scale bars: **A**: 100 µm, also applies to B. **H**: 60 µm, also applies to D, E and G.

4.4 PAPER IV: AXON-SEQ DECODES THE MOTOR AXON TRANSCRIPTOME AND ITS MODULATION IN RESPONSE TO ALS

In *Paper IV*, we shifted our focus to understanding why specifically the distal axon is a highly vulnerable compartment of motor neurons. Towards this goal we developed a method called Axon-Seq, to allow the investigation of the axonal transcriptome separated from the somatic (cell body) transcriptome.

We generated spinal motor neurons from mouse ESCs (see section 3.1). Microfluidic culturing of these motor neurons was used to separate axons from somas (see section 3.2). To allow RNA-sequencing to be performed on single devices, concentration of the axonal lysate was combined with optimisation of the Smart-Seq2 protocol for library preparation. Together, we managed to generate cDNA libraries from single device axon preparations.

First, we assessed the overall size of the axonal transcriptome and found that the number of uniquely detected transcripts in axons was lower than in somas. Axons expressed on average around 5,000 transcripts, compared to 15-17,000 in somas (Fig. 12A). We also noticed that some axonal samples appeared to have an increased number of detected genes. Analysis of marker gene expression and unbiased clustering led us to the conclusion that these samples were likely contaminated with one or more cells that shifted the transcriptome entirely. We then proceeded to routinely and thoroughly check all samples for somatic contamination.

4.4.1 The axonal transcriptome contains mRNAs for essential cellular functions

Several hundred transcripts were enriched in the axonal compared to the somatic transcriptome. We found strong overrepresentation of transcripts encoding proteins for essential cellular functions, such as ribosomal subunits and components of the mitochondrial respiratory electron transport chain, even in only the top 25 most axon-enriched transcripts (Fig. 12B). This makes sense, as mitochondria can multiply by fission in axons (Amiri and Hollenbeck, 2008). However, they would need to locally build up their repertoire of proteins for energy production. Local translation of these mRNAs would allow for an energy and storage-efficient way of coping with this. Gene set enrichment analysis confirmed the enrichment of the complete respiratory electron transport pathways in axons (Fig. 12C). As for ribosomal subunits, we also detected essentially the entire pathway *Ribosome* enriched in axons (Fig. 12D). It was long unknown whether ribosomes can be created in axons, as the presence of their subunits at mRNA level would suggest. Ribosome biogenesis traditionally occurs in the nucleolus, where

rRNA and proteins come together and are assembled into the small and large components (reviewed in Peña et al., 2017). Subsequently, mRNAs are then shuttled into axons already loaded on polysomes, essentially carrying ribosomes along from the start (Crispino et al., 1997). Additionally, ribosome components (completed small and large subunits) can be transferred from adjacent glia, such as Schwann cells, into axons (Court et al., 2008). However, recently it was demonstrated that fully functional ribosomes can exchange subunits in axons, and local translation of these individual ribosome subunits might therefore benefit the local ribosomes by possibly extending their lifespan (Shigeoka et al., 2019).

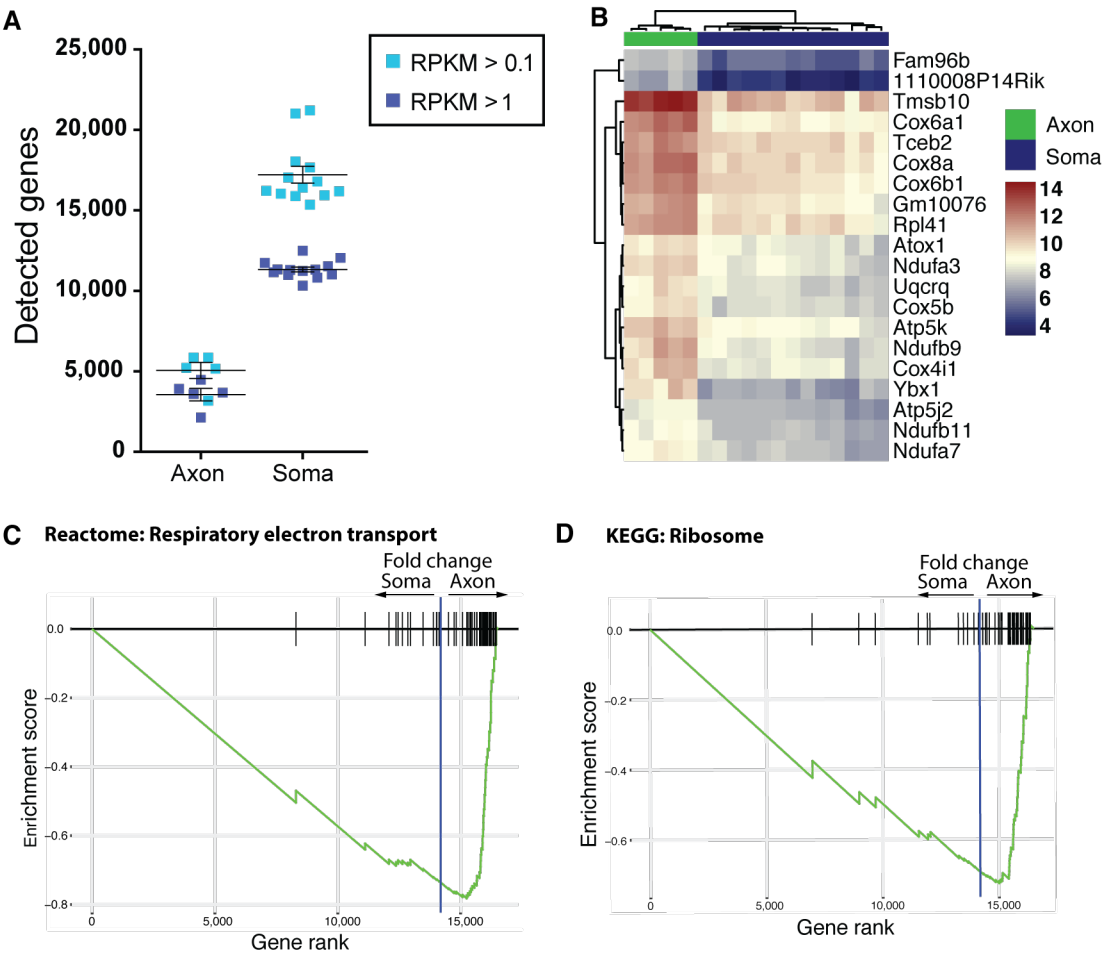

Figure 12. General characteristics of the motor axonal transcriptome. A. Number of uniquely detected genes in mouse ESC-derived motor neuron somas and axons. **B.** Heatmap showing the expression in axons and somas of the top 25 most axon-enriched genes. A large number of these genes encode mitochondrial proteins or ribosomal subunits. **C,D.** Gene set enrichment analysis plots showing an axonal enrichment of the pathways *respiratory electron transport* and *ribosome*.

An interesting finding was the localisation of a number of transcription factor mRNAs into axons. There is considerable overlap among the highest expressed transcription factors in somas and axons, even though they may perform entirely different functions in the different

subcellular compartments. As such, axons appear to have a repertoire of specific local transcription factors than possibly perform non-canonical roles rather than their classical role as a DNA-binding factor. For example, the most axon-enriched transcription factor, Ybx1, is known to have roles in alternative splicing and mRNA transport (Lyabin et al., 2014). It's very high expression in axons suggests that it has important local functions in mRNA metabolism. In addition, some of these transcription factors might be present locally as signalling/survival cues to other cells *in vivo*, e.g. Schwann cells or muscle. Along these lines, it was shown that targeted secretion of the homeobox family transcription factor Otx2 from one neuron to another can promote the receiver neuron's survival (Kim et al., 2016).

4.4.2 The ALS-causative SOD1^{G93A} mutation causes dysregulation in the axonal transcriptome

Finally, we set out to compare the axonal transcriptome of control mouse ESC-derived motor neurons with that of cells carrying the ALS-causative SOD1^{G93A} mutation. We detected high expression of the SOD1^{G93A} transgene both in cell bodies and in axons (Fig. 13A). This is not unexpected, as the endogenous *Sod1* also is highly expressed in axons (Fig. 13B). We uncovered dysregulation of 121 genes in the SOD1^{G93A} mutant motor axons (Fig. 13C). We cross-compared with published data of similar microfluidic chambers coupled with primary motor neurons, where *Smn* was knocked down as a model for SMA. We found 16 transcripts that were dysregulated across ALS and SMA, among which one commonly downregulated gene: *Nrp1*, a semaphorin co-receptor. These data indicate that loss of Nrp1 in axons could be an early disease phenotype across motor neuron diseases.

Among the dysregulated transcripts in the SOD1^{G93A} axons was also the RNA binding proteins *Rbpms*, which was shown to have a severe impact on axonal branching in retinal ganglion neurons (Hornberg et al., 2013), *Dbn1*, an actin-binding protein strongly involved in cytoskeleton remodelling in dendrites (Mizui et al., 2005) and *Nek1*, the function of which has not been entirely elucidated yet but whose loss of function causes ALS (Kenna et al., 2016).

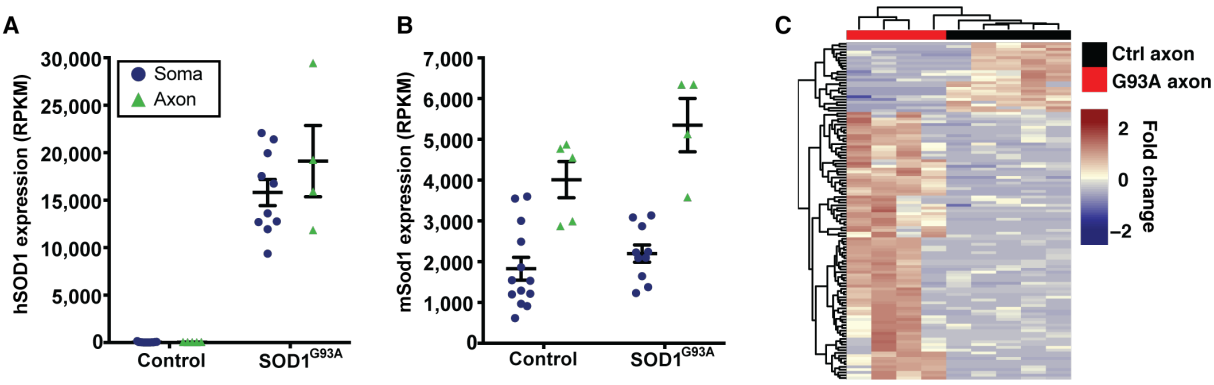

Figure 13. Mutant SOD1^{G93A} induces gene dysregulation in motor axons. A. Mutant human SOD1^{G93A} is expressed in both somas and axons at very high levels (> 10,000 RPKM). **B.** Endogenous mouse Sod1 is enriched in axons and expressed at lower levels than the human SOD1, but nonetheless high (1,000 – 5,000 RPKM). **C.** Heatmap showing the 121 dysregulated transcripts in the SOD1^{G93A} motor axons.

4.4.3 Cross-comparison with published data reveals a core axonal transcriptome

Throughout the paper we cross-compare our motor axon transcriptome with published datasets of axonal transcriptomes generated with RNA-sequencing. We compared to data from primary embryonic mouse motor neurons grown in microfluidic devices (Briese et al., 2016) or cell culture insets (Rotem et al., 2017), as well as sensory neuron axons from dorsal root ganglia grown on cell culture insets (Minis et al., 2014). One striking difference to us was that the number of detected genes in our axonal samples was drastically lower (~5,000) compared to all other datasets (10,000+) (Fig. 14A, B). In fact, all published datasets showed a similar number of transcripts in axons as in somas. We only observed these high numbers in axon samples that we deemed 'contaminated' with cell bodies. We then clustered all our samples, axons and somas, as well as those of published datasets together based on neuronal and glial marker genes (after remapping everything through the same pipeline to avoid mapping bias). Here we observed clustering of the published axon samples together with our soma samples, strengthening our suspicion of cellular contamination in the published axon samples (Fig. 14C). To analyse what made up the difference in number of detected genes, we ran GO-term analysis on the non-overlapping genes between the axonal samples in our data and the published datasets. This resulted in a clear enrichment of proliferative processes (*DNA-dependent DNA replication, Mitotic nuclear division*), confirming that these samples contained proliferative cells or fractions of cells in their axonal samples (Fig. 14A,B).

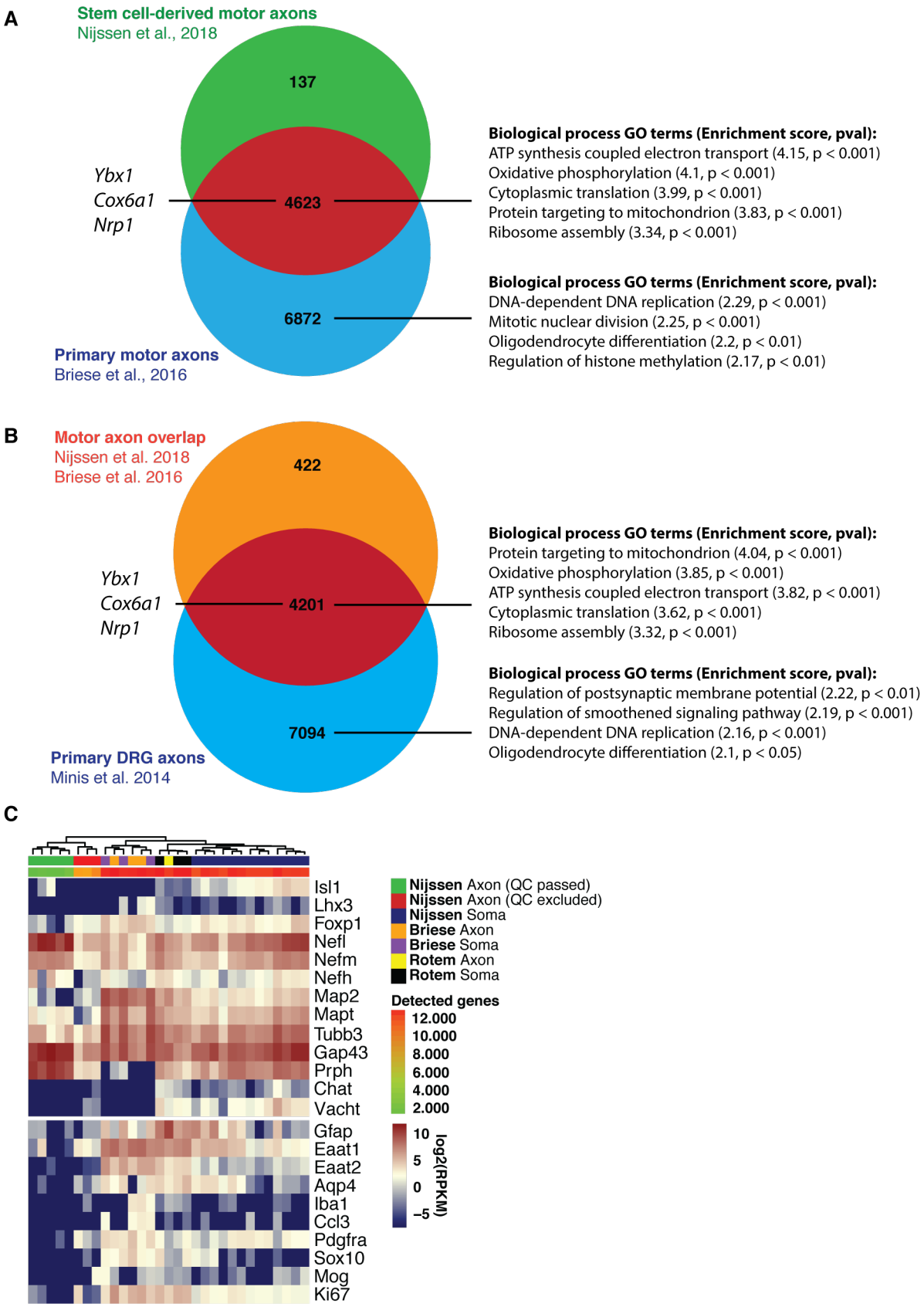

Figure 14. Cross-comparison with published axon transcriptomes reveals a core axonal mRNA pool. A. Venn diagram of genes detected in axons in this study and motor axons in Briese et al., 2016. Enriched GO-terms are shown on the side pertaining to the genes in the respective compartment. **B.** Comparison of the genes found to be overlapping in (A) with the axon-detected genes in DRG axons in Minis et al. (2014). Enriched GO-terms are

shown on the side pertaining to the genes in the respective compartment. **C.** Heatmap showing expression levels of marker genes in all published motor axon datasets (Briese et al., 2016; Rotem et al., 2017).

However, we did manage to pinpoint a core motor axon mRNA pool through cross-comparison with the embryonic primary motor neurons (Briese et al., 2015; Rotem et al., 2017), as well as a core peripheral axon pool through cross-comparison with the sensory neurons (Minis et al., 2014). These findings regarding sample purity were subsequently validated in a recent study looking at *in vivo* micro-dissected axons and cross-comparing with previous work including our study (Farias et al., 2020). Our dataset nearly completely overlapped with the core axon transcriptome reported in this study and subtle differences are likely due to developmental differences, e.g. myelination.

In conclusion, we have developed a technique called Axon-Seq that is highly sensitive to detect axonal mRNAs. Coupled with a bioinformatic control step we can isolate pure axonal samples without cross-contamination of other cell types. We identify a high abundance of ribosomal and mitochondrial proteins among the axonal transcripts, in line with their essential functions in the neuron, as well as transcription factors, an exciting avenue for further research as they must perform a non-canonical function in axons. We show dysregulation of the axonal transcriptome in an ALS model based on the $SOD1^{G93A}$ mutation and through cross-comparison with published datasets we can highlight a core motor axonal transcript pool of just over 4,000 unique mRNAs.

4.5 PAPER V: MUTATIONS IN THE ALS-CAUSATIVE GENES FUS AND TDP-43 CAUSE DISTINCT DYSREGULATION OF SOMATIC AND AXONAL TRANSCRIPTOMES

In *Paper V* we furthered the microfluidic Axon-Seq platform that has been set up in *Paper IV* to investigate human iPSC-derived motor neurons carrying ALS-causative mutations in FUS and TDP-43. We adapted published protocols to generate a high proportion (~85%) mature spinal motor neurons from human iPSCs (see section 3.1). Next, we differentiated lines carrying homozygous FUS^{P525L}, TDP-43^{M337V} and FUS KO mutations into motor neurons to enable analysis of transcriptome dysregulation in somas and axons due to mutations in these RNA-binding proteins.

4.5.1 Cellular distribution of FUS and TDP-43 is altered between our iPSC-derived motor neurons

Firstly, however, we investigated the distribution of FUS and TDP-43 themselves in the motor neurons carrying the ALS mutations. We observed a reduction in nuclear FUS, as well as overt mislocalisation to the cytoplasm in the FUS^{P525L} line. This is expected, given that this mutation perturbs the nuclear localisation signal and effectively maintains FUS outside of the nucleus. Interestingly, also the TDP-43^{M337V} line displayed a reduction in nuclear FUS, but no cytoplasmic mislocalisation, indicating a crosstalk between the two proteins.

The TDP-43^{M337V} line also displayed a reduction in nuclear TDP-43 signal, but without mislocalisation to the cytoplasm. This mutation does not directly affect nuclear localisation, as it is located in the glycine-rich domain of TDP-43. Thus, this reduction is not directly caused by mislocalisation, but rather other processes that render the protein less detectable. RNA levels of TDP-43 were not altered, yet decreased translation efficiency remains a possibility. Alternatively, given that the TDP-43^{M337V} mutations renders the protein more prone to aggregate, it is tempting to think that aggregation of part of the TDP-43 pool renders the antibody epitope inaccessible. In the FUS^{P525L} line no alterations in TDP-43 distribution were observed.

In conclusion, this data shows that mutations in both FUS and TDP-43 have the capability to alter the nuclear levels of FUS, while nuclear TDP-43 levels are only altered by mutations in TDP-43 but not FUS. This makes sense, considering the lack of TDP-43 inclusion pathology in ALS caused by mutations in FUS (King et al., 2015). Vice versa, mislocalisation of FUS has

been observed in post-mortem tissue from patients with mutations in FUS, TDP-43, VCP or even sALS (Deng et al., 2010; Ikenaka et al., 2020; Tyzack et al., 2019).

4.5.2 The somatic transcriptome is dysregulated in motor neurons carrying mutations in FUS and TDP-43

Having established that our iPSC-derived motor neurons display ALS-like intracellular pathology, we then performed RNA-sequencing on the bulk cultures to investigate the transcriptomic alterations induced by the FUS and TDP-43 mutations. What we found was a largely distinct pattern of gene regulation between mutations (Fig. 15A). A set of 12 genes was commonly dysregulated between the FUS^{P525L} and $TDP\text{-}43^{M337V}$ mutant lines. Nine of these were downregulated in both, including galectin-1 (*LGALS1*) and the endosome recycling protein *RAB11FIP1*, responsible for integrin recycling at distal axonal tips (Eva et al., 2010). Its downregulation might exert a deleterious effect on axonal outgrowth and synaptic maintenance. Only one gene, *REG1A*, was commonly upregulated. Its encoded protein is known to induce regeneration in several somatic tissues, and its expression in neurons improves neurite outgrowth (Ba et al., 2011). In our lines, the upregulation of REG1A is possibly a compensatory mechanism to counter the loss of other important neuronal functions.

Two genes were dysregulated in opposite directions: *SLITRK4* and *USP51*. Both had increased expression in the FUS^{P525L} line compared to control, but lower expression in the $TDP\text{-}43^{M337V}$ line. In addition, 5 genes were dysregulated across our two ALS lines and the FUS KO line. Among these was *MAGEH1*, that interacts with the p75 neurotrophic receptor ($p75^{NTR}$) and has neuroprotective and anti-apoptotic effects in an *in vitro* model of frontotemporal dementia (Ehrlich et al., 2015). *MAGEH1*, similar to *SLITRK4* and *USP51*, also showed upregulation in the FUS^{P525L} line (as well as the FUS KO line), but downregulation in the $TDP\text{-}43^{M337V}$ motor neurons. Due to the comparison with the FUS KO line, this indicates that the dysregulation of *MAGEH1* is driven by the loss of nuclear FUS, while *SLITRK4* and *USP51* are likely dysregulated due to gain-of-function of the mutant FUS^{P525L}.

To gain a better overview of dysregulated processes in our motor neurons, we then performed gene set enrichment analysis. We found many pathways significantly regulated in our lines, with a larger proportion of overlap between them as with individual dysregulated genes. Again, this analysis allowed us to pinpoint pathways that were unique to either the $TDP\text{-}43^{M337V}$ or FUS^{P525L} mutation, common to both and/or driven by FUS loss of nuclear function.

In the TDP-43^{M337V} motor neurons, we identified pathways pertaining to neural cell-cell adhesion enriched, as well as pathways related to GABA-receptor activity and transport of sodium and chloride ions. Downregulated were metabolic pathways, such as *monosaccharide catabolic process* and *peptide metabolic process*, as well as the GO-term *mitochondrial matrix*. The FUS^{P525L} line showed unique upregulation of lysosomal pathways and *microtubule bundle formation*, while showing downregulation of splicing pathways and neurotrophic signalling.

Both lines showed common enrichment of transmembrane transport pathways of several classes of molecules, as well as *potassium ion transport*. The pathway *ribonucleoprotein complex biogenesis* was downregulated in both the TDP-43^{M337V} and FUS^{P525L} lines.

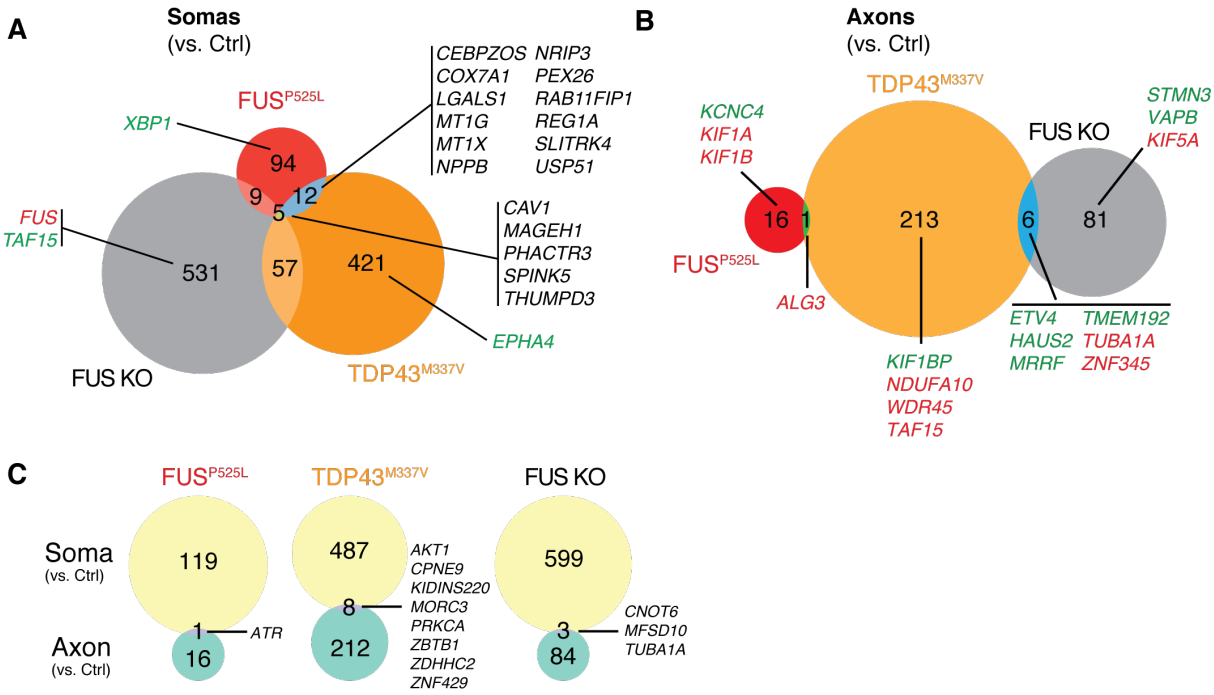

Figure 15. Gene dysregulation in somas and axons of iPSC-derived motor neurons, induced by mutations in and knock-out of FUS and TDP-43. A. Differentially expressed genes in somas of FUS^{P525L}, TDP-43^{M337V} and FUS KO motor neurons, compared to isogenic control motor neurons. Green means upregulated in the mutant line, red means downregulated as compared to control **B.** Differentially expressed genes in axons of FUS^{P525L}, TDP-43^{M337V} and FUS KO motor neurons, compared to isogenic control motor neurons. Green means upregulated in the mutant line, red means downregulated as compared to control. **C.** Venn diagram cross-comparing the differentially expressed genes per line between axon and soma.

As these pathways mentioned so far for the FUS^{P525L} line were non-overlapping with the FUS KO line, it is implicated that these specific pathways are dysregulated due to gain-of-function of the mutant FUS. When investigating the dysregulated pathways in the FUS KO line, and its

overlap with the FUS^{P525L} line it is interesting to note that here many pathways relating to synaptic functioning and signalling, synaptic membrane as well as vesicle transport are downregulated. This would suggest that while splicing defects are dysregulated in the FUS^{P525L} line only, pathways implicated in synaptic dysfunction are mediated by loss of nuclear FUS.

4.5.3 The axonal transcriptome is also dysregulated, but distinct from the events in somas

Next, we turned to the transcriptomes from our motor axons. Similar to the mouse motor axons in *Paper IV*, we found that human motor axons contain approximately 5,000 unique transcripts with a strong enrichment for transcripts encoding proteins required for mitochondrial respiration, as well as ribosome subunits. An additional finding is the detection of the *C9orf16* transcript being strongly enriched in axons compared to somas. In *Paper IV*, we identified the mouse homolog *1110008P14Rik* as being similarly enriched (Fig. 11B). Homologs exist only in vertebrates, and while its exact function is unknown, the protein is predicted to localise to microtubules. Even though *C9orf16* appears to not be dysregulated in disease, it is still intriguing to find such a similar and strong axonal enrichment for this protein, indicating that it likely has an important function in axonal cytoskeletal formation and/or maintenance.

Our ALS mutations induced dysregulation of a number of transcripts in axons (Fig. 15B). Out of the 17 dysregulated genes in the FUS^{P525L} line, two were *KIF1A* and *KIF1B*. These transcripts encode kinesin motor proteins, that mediate anterograde transport of various types of cargo, including synaptic vesicles (Okada et al., 1995). Their decreased expression in axons potentially disrupts axonal transport and vesicle release.

In the TDP-43^{M337V} line, the axonal transcriptome hinted at metabolic dysregulation. A key component for the formation of the first complex in the mitochondrial respiratory chain, *NDUFA10*, was downregulated. In addition, *WDR45* was downregulated. This protein is implicated in organellar autophagy, and reduced levels were shown to impair mitochondrial function, increase oxidative stress and indeed impair autophagic pathways (Seibler et al., 2018; Wan et al., 2019). Meanwhile, *KIF1BP* was upregulated in the TDP-43^{M337V} axons. This kinesin binding protein confers transport specificity to mitochondria, and its depletion causes the intracellular aggregation of mitochondria (Wozniak et al., 2005). Potentially, the neuron compensates for decreased mitochondrial function in axons by attempting to increase the transport inflow of mitochondria.

Finally, we observed that the transcriptome dysregulations due to mutations in FUS or TDP-43 were largely distinct between axons and somas, with only a handful of genes being regulated in both compartments (Fig. 15C). In TDP-43^{M337V} somas and axons, *AKT1* was downregulated. As a known pro-survival factor, its downregulated may predispose these mutant neurons to be more prone to cellular stress. Other genes were regulated in different directions in the two cellular compartments. *MORC3* was upregulated in somas in the TDP-43^{M337V} line compared to control somas, but downregulated in the mutant axons. In the FUS^{P525L} line, *ATR*, showed a similar pattern of expression. Both proteins are known to have important functions in the nucleus, with MORC able to generate ATP-dependent liquid-liquid phase separated droplets in the nucleus with a likely function to bring together DNA and DNA-binding proteins (Zhang et al., 2019), and ATR having a canonical role in DNA damage repair sensing and repair (Zou and Elledge, 2003). Their presence in axons suggests possible local non-canonical roles, however in the disease situation it appears that these proteins are recruited back to the soma, at the cost of their axonal expression.

Taken together, our data shows that ALS-causative mutations in FUS and TDP-43 result in dysregulation of both the somatic and axonal transcriptomes. However, the pattern of gene regulation is largely unique to each mutation, implying that the initial upstream events occurring due to these mutations are non-overlapping. Using the FUS KO line, we were able to dissect out the gene regulation that is likely caused by loss of nuclear FUS, as well as which dysregulation is initiated by gain-of-function of FUS^{P525L}. Our lines also showed distinct gene regulation in axons and somas, with both compartments presenting with sets of pathways or differentially expressed genes that in the future may present both central and peripheral targets for therapeutic intervention.

5 FUTURE PERSPECTIVES

In this thesis work, we first investigated the selective resistance to degeneration of oculomotor neurons compared to more vulnerable spinal motor neurons in both ALS and SMA. We employed both *in vivo* and *in vitro* approaches, by performing a transcriptomic analysis on different motor neuron pools in SMA mice, as well as generating oculomotor neurons from mouse stem cells. In doing so, we elucidated factors that can transfer resilience onto more vulnerable motor neurons, as exemplified most clearly by the protective effect of GDF15. This, combined with previous work of our lab showing the beneficial effects of expression of IGF-2 and SYT13, provides novel therapeutic targets that can be applied across motor neuron diseases. One future direction is to assess synergistic effects of combinations of these factors, as they affect different aspects of neuronal physiology, providing strength to a combined therapeutic approach.

An additional exciting avenue to pursue is the generation of human iPSC-derived oculomotor neurons. As we have shown in *Paper V*, mutations in ALS-causative genes affect the transcriptome and distribution of mutant proteins in iPSC-derived motor neurons. Being able to model spinal as well as oculomotor neurons will provide novel insights in how the resistant oculomotor neurons respond to varying mutations. This will go beyond identifying only pathways of degeneration in spinal motor neurons. In addition, potential differences in protein distribution, mislocalisation and aggregation in oculomotor neurons can be investigated. Oculomotor neurons possess multiple aspects rendering them more resistant, such as increased calcium-buffering potential, improved proteasome function, higher levels of pro-survival (Akt) signalling and upregulation of anti-apoptotic pathways in disease. Identifying which of these are most important in the face of mutations in various ALS-causative genes by modifying expression of components of these pathways will give important clues regarding how vulnerable neurons can be shielded best using endogenous signalling cascades in different disease contexts.

The second part of this thesis concerns the selective vulnerability of the distal motor axon compared to the soma. As we showed in *Paper I*, neuromuscular defects in ALS start with pre-synaptic dysfunction and denervation of the motor neuron at the NMJ. We then showed in *Paper IV* and *Paper V* that the presence of ALS-causative mutations in motor neurons causes transcriptome dysregulation. Together these papers highlight the cell-intrinsic processes

occurring in the motor neurons and particularly their axons, rendering stem cell-derived motor neurons and their isolated axons a novel and useful tool to study transcriptomic changes in the neuron itself. However, to recapitulate the *in vivo* environment more truthfully, as well as any pathological changes occurring to a neuromuscular synapse directly, the future development of this system should aim at generating functional *in vitro* NMJs.

For one it will enable studying the details of whether and how local transcriptomic dysregulation in axons affects neuromuscular stability, maintenance and degeneration in ALS. Moreover, this system will push further maturation of the motor neurons, as they now synapse onto their physiological targets. It is expected that formation of a synapse will stabilise the developing motor axon transcriptome, as the requirements for growth and pathfinding disappear while the need for synaptic signalling and neurotransmitter release increase. Moreover, since dysfunction at the NMJ is one of the earliest phenotypes observed in ALS, this will provide novel ways for *in vitro* approaches to study motor neuron dysfunction, potentially without requiring external stressors or long periods of time to observe neuronal degeneration.

The most exciting way to approach this would be to generate myofibres directly from iPSCs, much in the same way as the motor neurons. Using this approach, motor units could be created with ALS-causative mutations in both cell types, or only one of the two. This will allow dissection of disease-induced changes exerted by neurons and muscle onto each other, as well as the intricacies of their cell-to-cell communication. In conclusion, this system has the potential to reveal pathways of synaptic degeneration that can be targeted so as to preserve NMJs or possibly even stimulate sprouting and re-innervation early on in disease.

6 ACKNOWLEDGEMENTS

Eva, it's hard to put into words how grateful I am to have had you as my supervisor. Of course, I could praise your scientific outlook, and how there always seemed to be a never-ending stream of great projects to work on :) But more than that I want to thank you for being such a genuine and caring person. Your personal approach and openness in leading the lab makes it an environment that goes beyond simply a workplace. You rock!

Laura and **Ilary**, you were the most awesome and inspiring internship supervisors I could have wished for when I came to the lab! You strengthened my scientific curiosity and jointly motivated and even made it possible for me to start this entire journey.

Christoph, Julio and **Nigel**, I count myself lucky to have been surrounded by all of you. Thank you for all the endless discussions and science-babble! You all made the lab a place that I enjoyed coming to every single day. Christoph, thank you for all the nerdy discussions we had over lunch and coffees and your superb sense of (dark) humour! Please never lose it. Nigel, I feel like every time we had a long science discussion new ideas were created for both our projects, something I valued immensely. Julio, we've worked on so many projects together that I lost count. Your optimism and always abundant smiles cheered up everyone around.

Susanne, my PhD buddy in the lab! You left some big footsteps to fill! Thank you for your happy presence and dedicated attitude to science. I promise I will keep wearing bike helmets from now on ;)

Salim, your teamwork attitude and cheerful smiles fit in well in the Hedlund lab and I hope it is going to lead to great things :)

All members of the **D7 quarter**, thanks both for creating such a nice shared space and fun and fikas at one or the other occasion.

A big thanks to both my Dutch students **Rein** and **Jacob**! Still not sure how that Dutch-coincidence happened… I am grateful for everything you both contributed to our projects!

Thank you to **Marlene, Christina, Ming, Gillian**, **Dana, Nora and Olga**. It was great to have your company in the lab and you all made it into a more fun and productive place!

Marc, Stefan, Jonas and Jutzi, even though we did not meet that often I feel that our projects were very interwoven. Thank you not only for being so generous with sharing protocols, reagents, and cells but also for the fun times we had hanging out at conferences!

I want to thank my co-supervisors **Ole Kiehn** and **Rickard Sandberg.** Thank you **Rickard** for allowing us to use your sequencer in the beginning of it all.

Thank you **Qiaolin** and **Shangli** for your bioinformatics support. You made it possible for some projects to even take off in the first place.

Staffan, it is too bad that we did not overlap more than we did. It was truly inspiring to have you join our meetings, and you always managed to pull another fact about motor neurons out of the hat that nobody knew yet. I'll make sure to carry the *Globen*-analogy for the length of axons forward from here on!

I want to thank my mentor, professor **Marc de Baets** for his guidance and help with setting up this whole adventure at the very start.

A big thanks goes to my amazing friends **Koen, Bryan, Frank** and **Jorn** for keeping me sane when it was necessary and for always providing fun distraction when it was much needed!

Thank you **Eeva** and **Kent** for making my move to Sweden so nice and easy. You were so inviting, friendly and open. I very much appreciate the start you gave me (and the Swedish lessons!).

Mijn ouders, **Wiel** en **May**, jullie hebben altijd achter elke beslissing gestaan die ik gemaakt heb en doen dat nog steeds. Daarvoor kan ik jullie niet genoeg bedanken.

My dear **Gill**, it feels strange to thank you here specifically as I am grateful for every moment we get to spend together. You make me a better person.

7 REFERENCES

Allodi, I., Comley, L., Nichterwitz, S., Nizzardo, M., Simone, C., Benitez, J.A., Cao, M., Corti, S., and Hedlund, E. (2016). Differential neuronal vulnerability identifies IGF-2 as a protective factor in ALS. Scientific Reports *6*, 25960.

Almeida, S., Gascon, E., Tran, H., Chou, H.J., Gendron, T.F., Degroot, S., Tapper, A.R., Sellier, C., Charlet-Berguerand, N., Karydas, A., et al. (2013). Modeling key pathological features of frontotemporal dementia with C9ORF72 repeat expansion in iPSC-derived human neurons. Acta Neuropathol *126*, 385–399.

Amiri, M., and Hollenbeck, P.J. (2008). Mitochondrial biogenesis in the axons of vertebrate peripheral neurons. Dev Neurobiol *68*, 1348–1361.

An, D., Fujiki, R., Iannitelli, D.E., Smerdon, J.W., Maity, S., Rose, M.F., Gelber, A., Wanaselja, E.K., Yagudayeva, I., Lee, J.Y., et al. (2019). Stem cell-derived cranial and spinal motor neurons reveal proteostatic differences between ALS resistant and sensitive motor neurons. Elife *8*, e44423.

Ash, P.E.A., Bieniek, K.F., Gendron, T.F., Caulfield, T., Lin, W.-L., DeJesus-Hernandez, M., van Blitterswijk, M.M., Jansen-West, K., Paul, J.W., Rademakers, R., et al. (2013). Unconventional Translation of C9ORF72 GGGGCC Expansion Generates Insoluble Polypeptides Specific to c9FTD/ALS. Neuron *77*, 639–646.

Atanasio, A., Decman, V., White, D., Ramos, M., Ikiz, B., Lee, H.-C., Siao, C.-J., Brydges, S., LaRosa, E., Bai, Y., et al. (2016). C9orf72 ablation causes immune dysregulation characterized by leukocyte expansion, autoantibody production, and glomerulonephropathy in mice. Sci Rep-Uk *6*, 23204.

Aulas, A., and Velde, C.V. (2015). Alterations in stress granule dynamics driven by TDP-43 and FUS: a link to pathological inclusions in ALS? Front Cell Neurosci *9*, 423.

Ayers, J.I., Xu, G., Pletnikova, O., Troncoso, J.C., Hart, P.J., and Borchelt, D.R. (2014). Conformational specificity of the C4F6 SOD1 antibody; low frequency of reactivity in sporadic ALS cases. Acta Neuropathologica Commun *2*, 55.

Ba, I.A.-T.V., Marchal, S., François, F., Silhol, M., Lleres, C., Michel, B., Benyamin, Y., Verdier, J.-M., Trousse, F., and Marcilhac, A. (2011). Regenerating Islet-derived 1α (Reg-1α) Protein Is New Neuronal Secreted Factor That Stimulates Neurite Outgrowth via Exostosin Tumor-like 3 (EXTL3) Receptor. J Biol Chem *287*, 4726–4739.

Becker, L.A., Huang, B., Bieri, G., Ma, R., Knowles, D.A., Jafar-Nejad, P., Messing, J., Kim, H.J., Soriano, A., Auburger, G., et al. (2017). Therapeutic reduction of ataxin-2 extends lifespan and reduces pathology in TDP-43 mice. Nature *544*, 367–371.

Bergmann, M., Völpel, M., and Kuchelmeister, K. (1995). Onuf's nucleus is frequently involved in motor neuron disease/amyotrophic lateral sclerosis. J Neurol Sci *129*, 141–146.

Bilican, B., Serio, A., Barmada, S.J., Nishimura, A.L., Sullivan, G.J., Carrasco, M., Phatnani, H.P., Puddifoot, C.A., Story, D., Fletcher, J., et al. (2012). Mutant induced pluripotent stem cell lines recapitulate aspects of TDP-43 proteinopathies and reveal cell-specific vulnerability. P Natl Acad Sci Usa *109*, 5803–5808.

Boillée, S., Yamanaka, K., Lobsiger, C.S., Copeland, N.G., Jenkins, N.A., Kassiotis, G., Kollias, G., and Cleveland, D.W. (2006). Onset and Progression in Inherited ALS Determined by Motor Neurons and Microglia. Science *312*, 1389–1392.

Briese, M., Saal, L., Appenzeller, S., Moradi, M., Baluapuri, A., and Sendtner, M. (2015). Whole transcriptome profiling reveals the RNA content of motor axons. Nucleic Acids Research.

Bruijn, L.I., Houseweart, M.K., Kato, S., Anderson, K.L., Anderson, S.D., Ohama, E., Reaume, A.G., Scott, R.W., and Cleveland, D.W. (1998). Aggregation and Motor Neuron Toxicity of an ALS-Linked SOD1 Mutant Independent from Wild-Type SOD1. Science *281*, 1851–1854.

Burge, C.B., Padgett, R.A., and Sharp, P.A. (1998). Evolutionary Fates and Origins of U12-Type Introns. Mol Cell *2*, 773–785.

Burke, R.E., and Tsairis, P. (1973). Anatomy and innervation ratios in motor units of cat gastrocnemius. J Physiology *234*, 749–765.

Burke, R.E., Levine, D.N., Zajac, F.E., Tsairis, P., and Engel, W.K. (1971). Mammalian Motor Units: Physiological-Histochemical Correlation in Three Types in Cat Gastrocnemius. Science *174*, 709–712.

Burkhardt, M.F., Martinez, F.J., Wright, S., Ramos, C., Volfson, D., Mason, M., Garnes, J., Dang, V., Lievers, J., Shoukat-Mumtaz, U., et al. (2013). A cellular model for sporadic ALS using patient-derived induced pluripotent stem cells. Mol Cell Neurosci *56*, 355–364.

Caligari, M., Godi, M., Guglielmetti, S., Franchignoni, F., and Nardone, A. (2013). Eye tracking communication devices in amyotrophic lateral sclerosis: Impact on disability and quality of life. Amyotroph Lat Scl Fr *14*, 546–552.

Campenot, R.B. (1977). Local control of neurite development by nerve growth factor. Proc National Acad Sci *74*, 4516–4519.

Chambers, S.M., Fasano, C.A., Papapetrou, E.P., Tomishima, M., Sadelain, M., and Studer, L. (2009). Highly efficient neural conversion of human ES and iPS cells by dual inhibition of SMAD signaling. Nat Biotechnol *27*, 275–280.

Chaytow, H., Huang, Y.-T., Gillingwater, T.H., and Faller, K.M.E. (2018). The role of survival motor neuron protein (SMN) in protein homeostasis. Cell Mol Life Sci Cmls *75*, 3877–3894.

Chen, H., Qian, K., Du, Z., Cao, J., Petersen, A., Liu, H., Blackbourn, L.W., Huang, C.-L., Errigo, A., Yin, Y., et al. (2014). Modeling ALS with iPSCs reveals that mutant SOD1 misregulates neurofilament balance in motor neurons. Cell Stem Cell *14*, 796–809.

Chiang, P.-M., Ling, J., Jeong, Y.H., Price, D.L., Aja, S.M., and Wong, P.C. (2010). Deletion of TDP-43 down-regulates Tbc1d1, a gene linked to obesity, and alters body fat metabolism. Proc National Acad Sci *107*, 16320–16324.

Cifuentes-Diaz, C., Nicole, S., Velasco, M.E., Borra-Cebrian, C., Panozzo, C., Frugier, T., Millet, G., Roblot, N., Joshi, V., and Melki, J. (2002). Neurofilament accumulation at the motor endplate and lack of axonal sprouting in a spinal muscular atrophy mouse model. Hum Mol Genet *11*, 1439–1447.

Clement, A.M., Nguyen, M.D., Roberts, E.A., Garcia, M.L., Boillée, S., Rule, M., McMahon, A.P., Doucette, W., Siwek, D., Ferrante, R.J., et al. (2003). Wild-Type Nonneuronal Cells Extend Survival of SOD1 Mutant Motor Neurons in ALS Mice. Science *302*, 113–117.

Comley, L., Allodi, I., Nichterwitz, S., Nizzardo, M., Simone, C., Corti, S., and Hedlund, E. (2015). Motor neurons with differential vulnerability to degeneration show distinct protein signatures in health and ALS. Neuroscience *291*, 216–229.

Court, F.A., Hendriks, W.T.J., MacGillavry, H.D., Alvarez, J., and Minnen, J. van (2008). Schwann cell to axon transfer of ribosomes: toward a novel understanding of the role of glia in the nervous system. J Neurosci Official J Soc Neurosci *28*, 11024–11029.

Crispino, M., Kaplan, B.B., Martin, R., Alvarez, J., Chun, J.T., Benech, J.C., and Giuditta, A. (1997). Active Polysomes Are Present in the Large Presynaptic Endings of the Synaptosomal Fraction from Squid Brain. J Neurosci *17*, 7694–7702.

Cruz, S.D., Bui, A., Saberi, S., Lee, S.K., Stauffer, J., McAlonis-Downes, M., Schulte, D., Pizzo, D.P., Parone, P.A., Cleveland, D.W., et al. (2017). Misfolded SOD1 is not a primary component of sporadic ALS. Acta Neuropathol *134*, 97–111.

Cudkowicz, M.E., McKenna-Yasek, D., Chen, C., Hedley-Whyte, E.T., and Brown, R.H. (1998). Limited corticospinal tract involvement in amyotrophic lateral sclerosis subjects with the A4V mutation in the copper/zinc superoxide dismutase gene. Ann Neurol *43*, 703–710.

DeJesus-Hernandez, M., Mackenzie, I.R., Boeve, B.F., Boxer, A.L., Baker, M., Rutherford, N.J., Nicholson, A.M., Finch, N.A., Flynn, H., Adamson, J., et al. (2011). Expanded GGGGCC Hexanucleotide Repeat in Noncoding Region of C9ORF72 Causes Chromosome 9p-Linked FTD and ALS. Neuron *72*, 245–256.

Deng, H.-X., Zhai, H., Bigio, E.H., Yan, J., Fecto, F., Ajroud, K., Mishra, M., Ajroud-Driss, S., Heller, S., Sufit, R., et al. (2010). FUS-immunoreactive inclusions are a common feature in sporadic and non-SOD1 familial amyotrophic lateral sclerosis. Ann Neurol *67*, 739–748.

Deng, Q., Andersson, E., Hedlund, E., Alekseenko, Z., Coppola, E., Panman, L., Millonig, J.H., Brunet, J.-F.F., Ericson, J., and Perlmann, T. (2011). Specific and integrated roles of Lmx1a, Lmx1b and Phox2a in ventral midbrain development. Development (Cambridge, England) *138*, 3399–3408.

Devlin, A.-C., Burr, K., Borooah, S., Foster, J.D., Cleary, E.M., Geti, I., Vallier, L., Shaw, C.E., Chandran, S., and Miles, G.B. (2015). Human iPSC-derived motoneurons harbouring TARDBP or C9ORF72 ALS mutations are dysfunctional despite maintaining viability. Nat Commun *6*, 5999.

Donnelly, C.J., Zhang, P.-W., Pham, J.T., Haeusler, A.R., Heusler, A.R., Mistry, N.A., Vidensky, S., Daley, E.L., Poth, E.M., Hoover, B., et al. (2013). RNA toxicity from the ALS/FTD C9ORF72 expansion is mitigated by antisense intervention. Neuron *80*, 415–428.

Egawa, N., Kitaoka, S., Tsukita, K., Naitoh, M., Takahashi, K., Yamamoto, T., Adachi, F., Kondo, T., Okita, K., Asaka, I., et al. (2012). Drug screening for ALS using patient-specific induced pluripotent stem cells. Sci Transl Med *4*, 145ra104.

Ehrlich, M., Hallmann, A.-L., Reinhardt, P., Araúzo-Bravo, M.J., Korr, S., Röpke, A., Psathaki, O.E., Ehling, P., Meuth, S.G., Oblak, A.L., et al. (2015). Distinct Neurodegenerative Changes in an Induced Pluripotent Stem Cell Model of Frontotemporal Dementia Linked to Mutant TAU Protein. Stem Cell Rep *5*, 83–96.

Elden, A.C., Kim, H.-J., Hart, M.P., Chen-Plotkin, A.S., Johnson, B.S., Fang, X., Armakola, M., Geser, F., Greene, R., Lu, M.M., et al. (2010). Ataxin-2 intermediate-length polyglutamine expansions are associated with increased risk for ALS. Nature *466*, 1069–1075.

Enoka, R.M. (1995). Morphological Features and Activation Patterns of Motor Units. J Clin Neurophysiol *12*, 538–559.

Epstein, C.J., Avraham, K.B., Lovett, M., Smith, S., Elroy-Stein, O., Rotman, G., Bry, C., and Groner, Y. (1987). Transgenic mice with increased Cu/Zn-superoxide dismutase activity: animal model of dosage effects in Down syndrome. Proc National Acad Sci *84*, 8044–8048.

Eva, R., Dassie, E., Caswell, P.T., Dick, G., ffrench-Constant, C., Norman, J.C., and Fawcett, J.W. (2010). Rab11 and its effector Rab coupling protein contribute to the trafficking of beta 1 integrins during axon growth in adult dorsal root ganglion neurons and PC12 cells. J Neurosci Official J Soc Neurosci *30*, 11654–11669.

Evans, M.J., and Kaufman, M.H. (1981). Establishment in culture of pluripotential cells from mouse embryos. Nature *292*, 154–156.

Farias, J., Holt, C.E., Sotelo, J.R., and Sotelo-Silveira, J.R. (2020). Axon micro-dissection and transcriptome profiling reveals the in vivo RNA content of fully differentiated myelinated motor axons. Rna New York N Y *26*, 595–612.

Ferrucci, M., Spalloni, A., Bartalucci, A., Cantafora, E., Fulceri, F., Nutini, M., Longone, P., Paparelli, A., and Fornai, F. (2010). A systematic study of brainstem motor nuclei in a mouse model of ALS, the effects of lithium. Neurobiol Dis *37*, 370–383.

Finkel, R.S., Chiriboga, C.A., Vajsar, J., Day, J.W., Montes, J., Vivo, D.C.D., Yamashita, M., Rigo, F., Hung, G., Schneider, E., et al. (2016). Treatment of infantile-onset spinal muscular atrophy with nusinersen: a phase 2, open-label, dose-escalation study. Lancet *388*, 3017–3026.

Fischer, L.R., Culver, D.G., Tennant, P., Davis, A.A., Wang, M., Castellano-Sanchez, A., Khan, J., Polak, M.A., and Glass, J.D. (2004). Amyotrophic lateral sclerosis is a distal axonopathy: evidence in mice and man. Experimental Neurology *185*, 232–240.

Forsberg, K., Jonsson, P.A., Andersen, P.M., Bergemalm, D., Graffmo, K.S., Hultdin, M., Jacobsson, J., Rosquist, R., Marklund, S.L., and Brännström, T. (2010). Novel Antibodies Reveal Inclusions Containing Non-Native SOD1 in Sporadic ALS Patients. Plos One *5*, e11552.

Freibaum, B.D., Lu, Y., Lopez-Gonzalez, R., Kim, N.C., Almeida, S., Lee, K.-H.H., Badders, N., Valentine, M., Miller, B.L., Wong, P.C., et al. (2015). GGGGCC repeat expansion in C9orf72 compromises nucleocytoplasmic transport. Nature *525*, 129–133.

Frey, D., Schneider, C., Xu, L., Borg, J., Spooren, W., and Caroni, P. (2000). Early and selective loss of neuromuscular synapse subtypes with low sprouting competence in motoneuron diseases. The Journal of Neuroscience : The Official Journal of the Society for Neuroscience *20*, 2534–2542.

Fujimori, K., Ishikawa, M., Otomo, A., Atsuta, N., Nakamura, R., Akiyama, T., Hadano, S., Aoki, M., Saya, H., Sobue, G., et al. (2018). Modeling sporadic ALS in iPSC-derived motor neurons identifies a potential therapeutic agent. Nat Med *24*, 1579–1589.

Gabanella, F., Butchbach, M.E.R., Saieva, L., Carissimi, C., Burghes, A.H.M., and Pellizzoni, L. (2007). Ribonucleoprotein Assembly Defects Correlate with Spinal Muscular Atrophy Severity and Preferentially Affect a Subset of Spliceosomal snRNPs. Plos One *2*, e921.

Gasset-Rosa, F., Lu, S., Yu, H., Chen, C., Melamed, Z., Guo, L., Shorter, J., Cruz, S.D., and Cleveland, D.W. (2019). Cytoplasmic TDP-43 De-mixing Independent of Stress Granules Drives Inhibition of Nuclear Import, Loss of Nuclear TDP-43, and Cell Death. Neuron *102*, 339-357.e7.

Giorgio, F., Carrasco, M.A., Siao, M.C., Maniatis, T., and Eggan, K. (2007). Non–cell autonomous effect of glia on motor neurons in an embryonic stem cell–based ALS model. Nature Neuroscience *10*, 608–614.

Giorgio, F.P.D., Boulting, G.L., Bobrowicz, S., and Eggan, K.C. (2008). Human Embryonic Stem Cell-Derived Motor Neurons Are Sensitive to the Toxic Effect of Glial Cells Carrying an ALS-Causing Mutation. Cell Stem Cell *3*.

Gould, T.W., Buss, R.R., Vinsant, S., Prevette, D., Sun, W., Knudson, C.M., Milligan, C.E., and Oppenheim, R.W. (2006). Complete Dissociation of Motor Neuron Death from Motor Dysfunction by Bax Deletion in a Mouse Model of ALS. J Neurosci *26*, 8774–8786.

Grad, L.I., Yerbury, J.J., Turner, B.J., Guest, W.C., Pokrishevsky, E., O'Neill, M.A., Yanai, A., Silverman, J.M., Zeineddine, R., Corcoran, L., et al. (2014). Intercellular propagated misfolding of wild-type Cu/Zn superoxide dismutase occurs via exosome-dependent and -independent mechanisms. P Natl Acad Sci Usa *111*, 3620–3625.

Gueritaud, J., Horcholle-Bossavit, G., Jami, L., Thiesson, D., and Tyc-Dumont, S. (1985). Resistance to glycogen depletion of motor units in the cat rectus lateralis muscle. Exp Brain Res *60*, 542–550.

Guidato, S., Barrett, C., and Guthrie, S. (2003). Patterning of motor neurons by retinoic acid in the chick embryo hindbrain in vitro. Mol Cell Neurosci *23*, 81–95.

Gumy, L.F., Yeo, G.S., Tung, Y.-C.L.C., Zivraj, K.H., Willis, D., Coppola, G., Lam, B.Y., Twiss, J.L., Holt, C.E., and Fawcett, J.W. (2011). Transcriptome analysis of embryonic and adult sensory axons reveals changes in mRNA repertoire localization. RNA (New York, N.Y.) *17*, 85–98.

Gurdon, J. (1962). The developmental capacity of nuclei taken from intestinal epithelium cells of feeding tadpoles. J Embryol Exp Morph *10*, 622–640.

Gurney, M., Pu, H., Chiu, A., Canto, D.M., Polchow, C., Alexander, D., Caliendo, J., Hentati, A., Kwon, Y., and Deng, H. (1994). Motor neuron degeneration in mice that express a human Cu,Zn superoxide dismutase mutation. Science (New York, N.Y.) *264*, 1772–1775.

Haenggeli, C., and Kato, A.C. (2002). Differential vulnerability of cranial motoneurons in mouse models with motor neuron degeneration. Neuroscience Letters *335*, 39–43.

Harding, B.N., Kariya, S., Monani, U.R., Chung, W.K., Benton, M., Yum, S.W., Tennekoon, G., and Finkel, R.S. (2015). Spectrum of neuropathophysiology in spinal muscular atrophy type I. Journal of Neuropathology and Experimental Neurology *74*, 15–24.

Hayward, L.J., Rodriguez, J.A., Kim, J.W., Tiwari, A., Goto, J.J., Cabelli, D.E., Valentine, J.S., and Brown, R.H. (2002). Decreased Metallation and Activity in Subsets of Mutant Superoxide Dismutases Associated with Familial Amyotrophic Lateral Sclerosis. J Biol Chem *277*, 15923–15931.

Hedlund, E., Karlsson, M., Osborn, T., Ludwig, W., and Isacson, O. (2010). Global gene expression profiling of somatic motor neuron populations with different vulnerability identify molecules and pathways of degeneration and protection. Brain *133*, 2313–2330.

Hegedus, J., Putman, C.T., and Gordon, T. (2007). Time course of preferential motor unit loss in the SOD1G93A mouse model of amyotrophic lateral sclerosis. Neurobiol Dis *28*, 154–164.

Heikinheimo, M., Lawshé, A., Shackleford, G.M., Wilson, D.B., and MacArthur, C.A. (1994). Fgf-8 expression in the post-gastrulation mouse suggests roles in the development of the face, limbs and central nervous system. Mech Develop *48*, 129–138.

Hicks, G.G., Singh, N., Nashabi, A., Mai, S., Bozek, G., Klewes, L., Arapovic, D., White, E.K., Koury, M.J., Oltz, E.M., et al. (2000). Fus deficiency in mice results in defective B-lymphocyte development and activation, high levels of chromosomal instability and perinatal death. Nat Genet *24*, 175–179.

Hornberg, H., Horck, F.W., Maurus, D., Zwart, M., Svoboda, H., Harris, W.A., and Holt, C.E. (2013). RNA-Binding Protein Hermes/RBPMS Inversely Affects Synapse Density and Axon Arbor Formation in Retinal Ganglion Cells In Vivo. J Neurosci *33*, 10384–10395.

Huang, C., Tong, J., Bi, F., Zhou, H., and Xia, X.-G. (2012). Mutant TDP-43 in motor neurons promotes the onset and progression of ALS in rats. J Clin Invest *122*, 107–118.

Ichiyanagi, N., Fujimori, K., Yano, M., Ishihara-Fujisaki, C., Sone, T., Akiyama, T., Okada, Y., Akamatsu, W., Matsumoto, T., Ishikawa, M., et al. (2016). Establishment of In Vitro FUS-Associated Familial Amyotrophic Lateral Sclerosis Model Using Human Induced Pluripotent Stem Cells. Stem Cell Reports.

Ikenaka, K., Ishigaki, S., Iguchi, Y., Kawai, K., Fujioka, Y., Yokoi, S., Abdelhamid, R.F., Nagano, S., Mochizuki, H., Katsuno, M., et al. (2020). Characteristic Features of FUS Inclusions in Spinal Motor Neurons of Sporadic Amyotrophic Lateral Sclerosis. J Neuropathology Exp Neurology *79*, 370–377.

Imamura, K., Izumi, Y., Watanabe, A., Tsukita, K., Woltjen, K., Yamamoto, T., Hotta, A., Kondo, T., Kitaoka, S., Ohta, A., et al. (2017). The Src/c-Abl pathway is a potential therapeutic target in amyotrophic lateral sclerosis. Sci Transl Med *9*, eaaf3962.

Jaarsma, D., Teuling, E., Haasdijk, E.D., Zeeuw, C.I.D., and Hoogenraad, C.C. (2008). Neuron-Specific Expression of Mutant Superoxide Dismutase Is Sufficient to Induce Amyotrophic Lateral Sclerosis in Transgenic Mice. J Neurosci *28*, 2075–2088.

Jablonka, S., Schrank, B., Kralewski, M., Rossoll, W., and Sendtner, M. (2000). Reduced survival motor neuron (Smn) gene dose in mice leads to motor neuron degeneration: an animal model for spinal muscular atrophy type III. Human Molecular Genetics *9*, 341–346.

Japtok, J., Lojewski, X., Naumann, M., Klingenstein, M., Reinhardt, P., Sterneckert, J., Putz, S., Demestre, M., Boeckers, T.M., Ludolph, A.C., et al. (2015). Stepwise acquirement of hallmark neuropathology in FUS-ALS iPSC models depends on mutation type and neuronal aging. Neurobiol Dis *82*, 420–429.

Jessell, T.M. (2000). Neuronal specification in the spinal cord: inductive signals and transcriptional codes. Nat Rev Genet *1*, 20–29.

Jiang, J., Zhu, Q., Gendron, T.F., Saberi, S., McAlonis-Downes, M., Seelman, A., Stauffer, J.E., Jafar-nejad, P., Drenner, K., Schulte, D., et al. (2016). Gain of Toxicity from ALS/FTD-Linked Repeat Expansions in C9ORF72 Is Alleviated by Antisense Oligonucleotides Targeting GGGGCC-Containing RNAs. Neuron *90*, 535–550.

Jovičić, A., Mertens, J., Boeynaems, S., Bogaert, E., Chai, N., Yamada, S.B., III, J.W., Sun, S., Herdy, J.R., Bieri, G., et al. (2015). Modifiers of C9orf72 dipeptide repeat toxicity connect nucleocytoplasmic transport defects to FTD/ALS. Nature Neuroscience *18*, 1226–1229.

Jutzi, D., Akinyi, M.V., Mechtersheimer, J., Frilander, M.J., and Ruepp, M.-D. (2018). The emerging role of minor intron splicing in neurological disorders. Cell Stress *2*, 40–54.

Kaplan, A., Spiller, K.J., Towne, C., Kanning, K.C., Choe, G.T., Geber, A., Akay, T., Aebischer, P., and Henderson, C.E. (2014). Neuronal Matrix Metalloproteinase-9 Is a Determinant of Selective Neurodegeneration. Neuron *81*, 333–348.

Karumbayaram, S., Kelly, T.K., Paucar, A.A., Roe, A.J.T., Umbach, J.A., Charles, A., Goldman, S.A., Kornblum, H.I., and Wiedau-Pazos, M. (2009). Human embryonic stem cell-derived motor neurons expressing SOD1 mutants exhibit typical signs of motor neuron degeneration linked to ALS. Dis Model Mech *2*, 189–195.

Kenna, K.P., Doormaal, P.T.C. van, Dekker, A.M., Ticozzi, N., Kenna, B.J., Diekstra, F.P., Rheenen, W. van, Eijk, K.R. van, Jones, A.R., Keagle, P., et al. (2016). NEK1 variants confer susceptibility to amyotrophic lateral sclerosis. Nat Genet *48*, 1037–1042.

Kim, H.-T., Prochiantz, A., and Kim, J.W. (2016). Donating Otx2 to support neighboring neuron survival. Bmb Rep *49*, 69–70.

King, A., Troakes, C., Smith, B., Nolan, M., Curran, O., Vance, C., Shaw, C.E., and Al-Sarraj, S. (2015). ALS-FUS pathology revisited: singleton FUS mutations and an unusual case with both a FUS and TARDBP mutation. Acta Neuropathologica Commun *3*, 62.

Kiskinis, E., Sandoe, J., Williams, L.A., Boulting, G.L., Moccia, R., Wainger, B.J., Han, S., Peng, T., Thams, S., Mikkilineni, S., et al. (2014). Pathways disrupted in human ALS motor neurons identified through genetic correction of mutant SOD1. Cell Stem Cell *14*, 781–795.

Klim, J.R., Williams, L.A., Limone, F., Juan, I.G.S., Davis-Dusenbery, B.N., Mordes, D.A., Burberry, A., Steinbaugh, M.J., Gamage, K.K., Kirchner, R., et al. (2019). ALS-implicated protein TDP-43 sustains levels of STMN2, a mediator of motor neuron growth and repair. Nat Neurosci *22*, 167–179.

Kraemer, B.C., Schuck, T., Wheeler, J.M., Robinson, L.C., Trojanowski, J.Q., Lee, V.M.Y., and Schellenberg, G.D. (2010). Loss of murine TDP-43 disrupts motor function and plays an essential role in embryogenesis. Acta Neuropathol *119*, 409–419.

Kreiter, N., Pal, A., Lojewski, X., Corcia, P., Naujock, M., Reinhardt, P., Sterneckert, J., Petri, S., Wegner, F., Storch, A., et al. (2018). Age-dependent neurodegeneration and organelle transport deficiencies in mutant TDP43 patient-derived neurons are independent of TDP43 aggregation. Neurobiol Dis *115*, 167–181.

Kubota, M., Sakakihara, Y., Uchiyama;, Y., Nara;, A., Nagata, T., Nitta, H., Ishimoto;, K., Oka, A., Horio, K., and Yanagisawa, M. (2000). New ocular movement detector system as a communication tool in ventilator-assisted Werdnig- Hoffmann disease. Developmental Medicine & Child Neurology *42*, 61–64.

Kwiatkowski, T.J., Bosco, D.A., LeClerc, A.L., Tamrazian, E., Vanderburg, C.R., Russ, C., Davis, A., Gilchrist, J., Kasarskis, E.J., Munsat, T., et al. (2009). Mutations in the FUS/TLS Gene on Chromosome 16 Cause Familial Amyotrophic Lateral Sclerosis. Science *323*, 1205–1208.

Lasek, R.J., Garner, J.A., and Brady, S.T. (1984). Axonal transport of the cytoplasmic matrix. J Cell Biology *99*, 212s–221s.

Lattante, S., Rouleau, G.A., and Kabashi, E. (2013). TARDBP and FUS mutations associated with amyotrophic lateral sclerosis: summary and update. Hum Mutat *34*, 812–826.

Le, T.T., Pham, L.T., Butchbach, M., Zhang, H.L., Monani, U.R., Coovert, D.D., Gavrilina, T.O., Xing, L., Bassell, G.J., and Burghes, A. (2005). SMNΔ7, the major product of the centromeric survival motor neuron (SMN2) gene, extends survival in mice with spinal muscular atrophy and associates with full-length SMN. Human Molecular Genetics *14*, 845–857.

Lefebvre, S., Bürglen, L., Reboullet, S., Clermont, O., Burlet, P., Viollet, L., Benichou, B., Cruaud, C., Millasseau, P., Zeviani, M., et al. (1995). Identification and characterization of a spinal muscular atrophy-determining gene. Cell *80*, 155–165.

Lenglet, T., Mirault, J., Veyrat-Masson, M., Funkiewiez, A., Amador, M. del M., Bruneteau, G., Forestier, N.L., Pradat, P.-F., Salachas, F., Vacher, Y., et al. (2019). Cursive Eye-Writing With Smooth-Pursuit Eye-Movement Is Possible in Subjects With Amyotrophic Lateral Sclerosis. Front Neurosci-Switz *13*, 538.

Lenzi, J., Santis, R.D., Turris, V. de, Morlando, M., Laneve, P., Calvo, A., Caliendo, V., Chio, A., Rosa, A., and Bozzoni, I. (2015). ALS mutant FUS proteins are recruited into stress granules in induced pluripotent stem cell-derived motoneurons. Dis Model Mech *8*, 755–766.

Li, X.-J., Du, Z.-W., Zarnowska, E.D., Pankratz, M., Hansen, L.O., Pearce, R.A., and Zhang, S.-C. (2005). Specification of motoneurons from human embryonic stem cells. Nat Biotechnol *23*, 215–221.

Lippmann, E.S., Williams, C.E., Ruhl, D.A., Estevez-Silva, M.C., Chapman, E.R., Coon, J.J., and Ashton, R.S. (2015). Deterministic HOX Patterning in Human Pluripotent Stem Cell-Derived Neuroectoderm. Stem Cell Reports.

Liu, K.X., Edwards, B., Lee, S., Finelli, M.J., Davies, B., Davies, K.E., and Oliver, P.L. (2015). Neuron-specific antioxidant OXR1 extends survival of a mouse model of amyotrophic lateral sclerosis. Brain J Neurology *138*, 1167–1181.

Liu, Q., Fischer, U., Wang, F., and Dreyfuss, G. (1997). The Spinal Muscular Atrophy Disease Gene Product, SMN, and Its Associated Protein SIP1 Are in a Complex with Spliceosomal snRNP Proteins. Cell *90*, 1013–1021.

Liu, Y., Pattamatta, A., Zu, T., Reid, T., Bardhi, O., Borchelt, D.R., Yachnis, A.T., and Ranum, L.P.W. (2016). C9orf72 BAC Mouse Model with Motor Deficits and Neurodegenerative Features of ALS/FTD. Neuron *90*, 521–534.

Lopez-Gonzalez, R., Lu, Y., Gendron, T.F., Karydas, A., Tran, H., Yang, D., Petrucelli, L., Miller, B.L., Almeida, S., and Gao, F.-B. (2016). Poly(GR) in C9ORF72-Related ALS/FTD Compromises Mitochondrial Function and Increases Oxidative Stress and DNA Damage in iPSC-Derived Motor Neurons. Neuron *92*, 383–391.

Luo, L., Song, Z., Li, X., Huiwang, Zeng, Y., Qinwang, Meiqi, and He, J. (2018). Efficacy and safety of edaravone in treatment of amyotrophic lateral sclerosis-a systematic review and meta-analysis. Neurological Sci Official J Italian Neurological Soc Italian Soc Clin Neurophysiology *40*, 235–241.

Lyabin, D.N., Eliseeva, I.A., and Ovchinnikov, L.P. (2014). YB-1 protein: functions and regulation. Wiley Interdiscip Rev Rna *5*, 95–110.

Mackenzie, I.R., Arzberger, T., Kremmer, E., Troost, D., Lorenzl, S., Mori, K., Weng, S.-M., Haass, C., Kretzschmar, H.A., Edbauer, D., et al. (2013). Dipeptide repeat protein pathology in C9ORF72 mutation cases: clinico-pathological correlations. Acta Neuropathol *126*, 859–879.

Mackenzie, I.R.A., Bigio, E.H., Ince, P.G., Geser, F., Neumann, M., Cairns, N.J., Kwong, L.K., Forman, M.S., Ravits, J., Stewart, H., et al. (2007). Pathological TDP- 43 distinguishes sporadic amyotrophic lateral sclerosis from amyotrophic lateral sclerosis with SOD1 mutations. Ann Neurol *61*, 427–434.

Maden, M. (2002). Retinoid signalling in the development of the central nervous system. Nat Rev Neurosci *3*, 843–853.

Mancuso, R., Oliván, S., Rando, A., Casas, C., Osta, R., and Navarro, X. (2012). Sigma-1R Agonist Improves Motor Function and Motoneuron Survival in ALS Mice. Neurotherapeutics *9*, 814–826.

Mannen, T., Iwata, M., Toyokura, Y., and Nagashima, K. (1982). The Onuf's nucleus and the external anal sphincter muscles in amyotrophic lateral sclerosis and Shy-Drager syndrome. Acta Neuropathol *58*, 255–260.

Marchetto, M., Muotri, A.R., Mu, Y., Smith, A.M., Cezar, G.G., and Gage, F.H. (2008). Non-Cell-Autonomous Effect of Human SOD1G37R Astrocytes on Motor Neurons Derived from Human Embryonic Stem Cells. Cell Stem Cell *3*.

Marrone, L., Poser, I., Casci, I., Japtok, J., Reinhardt, P., Janosch, A., Andree, C., Lee, H.O., Moebius, C., Koerner, E., et al. (2018). Isogenic FUS-eGFP iPSC Reporter Lines Enable Quantification of FUS Stress Granule Pathology that Is Rescued by Drugs Inducing Autophagy. Stem Cell Rep *10*, 375–389.

Martin, G.R. (1981). Isolation of a pluripotent cell line from early mouse embryos cultured in medium conditioned by teratocarcinoma stem cells. Proc National Acad Sci *78*, 7634–7638.

Maury, Y., Côme, J., Piskorowski, R.A., Salah-Mohellibi, N., Chevaleyre, V., Peschanski, M., Martinat, C., and Nedelec, S. (2015). Combinatorial analysis of developmental cues efficiently converts human pluripotent stem cells into multiple neuronal subtypes. Nat Biotechnol *33*, 89–96.

Mazzoni, E.O., Mahony, S., Closser, M., Morrison, C.A., Nedelec, S., Williams, D.J., An, D., Gifford, D.K., and Wichterle, H. (2013). Synergistic binding of transcription factors to cell-specific enhancers programs motor neuron identity. Nature Neuroscience *16*, 1219–1227.

Melamed, Z., López-Erauskin, J., Baughn, M.W., Zhang, O., Drenner, K., Sun, Y., Freyermuth, F., McMahon, M.A., Beccari, M.S., Artates, J.W., et al. (2019). Premature polyadenylation-mediated loss of stathmin-2 is a hallmark of TDP-43-dependent neurodegeneration. Nat Neurosci *22*, 180–190.

Miller, R.G., Mitchell, J.D., and Moore, D.H. (2012). Riluzole for amyotrophic lateral sclerosis (ALS)/motor neuron disease (MND). Cochrane Database Syst Rev *3*, CD001447.

Minis, A., Dahary, D., Manor, O., Leshkowitz, D., Pilpel, Y., and Yaron, A. (2014). Subcellular transcriptomics-dissection of the mRNA composition in the axonal compartment of sensory neurons. Developmental Neurobiology *74*, 365–381.

Mirra, A., Rossi, S., Scaricamazza, S., Salvio, M.D., Salvatori, I., Valle, C., Rusmini, P., Poletti, A., Cestra, G., Carrì, M.T., et al. (2017). Functional interaction between FUS and SMN underlies SMA-like splicing changes in wild-type hFUS mice. Sci Rep-Uk *7*, 2033.

Mitchell, J.C., McGoldrick, P., Vance, C., Hortobagyi, T., Sreedharan, J., Rogelj, B., Tudor, E.L., Smith, B.N., Klasen, C., Miller, C.C.J., et al. (2012). Overexpression of human wild-type FUS causes progressive motor neuron degeneration in an age- and dose-dependent fashion. Acta Neuropathol *125*, 273–288.

Mizielinska, S., Gronke, S., Niccoli, T., Ridler, C.E., Clayton, E.L., Devoy, A., Moens, T., Norona, F.E., Woollacott, I.O.C., Pietrzyk, J., et al. (2014). C9orf72 repeat expansions cause neurodegeneration in Drosophila through arginine-rich proteins. Science *345*, 1192–1194.

Mizui, T., Takahashi, H., Sekino, Y., and Shirao, T. (2005). Overexpression of drebrin A in immature neurons induces the accumulation of F-actin and PSD-95 into dendritic filopodia, and the formation of large abnormal protrusions. Mol Cell Neurosci *30*, 149–157.

Moens, T.G., Mizielinska, S., Niccoli, T., Mitchell, J.S., Thoeng, A., Ridler, C.E., Grönke, S., Esser, J., Heslegrave, A., Zetterberg, H., et al. (2018). Sense and antisense RNA are not toxic in Drosophila models of C9orf72-associated ALS/FTD. Acta Neuropathol *135*, 445–457.

Monani, U., Sendtner, M., Coovert, D., Parsons, D., Andreassi, C., Le, T., Jablonka, S., Schrank, B., Rossoll, W., Rossol, W., et al. (2000). The human centromeric survival motor neuron gene (SMN2) rescues embryonic lethality in Smn–/– mice and results in a mouse with spinal muscular atrophy. Human Molecular Genetics *9*, 333–339.

Mong, J., Panman, L., Alekseenko, Z., Kee, N., Stanton, L.W., Ericson, J., and Perlmann, T. (2014). Transcription factor-induced lineage programming of noradrenaline and motor neurons from embryonic stem cells. Stem Cells (Dayton, Ohio) *32*, 609–622.

Mori, K., Weng, S.-M., Arzberger, T., May, S., Rentzsch, K., Kremmer, E., Schmid, B., Kretzschmar, H.A., Cruts, M., Broeckhoven, C.V., et al. (2013). The C9orf72 GGGGCC Repeat Is Translated into Aggregating Dipeptide-Repeat Proteins in FTLD/ALS. Science *339*, 1335–1338.

Murray, M.E., DeJesus-Hernandez, M., Rutherford, N.J., Baker, M., Duara, R., Graff-Radford, N.R., Wszolek, Z.K., Ferman, T.J., Josephs, K.A., Boylan, K.B., et al. (2011). Clinical and neuropathologic heterogeneity of c9FTD/ALS associated with hexanucleotide repeat expansion in C9ORF72. Acta Neuropathol *122*, 673–690.

Nagahisa, H., Okabe, K., Iuchi, Y., Fujii, J., and Miyata, H. (2016). Characteristics of Skeletal Muscle Fibers of SOD1 Knockout Mice. Oxid Med Cell Longev *2016*, 1–8.

Nassif, M., Woehlbier, U., and Manque, P.A. (2017). The Enigmatic Role of C9ORF72 in Autophagy. Front Neurosci-Switz *11*, 442.

Naumann, M., Pal, A., Goswami, A., Lojewski, X., Japtok, J., Vehlow, A., Naujock, M., Günther, R., Jin, M., Stanslowsky, N., et al. (2018). Impaired DNA damage response signaling by FUS-NLS mutations leads to neurodegeneration and FUS aggregate formation. Nature Communications *9*, 335.

Naumann, M., Peikert, K., Günther, R., Kooi, A.J., Aronica, E., Hübers, A., Danel, V., Corcia, P., Pan-Montojo, F., Cirak, S., et al. (2019). Phenotypes and malignancy risk of different FUS mutations in genetic amyotrophic lateral sclerosis. Ann Clin Transl Neur *6*, 2384–2394.

Neumann, M., Sampathu, D.M., Kwong, L.K., Truax, A.C., Micsenyi, M.C., Chou, T.T., Bruce, J., Schuck, T., Grossman, M., Clark, C.M., et al. (2006). Ubiquitinated TDP-43 in Frontotemporal Lobar Degeneration and Amyotrophic Lateral Sclerosis. Science *314*, 130–133.

Nguyen, L., Montrasio, F., Pattamatta, A., Tusi, S.K., Bardhi, O., Meyer, K.D., Hayes, L., Nakamura, K., Banez-Coronel, M., Coyne, A., et al. (2020). Antibody Therapy Targeting RAN Proteins Rescues C9 ALS/FTD Phenotypes in C9orf72 Mouse Model. Neuron *105*, 645-662.e11.

Nichterwitz, S., Chen, G., Benitez, J., Yilmaz, M., Storvall, H., Cao, M., Sandberg, R., Deng, Q., and Hedlund, E. (2016). Laser capture microscopy coupled with Smart-seq2 for precise spatial transcriptomic profiling. Nature Communications *7*, 12139.

Nichterwitz, S., Benitez, J.A., Hoogstraaten, R., Deng, Q., and Hedlund, E. (2018). RNA Detection, Methods and Protocols. Methods Mol Biology Clifton N J *1649*, 95–110.

Nijssen, J., Comley, L.H., and Hedlund, E. (2017). Motor neuron vulnerability and resistance in amyotrophic lateral sclerosis. Acta Neuropathologica *133*, 863–885.

Nizzardo, M., Taiana, M., Rizzo, F., Benitez, J.A., Nijssen, J., Allodi, I., Melzi, V., Bresolin, N., Comi, G.P., Hedlund, E., et al. (2020). Synaptotagmin 13 is neuroprotective across motor neuron diseases. Acta Neuropathol 1–17.

Nölle, A., Zeug, A., Bergeijk, J. van, Tönges, L., Gerhard, R., Brinkmann, H., Rayes, S.A., Hensel, N., Schill, Y., Apkhazava, D., et al. (2011). The spinal muscular atrophy disease protein SMN is linked to the Rho-kinase pathway via profilin. Hum Mol Genet *20*, 4865–4878.

Okada, Y., Yamazaki, H., Sekine-Aizawa, Y., and Hirokawa, N. (1995). The neuron-specific kinesin superfamily protein KIF1A is a uniqye monomeric motor for anterograde axonal transport of synaptic vesicle precursors. Cell *81*, 769–780.

Paré, B., Lehmann, M., Beaudin, M., Nordström, U., Saikali, S., Julien, J.-P., Gilthorpe, J.D., Marklund, S.L., Cashman, N.R., Andersen, P.M., et al. (2018). Misfolded SOD1 pathology in sporadic Amyotrophic Lateral Sclerosis. Sci Rep-Uk *8*, 14223.

Pattyn, A., Morin, X., Cremer, H., Goridis, C., and Brunet, J.F. (1997). Expression and interactions of the two closely related homeobox genes Phox2a and Phox2b during neurogenesis. Dev Camb Engl *124*, 4065–4075.

Peña, C., Hurt, E., and Panse, V.G. (2017). Eukaryotic ribosome assembly, transport and quality control. Nat Struct Mol Biol *24*, 689–699.

Perera, N.D., Sheean, R.K., Crouch, P.J., White, A.R., Horne, M.K., and Turner, B.J. (2016). Enhancing survival motor neuron expression extends lifespan and attenuates neurodegeneration in mutant TDP-43 mice. Hum Mol Genet *25*, 4080–4093.

Picelli, S., Björklund, Å.K., Faridani, O.R., Sagasser, S., Winberg, G., and Sandberg, R. (2013). Smart-seq2 for sensitive full-length transcriptome profiling in single cells. Nat Methods *10*, nmeth.2639.

Pun, S., Santos, A.F., Saxena, S., Xu, L., and Caroni, P. (2006). Selective vulnerability and pruning of phasic motoneuron axons in motoneuron disease alleviated by CNTF. Nat Neurosci *9*, 408–419.

Pupillo, E., Messina, P., Logroscino, G., Beghi, E., and Group, S. (2014). Long-term survival in amyotrophic lateral sclerosis: a population-based study. Ann Neurol *75*, 287–297.

Reaume, A.G., Elliott, J.L., Hoffman, E.K., Kowall, N.W., Ferrante, R.J., Siwek, D.R., Wilcox, H.M., Flood, D.G., Beal, M.F., Brown, R.H., et al. (1996). Motor neurons in Cu/Zn superoxide dismutase-deficient mice develop normally but exhibit enhanced cell death after axonal injury. Nat Genet *13*, 43–47.

Reber, S., Stettler, J., Filosa, G., Colombo, M., Jutzi, D., Lenzken, S.C., Schweingruber, C., Bruggmann, R., Bachi, A., Barabino, S.M., et al. (2016). Minor intron splicing is regulated by FUS and affected by ALS-associated FUS mutants. Embo J *35*, 1504–1521.

Renton, A.E., Majounie, E., Waite, A., Simón-Sánchez, J., Rollinson, S., Gibbs, J.R., Schymick, J.C., Laaksovirta, H., Swieten, J.C. van, Myllykangas, L., et al. (2011). A hexanucleotide repeat expansion in C9ORF72 is the cause of chromosome 9p21-linked ALS-FTD. Neuron *72*, 257–268.

Renton, A.E., Chiò, A., and Traynor, B.J. (2014). State of play in amyotrophic lateral sclerosis genetics. Nature Neuroscience *17*, 17–23.

Rosen, D.R., Siddique, T., Patterson, D., Figlewicz, D.A., Sapp, P., Hentati, A., Donaldson, D., Goto, J., O'Regan, J.P., Deng, H.-X., et al. (1993). Mutations in Cu/Zn superoxide dismutase gene are associated with familial amyotrophic lateral sclerosis. Nature *362*, 59–62.

Rotem, N., Magen, I., Ionescu, A., Gershoni-Emek, N., Altman, T., Costa, C.J., Gradus, T., Pasmanik-Chor, M., Willis, D.E., Ben-Dov, I.Z., et al. (2017). ALS Along the Axons - Expression of Coding and Noncoding RNA Differs in Axons of ALS models. Scientific Reports *7*, 44500.

Ruegsegger, C., Maharjan, N., Goswami, A., L'Etang, A.F. de, Weis, J., Troost, D., Heller, M., Gut, H., and Saxena, S. (2015). Aberrant association of misfolded SOD1 with Na(+)/K(+)ATPase-α3 impairs its activity and contributes to motor neuron vulnerability in ALS. Acta Neuropathologica.

Saal, L., Briese, M., Kneitz, S., Glinka, M., and Sendtner, M. (2014). Subcellular transcriptome alterations in a cell culture model of spinal muscular atrophy point to widespread defects in axonal growth and presynaptic differentiation. RNA (New York, N.Y.) *20*, 1789–1802.

Schaefer, A.M., Sanes, J.R., and Lichtman, J.W. (2005). A compensatory subpopulation of motor neurons in a mouse model of amyotrophic lateral sclerosis. Journal of Comparative Neurology *490*, 209–219.

Schrank, B., Gotz, R., Gunnersen, J.M., Ure, J.M., Toyka, K.V., Smith, A.G., and Sendtner, M. (1997). Inactivation of the survival motor neuron gene, a candidate gene for human spinal muscular atrophy, leads to massive cell death in early mouse embryos. Proc National Acad Sci *94*, 9920–9925.

Seibler, P., Burbulla, L.F., Dulovic, M., Zittel, S., Heine, J., Schmidt, T., Rudolph, F., Westenberger, A., Rakovic, A., Münchau, A., et al. (2018). Iron overload is accompanied by mitochondrial and lysosomal dysfunction in WDR45 mutant cells. Brain J Neurology *141*, 3052–3064.

Serio, A., Bilican, B., Barmada, S.J., Ando, D.M., Zhao, C., Siller, R., Burr, K., Haghi, G., Story, D., Nishimura, A.L., et al. (2013). Astrocyte pathology and the absence of non-cell autonomy in an induced pluripotent stem cell model of TDP-43 proteinopathy. Proc National Acad Sci *110*, 4697–4702.

Sharma, A., Lyashchenko, A.K., Lu, L., Nasrabady, S.E., Elmaleh, M., Mendelsohn, M., Nemes, A., Tapia, J.C., Mentis, G.Z., and Shneider, N.A. (2016). ALS-associated mutant FUS induces selective motor neuron degeneration through toxic gain of function. Nature Communications *7*, 10465.

Shi, Y., Lin, S., Staats, K.A., Li, Y., Chang, W.-H., Hung, S.-T., Hendricks, E., Linares, G.R., Wang, Y., Son, E.Y., et al. (2018). Haploinsufficiency leads to neurodegeneration in C9ORF72 ALS/FTD human induced motor neurons. Nat Med *24*, 313–325.

Shigeoka, T., Jung, H., Jung, J., Turner-Bridger, B., Ohk, J., Lin, J.Q., Amieux, P.S., and Holt, C.E. (2016). Dynamic Axonal Translation in Developing and Mature Visual Circuits. Cell *166*, 181–192.

Shigeoka, T., Koppers, M., Wong, H.H.-W., Lin, J.Q., Cagnetta, R., Dwivedy, A., Nascimento, J. de F., Tartwijk, F.W. van, Ströhl, F., Cioni, J.-M., et al. (2019). On-Site Ribosome Remodeling by Locally Synthesized Ribosomal Proteins in Axons. Cell Reports *29*, 3605-3619.e10.

Simon, D.J., Pitts, J., Hertz, N.T., Yang, J., Yamagishi, Y., Olsen, O., Mark, M.T., Molina, H., and Tessier-Lavigne, M. (2016). Axon Degeneration Gated by Retrograde Activation of Somatic Pro-apoptotic Signaling. Cell *164*, 1031–1045.

Sleigh, J.N., Tosolini, A.P., Gordon, D., Devoy, A., Fratta, P., Fisher, E.M.C., Talbot, K., and Schiavo, G. (2020). Mice Carrying ALS Mutant TDP-43, but Not Mutant FUS, Display In Vivo Defects in Axonal Transport of Signaling Endosomes. Cell Reports *30*, 3655-3662.e2.

Solomon, D.A., Stepto, A., Au, W.H., Adachi, Y., Diaper, D.C., Hall, R., Rekhi, A., Boudi, A., Tziortzouda, P., Lee, Y.-B., et al. (2018). A feedback loop between dipeptide-repeat protein, TDP-43 and karyopherin-α mediates C9orf72-related neurodegeneration. Brain *141*, 2908–2924.

Sreedharan, J., Blair, I.P., Tripathi, V.B., Hu, X., Vance, C., Rogelj, B., Ackerley, S., Durnall, J.C., Williams, K.L., Buratti, E., et al. (2008). TDP-43 mutations in familial and sporadic amyotrophic lateral sclerosis. Sci New York N Y *319*, 1668–1672.

Sudria-Lopez, E., Koppers, M., Wit, M. de, Meer, C. van der, Westeneng, H.-J., Zundel, C.A.C., Youssef, S.A., Harkema, L., Bruin, A. de, Veldink, J.H., et al. (2016). Full ablation of C9orf72 in mice causes immune system-related pathology and neoplastic events but no motor neuron defects. Acta Neuropathol *132*, 145–147.

Swinnen, B., and Robberecht, W. (2014). The phenotypic variability of amyotrophic lateral sclerosis. Nature Reviews Neurology *10*, 661–670.

Swinnen, B., Bento-Abreu, A., Gendron, T.F., Boeynaems, S., Bogaert, E., Nuyts, R., Timmers, M., Scheveneels, W., Hersmus, N., Wang, J., et al. (2018). A zebrafish model for C9orf72 ALS reveals RNA toxicity as a pathogenic mechanism. Acta Neuropathol *135*, 427–443.

Takahashi, K., and Yamanaka, S. (2006). Induction of Pluripotent Stem Cells from Mouse Embryonic and Adult Fibroblast Cultures by Defined Factors. Cell *126*, 663–676.

Takahashi, K., Tanabe, K., Ohnuki, M., Narita, M., Ichisaka, T., Tomoda, K., and Yamanaka, S. (2007). Induction of Pluripotent Stem Cells from Adult Human Fibroblasts by Defined Factors. Cell *131*, 861–872.

Taylor, A.M., Blurton-Jones, M., Rhee, S., Cribbs, D.H., Cotman, C.W., and Jeon, N. (2005). A microfluidic culture platform for CNS axonal injury, regeneration and transport. Nature Methods *2*, 599–605.

Taylor, A.M., Berchtold, N.C., Perreau, V.M., Tu, C.H., Jeon, N.L., and Cotman, C.W. (2009). Axonal mRNA in Uninjured and Regenerating Cortical Mammalian Axons. J Neurosci *29*, 4697–4707.

Taylor, P.J., Jr, R.H., and Cleveland, D.W. (2016). Decoding ALS: from genes to mechanism. Nature 197–206.

Thomson, J.A., Itskovitz-Eldor, J., Shapiro, S.S., Waknitz, M.A., Swiergiel, J.J., Marshall, V.S., and Jones, J.M. (1998). Embryonic Stem Cell Lines Derived from Human Blastocysts. Science *282*, 1145–1147.

Tyzack, G.E., Luisier, R., Taha, D.M., Neeves, J., Modic, M., Mitchell, J.S., Meyer, I., Greensmith, L., Newcombe, J., Ule, J., et al. (2019). Widespread FUS mislocalization is a molecular hallmark of amyotrophic lateral sclerosis. Brain *142*, 2572–2580.

Vance, C., Rogelj, B., Hortobágyi, T., Vos, K.J.D., Nishimura, A.L., Sreedharan, J., Hu, X., Smith, B., Ruddy, D., Wright, P., et al. (2009). Mutations in FUS, an RNA processing protein, cause familial amyotrophic lateral sclerosis type 6. Sci New York N Y *323*, 1208–1211.

Vanselow, B.K., and Keller, B.U. (2000). Calcium dynamics and buffering in oculomotor neurones from mouse that are particularly resistant during amyotrophic lateral sclerosis (ALS)-related motoneurone disease. J Physiology *525*, 433–445.

Wächter, N., Storch, A., and Hermann, A. (2015). Human TDP-43 and FUS selectively affect motor neuron maturation and survival in a murine cell model of ALS by non-cell-autonomous mechanisms. Amyotrophic Lateral Sclerosis & Frontotemporal Degeneration *16*, 431–441.

Waddington, C. (1957). The strategy of the genes: a discussion of some aspects of theoretical biology.

Walker, A.K., Spiller, K.J., Ge, G., Zheng, A., Xu, Y., Zhou, M., Tripathy, K., Kwong, L.K., Trojanowski, J.Q., and Lee, V.M. (2015). Functional recovery in new mouse models of ALS/FTLD after clearance of pathological cytoplasmic TDP-43. Acta Neuropathologica *130*, 643–660.

Wan, H., Wang, Q., Chen, X., Zeng, Q., Shao, Y., Fang, H., Liao, X., Li, H.-S., Liu, M.-G., Xu, T.-L., et al. (2019). WDR45 contributes to neurodegeneration through regulation of ER homeostasis and neuronal death. Autophagy *16*, 531–547.

Wang, M.Z., Jin, P., Bumcrot, D.A., Marigo, V., Mcmahon, A.P., Wang, E.A., Woolf, T., and Pang, K. (1995). Induction of dopaminergic neuron phenotype in the midbrain by Sonic hedgehog protein. Nat Med *1*, 1184–1188.

Wichterle, H., Lieberam, I., Porter, J.A., and Jessell, T.M. (2002). Directed Differentiation of Embryonic Stem Cells into Motor Neurons. Cell *110*, 385–397.

Wils, H., Kleinberger, G., Janssens, J., Pereson, S., Joris, G., Cuijt, I., Smits, V., Groote, C.C., Broeckhoven, C.V., and Kumar-Singh, S. (2010). TDP-43 transgenic mice develop spastic paralysis and neuronal inclusions characteristic of ALS and frontotemporal lobar degeneration. Proc National Acad Sci *107*, 3858–3863.

Wong, P.C., Pardo, C.A., Borchelt, D.R., Lee, M.K., Copeland, N.G., Jenkins, N.A., Sisodia, S.S., Cleveland, D.W., and Price, D.L. (1995). An adverse property of a familial ALS-linked SOD1 mutation causes motor neuron disease characterized by vacuolar degeneration of mitochondria. Neuron *14*, 1105–1116.

Wozniak, M.J., Melzer, M., Dorner, C., Haring, H.-U., and Lammers, R. (2005). The novel protein KBP regulates mitochondria localization by interaction with a kinesin-like protein. Bmc Cell Biol *6*, 35.

Yamanaka, K., Chun, S.J., Boillee, S., Fujimori-Tonou, N., Yamashita, H., Gutmann, D.H., Takahashi, R., Misawa, H., and Cleveland, D.W. (2008). Astrocytes as determinants of disease progression in inherited amyotrophic lateral sclerosis. Nat Neurosci *11*, 251–253.

Yamazaki, T., Chen, S., Yu, Y., Yan, B., Haertlein, T.C., Carrasco, M.A., Tapia, J.C., Zhai, B., Das, R., Lalancette-Hebert, M., et al. (2012). FUS-SMN Protein Interactions Link the Motor Neuron Diseases ALS and SMA. Cell Reports *2*, 799–806.

Ye, W., Shimamura, K., Rubenstein, J.L.R., Hynes, M.A., and Rosenthal, A. (1998). FGF and Shh Signals Control Dopaminergic and Serotonergic Cell Fate in the Anterior Neural Plate. Cell *93*, 755–766.

Young, P.J., Le, T.T., Man, N. thi, Burghes, A.H.M., and Morris, G.E. (2000). The Relationship between SMN, the Spinal Muscular Atrophy Protein, and Nuclear Coiled Bodies in Differentiated Tissues and Cultured Cells. Exp Cell Res *256*, 365–374.

Yu, J., Vodyanik, M.A., Smuga-Otto, K., Antosiewicz-Bourget, J., Frane, J.L., Tian, S., Nie, J., Jonsdottir, G.A., Ruotti, V., Stewart, R., et al. (2007). Induced Pluripotent Stem Cell Lines Derived from Human Somatic Cells. Science *318*, 1917–1920.

Zhang, H., Xing, L., Rossoll, W., Wichterle, H., Singer, R.H., and Bassell, G.J. (2006). Multiprotein Complexes of the Survival of Motor Neuron Protein SMN with Gemins Traffic to Neuronal Processes and Growth Cones of Motor Neurons. J Neurosci *26*, 8622–8632.

Zhang, K., Donnelly, C.J., Haeusler, A.R., Grima, J.C., Machamer, J.B., Steinwald, P., Daley, E.L., Miller, S.J., Cunningham, K.M., Vidensky, S., et al. (2015). The C9orf72 repeat expansion disrupts nucleocytoplasmic transport. Nature *525*, 56–61.

Zhang, Y., Bertulat, B., Tencer, A.H., Ren, X., Wright, G.M., Black, J., Cardoso, M.C., and Kutateladze, T.G. (2019). MORC3 Forms Nuclear Condensates through Phase Separation. Iscience *17*, 182–189.

Zhang, Z., Almeida, S., Lu, Y., Nishimura, A.L., Peng, L., Sun, D., Wu, B., Karydas, A.M., Tartaglia, M.C., Fong, J.C., et al. (2013). Downregulation of microRNA-9 in iPSC-derived neurons of FTD/ALS patients with TDP-43 mutations. Plos One *8*, e76055.

Zivraj, K.H., Tung, Y.C., Piper, M., Gumy, L., Fawcett, J.W., Yeo, G.S., and Holt, C.E. (2010). Subcellular profiling reveals distinct and developmentally regulated repertoire of growth cone mRNAs. The Journal of Neuroscience : The Official Journal of the Society for Neuroscience *30*, 15464–15478.

Zou, L., and Elledge, S.J. (2003). Sensing DNA Damage Through ATRIP Recognition of RPA-ssDNA Complexes. Science *300*, 1542–1548.

Zu, T., Gibbens, B., Doty, N.S., Gomes-Pereira, M., Huguet, A., Stone, M.D., Margolis, J., Peterson, M., Markowski, T.W., Ingram, M.A.C., et al. (2010). Non-ATG–initiated translation directed by microsatellite expansions. Proc National Acad Sci *108*, 260–265.